CLEARINGHOUSE FOR FEDERAL SCIENTIFIC AND TECHNICAL INFORMATION CFSTI
DOCUMENT MANAGEMENT BRANCH 410.11

LIMITATIONS IN REPRODUCTION QUALITY

ACCESSION # AD 607036

- [x] 1. WE REGRET THAT LEGIBILITY OF THIS DOCUMENT IS IN PART UNSATISFACTORY. REPRODUCTION HAS BEEN MADE FROM BEST AVAILABLE COPY.
- [ ] 2. A PORTION OF THE ORIGINAL DOCUMENT CONTAINS FINE DETAIL WHICH MAY MAKE READING OF PHOTOCOPY DIFFICULT.
- [ ] 3. THE ORIGINAL DOCUMENT CONTAINS COLOR, BUT DISTRIBUTION COPIES ARE AVAILABLE IN BLACK-AND-WHITE REPRODUCTION ONLY.
- [ ] 4. THE INITIAL DISTRIBUTION COPIES CONTAIN COLOR WHICH WILL BE SHOWN IN BLACK-AND-WHITE WHEN IT IS NECESSARY TO REPRINT.
- [ ] 5. LIMITED SUPPLY ON HAND: WHEN EXHAUSTED, DOCUMENT WILL BE AVAILABLE IN MICROFICHE ONLY.
- [ ] 6. LIMITED SUPPLY ON HAND: WHEN EXHAUSTED DOCUMENT WILL NOT BE AVAILABLE.
- [ ] 7. DOCUMENT IS AVAILABLE IN MICROFICHE ONLY.
- [ ] 8. DOCUMENT AVAILABLE ON LOAN FROM CFSTI (TT DOCUMENTS ONLY).
- [ ] 9.

NBS 9/64 PROCESSOR:

FDL-TDR 64-66

STUDY OF PARACHUTE PERFORMANCE AND DESIGN PARAMETERS FOR HIGH DYNAMIC PRESSURE OPERATION

TECHNICAL DOCUMENTARY REPORT NO. FDL-TDR 64-66

MAY 1964

AIR FORCE FLIGHT DYNAMICS LABORATORY
RESEARCH AND TECHNOLOGY DIVISION
AIR FORCE SYSTEMS COMMAND
WRIGHT-PATTERSON AIR FORCE BASE, OHIO

PROJECT NO. 6065 TASK NO. 606505

(Prepared under Contract AF 33 (657)-9182
by Tech-Center Division, Cook Electric Company
Morton Grove, Illinois; P. E. Pedersen, Author)

FDL-TDR 64-66

STUDY OF PARACHUTE PERFORMANCE AND DESIGN PARAMETERS FOR HIGH DYNAMIC PRESSURE OPERATION

TECHNICAL DOCUMENTARY REPORT NO. FDL-TDR 64-66

MAY 1964

AIR FORCE FLIGHT DYNAMICS LABORATORY
RESEARCH AND TECHNOLOGY DIVISION
AIR FORCE SYSTEMS COMMAND
WRIGHT-PATTERSON AIR FORCE BASE, OHIO

PROJECT NO. 6065 - TASK NO. 606505

(Prepared under Contract AF 33 (657)-9182
by Tech-Center Division, Cook Electric Company
Morton Grove, Illinois; P. E. Pedersen, Author)

BEST AVAILABLE COPY

FOREWORD

This report was prepared by the Cook Research Laboratories, Tech-Center Division of the Cook Electric Company, Morton Grove, Illinois, in compliance with United States Air Force Contract No. AF 33(657)-9182. The contract was initiated under USAF Project 6065, Task No. 606505 by the Flight Dynamics Laboratory, AFSC Research and Technology Division, Wright-Patterson Air Force Base, Ohio, with Mr. Arnold B. Riffle as Project Officer.

The work at the Cook Research Laboratories was conducted under the supervision of Mr. R. C. Edwards, Director, Cook Research Laboratories; Mr. L. J. Lorenz, Manager; and Dr. R. J. Benjamin, Director of Engineering, Aerospace Technology Section. The program was directed by Mr. P. E. Pedersen, Program Manager and Mr. C. V. Bidne, Project Engineer in the field.

Work on the program, designated as Cook Project P-3752, was initiated on 1 July 1962 and was completed on 31 December 1963.

Staff members who contributed to the project included F. A. Ruprecht, Supervisor, Parachute Department, and Mr. E. J. Biedron, Junior Engineer, Parachute Design and Data Analysis.

Operations on the program at the Track Test Facility at AFMDC, New Mexico, was under the direction of Capt. D. S. Jones, Track Project Officer.

ABSTRACT

Parachute design and performance data were obtained on a series of 24 rocket-powered sled tests conducted on the track test facility at the Air Force Missile Development Center, Holloman Air Force Base, New Mexico. The program was conducted to advance the state of the art of textile parachute technology with respect to high dynamic pressure operation. Parachute deployment velocities, ranging between Mach 1.0 and 1.5, were obtained with the Tomahawk parachute test sled operating in either single stage or double stage, pusher configuration. Parachute types that were investigated included Hyperflo, Hemisflo, Reefed Conical Ribbon and Supersonic Guide Surface designs.

The data obtained included inflation characteristics, opening shock factors, drag coefficients, inflated areas, stability, canopy temperatures and general structural and aerodynamic design considerations.

From this parachute decelerator test program, it may be concluded that the Hyperflo type parachute, both mesh and ribbon roof designs, and the Hemisflo type parachute can be fabricated to withstand and operate successfully in the high dynamic pressure region of 3000 psf. Supersonic reefed operation and disreef to full open was also demonstrated as practical with a Conical Ribbon type parachute design.

The test vehicle system including associated deployment and release techniques and the data acquisition system are also discussed.

PUBLICATION REVIEW

TABLE OF CONTENTS

TABLE OF CONTENTS (cont'd)

ILLUSTRATIONS

ILLUSTRATIONS (cont'd)

ILLUSTRATIONS (cont'd)

TABLES

TABLES

LIST OF SYMBOLS

A_R*	Area Ratio-Ratio of instantaneous projected area of inflated canopy (S_{p_i}) to nominal design surface area (S_o) or theoretical projected area (S_p) whichever is applicable - (percent)
A_{VR}	Vertical ribbon width - (in.)
a	Speed of sound in air - ft/sec
a_{VR}	Distance between vertical ribbons - (in.)
B_{HR}	Horizontal ribbon width - (in.)
b_{HR}	Distance between horizontal ribbons - (in.)
C*	Radial ribbon width - (in.)
C_{D_o}	Drag coefficient of parachute canopy based on total cloth area. S_o - (dimensionless)
C_{D_p}	Drag coefficient of parachute canopy based on inflated (projected) canopy area - (dimensionless)
D_b*	Diameter, base (conical parachutes)(ft)
D_c	Diameter, constructed - (ft)
D_o	Diameter, nominal: equal to $\sqrt{\frac{4S_o}{\pi}}$ - (ft)
D_p	Projected or inflated canopy diameter - (ft)
e_g	Base width of gore - (in.)
e_{g_v}	Gore width at vent - (in.)
e_{g_m}*	Maximum gore width - (in.)
F	Drag force of parachute as transmitted to sled - (lb)
F_c	Constant drag force on fully inflated canopy - (lb)

F_o	Maximum opening force - (lb)
F_s	Peak snatch force - (lb)
h_g	Height of gore - (in.)
l_s	Length of suspension lines from canopy skirt to confluence point - (ft)
M	Mach number = V/a (dimensionless)
n_g	Number of gores (dimensionless)
q	Dynamic pressure $= \frac{\rho}{2} V^2$ - (lb/ft^2)
q_s	Dynamic pressure corresponding to the velocity at peak snatch force - (lb/ft^2)
q_o	Dynamic pressure corresponding to the velocity at maximum opening force - (lb/ft^2)
r^*	Turbulent recovery factor (dimensionless)
S_o	Total cloth area of canopy, or design surface area including slots and vent - (ft^2)
S_p	Theoretical projected area of inflated canopy - (ft^2)
$S_{p_i}{}^*$	Instantaneous (measured) projected area of inflated canopy - (ft^2)
T^*	Temperature (^{o}R)
$T_R{}^*$	Temperature, recovery - (^{o}R)
$T_\infty{}^*$	Temperature, free stream - (^{o}R)
t_d	Deployment time from release to completion of canopy line stretch (sec)
t_f	Inflation time (filling time) (sec)

t_{s_o}	Time to maximum opening force (sec)
X	Opening shock factor - (dimensionless), denotes the relationship between maximum opening force, F_o, and constant drag force, F_c, at equivalent velocity
α*	Conical angle (conical parachutes) = $\cos^{-1} \frac{D_b}{D_c}$ - (degrees)
λ_t	Total canopy porosity (percent)
ϕ	Angular displacement (stability) of parachute or parachute system from reference axis (degrees)

*Denotes that the definition is not included in the Parachute Handbook (Reference 1) or that the definition in the Handbook has been modified.

SECTION 1

INTRODUCTION

The use of rocket-powered track-borne parachute test vehicles for the detailed study of parachute behavior and operational characteristics has become a valuable and accepted method of obtaining parachute structural data and performance information not easily or otherwise available by other testing techniques.

This report contains the results of a comprehensive high speed sled parachute research program entitled "A Study of Parachute Performance and Design Parameters for High Dynamic Pressure Operation", conducted in accordance with the provisions of Contract AF 33(657)-9182. A total of 24 test runs were made with parachutes of the Hyperflo, Hemisflo, Conical Ribbon and Supersonic Guide Surface (Cone-Cup) types. Except for one test which was conducted with a cluster configuration of three parachutes, all of the tests were made with single test parachutes.

The primary objective of the test program was to advance the state of the art of textile parachute technology by investigating the aerodynamic and strength characteristics of parachute canopies operating at high dynamic pressures. A secondary objective was to add to the range of data obtained with Hyperflo and Hemisflo parachutes in previous wind tunnel and free-flight test programs (Refs. 2, 3, and 4). The test regime was to be confined to a Mach number range between 1.0 and 1.5 with specific test points being conducted at Mach numbers 1.1, 1.3, and 1.5. The corresponding dynamic pressures ranged from 1550 to 2900 psf.

The major parameters which were to be measured or derived included parachute force, drag coefficient, inflated areas and stability as a function of time, velocity, Mach number, and dynamic pressure. In addition, the temperature environment of the parachute canopy was also to be determined in applicable tests.

Manuscript released by the author April 1964
for publication as a FDL-Technical Documentary
Report

Parachute testing, using specially constructed rocket-powered, track-borne sleds as the test platform has been accomplished by the Tech-Center Division of Cook Electric Company on two previous programs initiated and monitored by the Recovery and Crew Stations Branch of the Air Force Flight Dynamics Laboratory. These programs, totaling 249 tests, were reported in Ref. 5 and 6. With the current series of 24 tests, a total of 273 parachute sled tests have been conducted.

On the above past programs, standard FIST type ribbon parachutes and special ribbon designs such as the Conicals, Equiflo and Hemisflo type parachutes, were developed to withstand dynamic pressures typical of sea level transonic operations. Under the present contract, the state of the art was advanced to include Hyperflo and Reefed Conical Ribbon type parachutes as well as Hemisflo type parachutes operating at dynamic pressures approaching 3000 psf (M 1.5).

SECTION 2

TEST CONDITIONS

2.1 TEST FACILITY

All of the parachute tests that were made during the program were conducted on the 35,000 foot track test facility at the Air Force Missile Development Center, Holloman Air Force Base, New Mexico. The parachutes were tested by deploying them from the Tomahawk rocket powered parachute test vehicle in accordance with pre-selected performance profiles. Details of the test vehicle system which was utilized in the conduct of the program is presented in Section 6 of this report.

2.2 TEST PROGRAM

Twenty-four tests were conducted with eleven configurations of four basic parachute types. Deployment velocities ranged from approximately Mach 1.0 to Mach 1.5. A chronological tabulation of the tests listing parachute type, parachute nominal diameter and deployment Mach number is presented in Table 2.2.1. A summary of the characteristics and performance of the parachute configurations which were tested are presented in Section 4 of this report. Detailed test results are included by parachute type and configuration in Section 5.

The program was conducted within limitations which are more or less inherent to this type of testing. Although not necessarily detrimental, the restrictions should be considered when reference is made to the data. The major limitations were as follows:

1. Parachute drag area was limited to 18 square feet at maximum velocity deployment conditions, based on a design subsonic drag coefficient of 0.5.

2. Deployment velocity was limited to a range between Mach 1.0 and Mach 1.5.

3. Altitude was limited to ground elevation at the test facility (approximately 4,100 m.s.l.)

4. Parachute performance was measured with respect to a fixed attachment point on the test vehicle (one degree of freedom).

TABLE 2.2.1

SCHEDULE OF TESTS CONDUCTED ON PROGRAM

Test No.	Test Date	Test Parachute - Type	Parachute Nominal Diameter	Deployment Mach No.
1	27 Nov. 1962	Hemisflo -EHR-137A	6.77	1.100
2	13 Dec. 1962	Hyperflo -HY-140A	6.06	1.058
3	19 Dec. 1962	Hemisflo -EHR-137B	6.77	1.316
4	17 Jan. 1963	Conical Ribbon-20CR-150B	8.44	1.270
5	30 Jan. 1963	Hyperflo -HY-141B	6.06	1.302
6	8 Feb. 1963	Hemisflo -EHR-138B	5.54	1.295
7	13 Feb. 1963	Hemisflo -EHR-137C	6.77	1.465
8	19 Feb. 1963	Hemisflo -EHR-139B	4.12	1.288
9	25 Feb. 1963	Hyperflo -HY-143B	3.69	1.310
10	7 Mar. 1963	Conical Ribbon-20CR-150B-A1	8.44	1.337
11	11 Mar. 1963	Hyperflo -HY-141C	6.06	1.466
12	13 Mar. 1963	Hyperflo -HY-142B	4.95	1.308
13	18 Mar. 1963	Hyperflo -HY-143C	3.69	1.491
14	25 Mar. 1963	Hemisflo -EHR-137B-A1	6.77	-
15	10 Apr. 1963	Hyperflo -HY-144A	3.69	1.078
16	12 Apr. 1963	Hemisflo -EHR-137B-A1	6.77	1.314
17	16 Apr. 1963	Hyperflo -HY-142C	4.95	1.378
18	26 Apr. 1963	Hyperflo -HY-143B(Cluster)	3 at 3.69	1.355
19	30 Apr. 1963	Supersonic Guide Surface	2.0	-
20	2 May 1963	Conical Ribbon-20CR-150B-A2	8.44	1.340
21	6 May 1963	Hyperflo -HY-144B	3.69	1.336
22	8 May 1963	Supersonic Guide Surface	2.0	1.040
23	13 May 1963	Hyperflo -HY-145A	4.95	1.026
24	16 May 1963	Supersonic Guide Surface	2.0	1.300

5. Infinite mass - The mass of the test vehicle was so great in comparison to the parachutes being tested that little velocity change occurred during the deployment and inflation process.

2.3 PARACHUTES

As shown in the schedule of tests listed in Table 2.2.1, the majority of the tests conducted on the program were conducted with Hyperflo and Hemisflo type parachute configurations. Several tests were also conducted with a reefed 20 degree Conical Ribbon type parachute and with a Supersonic Guide Surface (cone-cup) type parachute configuration. The Hyperflo and Hemisflo type parachutes were each designed in three drag area ranges. The other two parachute types were designed for special purpose tests that were conducted on one primary design of each of the parachute types. The general types and configuration variations which were investigated are listed below. Drag areas indicated are based on average measured subsonic drag coefficients.

Hyperflo Type Parachutes

1. 6.06 foot dia. (D_o), 20 gore, $C_DA = 12$
2. 4.95 foot dia. (D_o), 16 gore, $C_DA = 8$
3. 3.69 foot dia. (D_o), 12 gore, $C_DA = 4.5$

Hemisflo Type Parachutes

1. 6.77 foot dia. (D_o), 20 gore, $C_DA = 15$
2. 5.54 foot dia. (D_o), 16 gore, $C_DA = 10$
3. 4.12 foot dia. (D_o), 16 gore, $C_DA = 5.5$

Conical Ribbon (20 degree) Type Parachute

1. 8.44 foot dia. (D_o), 16 gore, $C_DA = 28$

Supersonic Guide Surface Type Parachute

1. 2.0 foot dia. (D_p), 12 gore, $C_DA = 3.0$

The two smaller sizes of Hyperflo type parachutes (4.95 and 3.69 foot nominal diameter) were tested with both ribbon and mesh roof construction and the 3.69 foot nominal diameter Hyperflo type parachute was also tested in a triple cluster configuration on a single suspension system.

Complete descriptions of the various parachute configurations are presented in Section 5 of this report, together with test data obtained on the individual tests of these particular types.

2.4 DATA ACQUISITION

Standard test facility telemetry instrumentation was carried on the test vehicle to provide parachute drag force information and sled space/time measurements. From these data other pertinent information such as maximum force, opening shock factor, drag coefficient, velocity, Mach number and dynamic pressure were determined.

Measurement of parachute inflation characteristics, areas and stability were obtained from sled-borne high speed motion picture cameras.

Additional operational information was obtained with stationary high speed motion picture and sequence cameras and still photography as required.

Further description of the instrumentation employed on the test program appears in Section 6.

SECTION 3

CONCLUSIONS AND RECOMMENDATIONS

3.1 CONCLUSIONS

3.1.1 Hyperflo Type Parachute

Subsonic and low supersonic drag data, in general, fit in with the range of data obtained in free-flight and wind tunnel tests.

The decrease in drag coefficient in the low supersonic speed regime was somewhat compensated by an increase in the projected canopy area in this regime, giving the effect of essentially constant drag area. This is obviously a desirable characteristic and may be an indication of a good supersonic design.

The mesh roof designs were found to be less sensitive to dynamic pressure change than the ribbon roof parachutes. This was evident by their lower increase in projected area than the ribbon roof designs and by the fact that much flatter roof geometry was maintained under equivalent high "q" conditions. Comparison with similar parachutes in free-flight tests also indicates that flatter roofs were maintained in the high "q" tests than in the low "q" tests.

No scale effects were noted with the three sizes of Hyperflo type parachutes that were tested. Such effects may not become evident in the small range of parachute sizes that were tested, or, if scale effects were a factor they were lost in the normal range of data variation.

On the one test conducted with a cluster of three Hyperflo type parachutes, no advantage was noted by utilizing this technique. Two of the parachutes in the cluster were delayed in inflating and performance characteristics were not improved. This cluster configuration also requires more storage volume than a single parachute of equivalent drag area.

Hyperflo type parachute stability at high dynamic pressures was generally excellent. Except for transient conditions immediately after inflation, the average angular displacement was on the order of 2 to 3 degrees.

Data points for filling time and time to maximum opening force did not follow any pattern supported by either theoretical or empirical data.

Both the mesh roof and the ribbon roof Hyperflo type parachutes were found to be structurally capable of providing satisfactory decelerator performance at an operational combination of low supersonic velocity and dynamic pressures approaching 3000 psf.

3.1.2 Hemisflo Type Parachutes

No substantial variation in drag coefficient was noted from the subsonic to the low supersonic regime. The larger Hemisflo type parachutes did, however, show a substantial increase in projected canopy area in the same transitional speed regime. This area increase may have been largely responsible for the maintenance of the high drag coefficient. It was not established from this series of tests if this is characteristic of these parachutes in general at high dynamic pressure-operation and if so, to what extent the projected canopy area will continue to increase.

The Hemisflo type parachute exhibited exceptional stability in the high "q" environment. Average angular displacements were generally under 1 degree and transient excursions rarely exceeded 2 degrees.

Like the data for the Hyperflo type parachutes, the inflation parameters for the Hemisflo type parachutes, filling time and time to maximum opening force, showed variations too scattered to conform to theoretical or empirical expressions.

The program produced Hemisflo type parachute designs which were capable of satisfactory performance in the low supersonic-high dynamic pressure operational environment while maintaining complete structural integrity.

3 1.3 Conical Ribbon Type Parachute (Reefing Tests)

The limited tests conducted with a reefed 20 degree Conical Ribbon type parachute demonstrated that reefed parachute operation at low supersonic speeds is practical and reliable providing that the reefed to disreefed drag area relationship is maintained above a certain minimum. This is probably a function of parachute type and size.

Drag coefficients of the reefed configurations were found to be approximately proportional to the drag area ratios.

No tendency to collapse or otherwise malfunction was observed during disreef operation in the transonic speed regime.

3.1.4 Supersonic Guide Surface (Cone-Cup) Type Parachute

No satisfactory test was obtained with the Supersonic Guide Surface type parachute. This was primarily because of deployment and structural difficulties and because of limited testing conducted with this configuration.

3.1.5 Aerodynamic Heating

Canopy temperature measurements made on a number of the higher velocity tests indicated a significant temperature rise at the low supersonic - high dynamic pressure conditions. Although material densities were not considered in the application of the sensors, the temperature environment indications showed that a temperature rise on the order of 85 percent of the theoretical recovery temperature can be expected.

3.2 RECOMMENDATIONS

Specific recommendations which can be made in regard to the tests conducted on the reported program include the following:

Additional tests should be conducted on Hyperflo and Hemisflo type designs to ascertain causes and effects of the drag coefficient area relationships noted on the tests conducted during the program. These tests should be run at increasing dynamic pressures so that the limits of the interaction of these parameters can be determined.

Additional reefing tests should be conducted with various sizes and types of parachutes to determine minimum allowable reefed/disreefed drag area ratios as a function of parachute type and size.

The Supersonic Guide Surface type parachutes should be investigated further in the higher dynamic pressure environment. Proper structural design and utilization of special deployment system components and methods can undoubtedly develop this parachute type to a useable supersonic aerodynamic decelerator.

In general, it can be stated that the use of high speed parachute test sleds are recommended to establish and confirm parachute structural design criteria. The relatively good control of test conditions and the ease and reliability of data acquisition of sled type testing provides an ideal means of evaluating structural and aerodynamic design parameter compatabilities. The high speed parachute test sled is particularly appropriate for evaluation of parachute canopies, which in the future may be constructed of unconventional materials and perhaps fabricated utilizing new techniques.

SECTION 4

PARACHUTE PERFORMANCE CHARACTERISTICS

4.1 GENERAL

Four basic parachute types, Hyperflo, Hemisflo, Conical Ribbon and Supersonic Guide Surface (Cone-Cup), were investigated during the test program. Of the total of twenty-four test operations which were conducted, eleven of the tests were made with Hyperflo type parachute configurations, seven of the tests were made with Hemisflo type parachute configurations and three each were conducted with reefed Conical Ribbon and Supersonic Guide Surface type parachute configurations.

The following paragraphs of this section of the report presents a summary of the operational characteristics of each parachute type which was investigated and provides general design information and parachute performance characteristics of the configurations which were deployed and which operated successfully in the low supersonic velocity range of Mach 1.1 to Mach 1.5. Performance characteristics which were obtained included opening shock factors, inflated canopy areas, drag coefficients and angular displacements (stability). Values of these parameters for each parachute configuration which yielded conclusive characteristic information are presented in tabular form in the paragraphs where each configuration is discussed. Corresponding data are also included in these tables to show basic physical and geometric properties of the parachute designs.

Where possible, curves and data have been included to show the effects and relationships of the various geometric and aerodynamic parameters on the performance of the parachute configurations or systems as they were investigated during this program.

4.2 HYPERFLO TYPE PARACHUTES

Six configurations of Hyperflo type parachutes were tested in the eleven test runs conducted with this parachute type. Four of the configurations used on eight of the tests were with parachutes having solid (non-porous) inlet cones and typical ribbon type of roof construction. Two of the configurations used on three tests were with parachutes having similar inlet cone construction, but with Perlon mesh roofs.

Major physical and geometric properties and average performance characteristics for the parachutes of this configuration group which operated satisfactorily are presented in Table 4.2.1.

Nine of the eleven tests yielded performance information through the complete operating range from deployment at supersonic velocity to mid-subsonic. On the remaining two tests, one parachute suffered severe structural damage and failed, and the other rotated itself into a collapsed state from which it did not recover. Data of the individual tests conducted with all the Hyperflo configurations are presented in detail in Section 5.1 of the report.

Several trends were noticed that showed parametric variations with Mach number and/or dynamic pressure. The drag coefficient was significantly lower in the supersonic speed regime than in the subsonic. Figure 4.2.1 illustrates the variation of drag coefficient with Mach number, velocity and dynamic pressure. The average drag coefficient variation, indicated by the heavy solid line, is the numerical average of all test data except that of the Hyperflo Type HY-141C from Test No. 11. The data from this test varied significantly from that obtained on other tests in this configuration group and is of questionable reliability.

No significant difference in drag coefficient between the ribbon roof and the mesh roof configurations was indicated. The subsonic drag coefficient was essentially the same for both parachute designs (mesh roof and ribbon roof) and supersonic data points appear to be converging toward the average as Mach number increases. This, of course, is to be expected considering that the porosities of the two designs of this parachute type were nearly identical. No significance is attached to the fact that the data points for the mesh roof parachutes appear to indicate a more pronounced transition from the supersonic level to the subsonic level.

The variation of inflated or projected canopy areas as a function of Mach number, velocity and dynamic pressure, is shown in Figure 4.2.2. It is evident from this display that the projected canopy areas were significantly higher during supersonic operation than they were during subsonic operation. Also readily noticeable is the fact that the mesh roof parachute designs did not inflate to as large projected areas as their ribbon roof counterparts. In subsonic operation, the area ratios of all three sizes of ribbon roof parachutes averaged approximately 115 percent of their respective design projected areas. In supersonic operation, however, this ratio varied from an average of 118 percent for the small 3.69 foot diameter parachute to 127 percent for the large 6.06 foot diameter parachute with the middle parachute, a 4.95 foot diameter design, averaging about 124 percent. For the mesh roof designs, these ratios were much lower. The small size

TABLE 4.2.1

AVERAGE PERFORMANCE CHARACTERISTICS - HYPERFLO TYPE PARACHUTES

Hyperflo Type	HY-141	HY-142	HY-143	HY-144	HY-145
Roof Construction	Ribbon	Ribbon	Ribbon	Mesh	Mesh
No. of Gores	20	16	12	12	16
Nominal Diameter, D_o (Ft)	6.06	4.95	3.69	3.69	4.95
Nominal Area, S_o (Ft^2)	28.85	19.22	10.67	10.67	19.22
Total Porosity, λ_t (Percent)	14.00	14.84	14.58	13.32	14.50
Weight, Canopy and Lines (Lbs)	19.5-22.7	13.4-14.1	7.3-8.0	6.5-6.7	10.5
Drag Coefficient, C_{D_o}	.47/.44	.37/.42	.35/.42	.35/.43	-/.42
Opening Shock Factor (X)	1.36/1.45	1.30/1.15	1.42/1.15	1.52/1.24	-/1.04
Area, S_{p_i}, (Ft^2)	17.5/15.5	11.4/10.6	6.2/5.8	5.4/5.2	-/9.8
Stability, ϕ (Degrees)	-	1.5±1.0	1.7±0.5	1.2±0.7	1.0±0.5
Deployment Mach No. Range	1.30-1.47	1.31-1.38	1.31-1.49	1.08-1.34	1.03

Numbers Separated By Slant (/) Indicates (Supersonic/Subsonic) Values

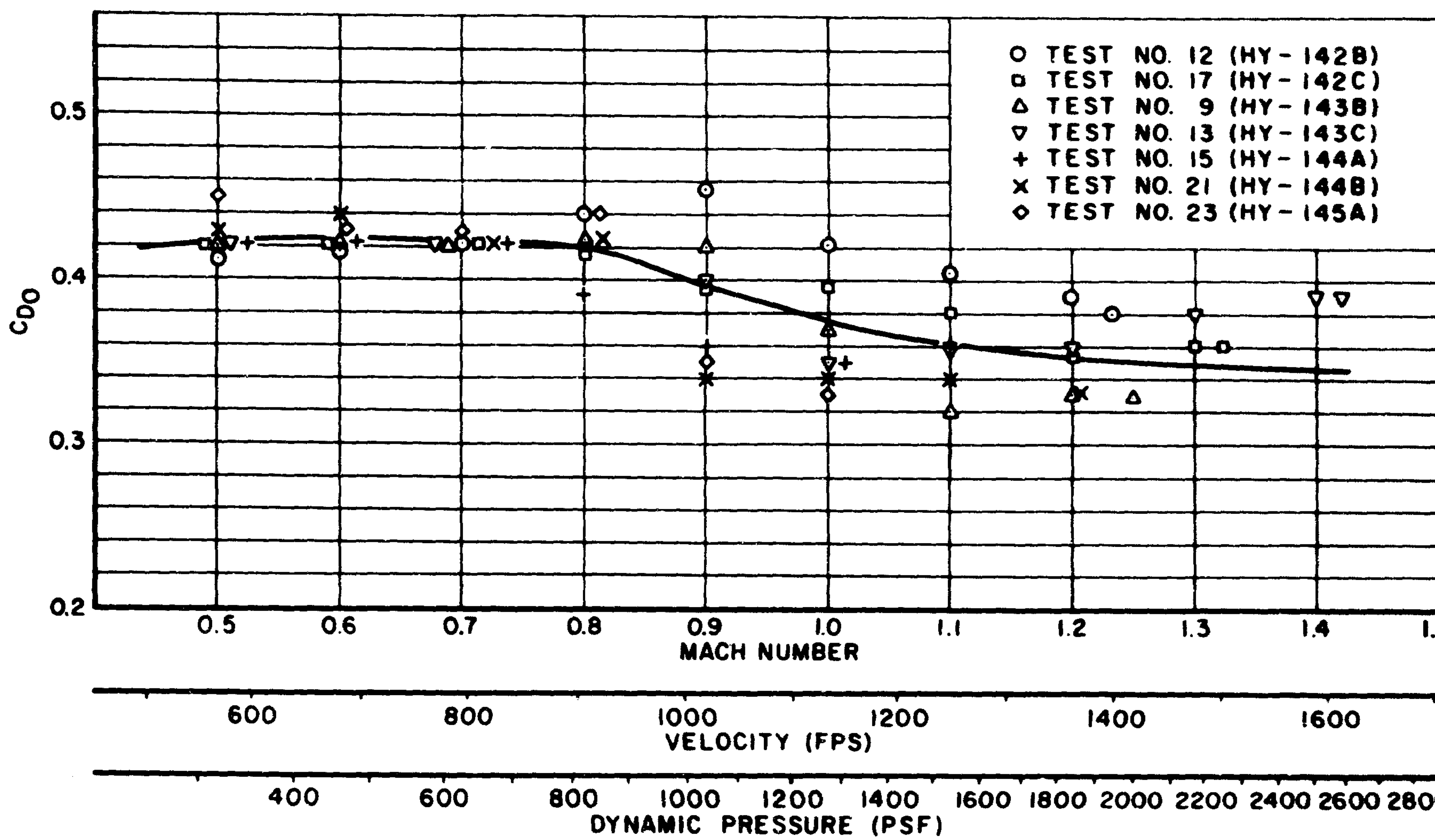

Figure 4.2.1. Variation of Drag Coefficient with Mach Number, Velocity and Dynamic Pressure - Hyperflo Type Parachutes

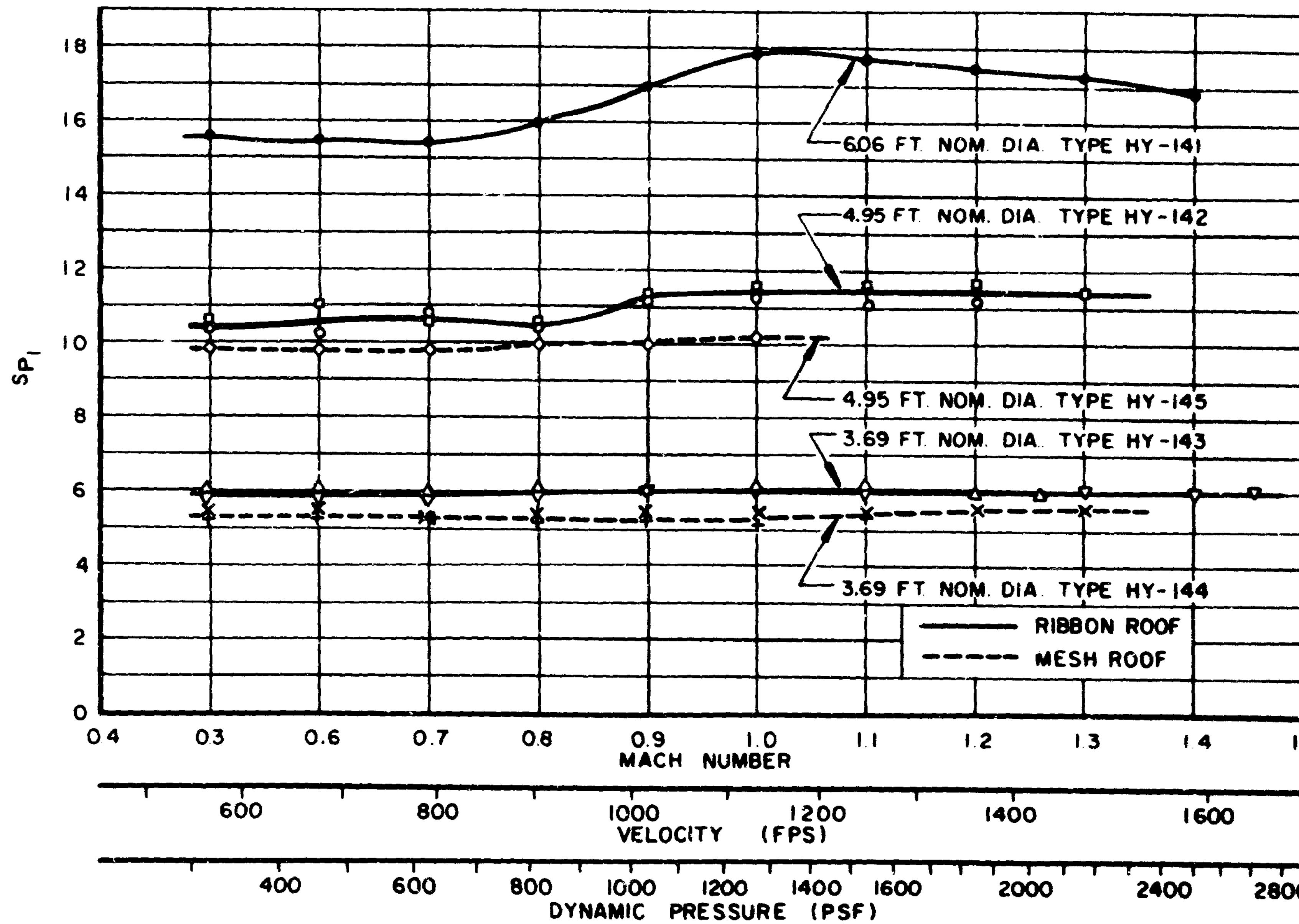

Figure 4.2.2. Variation of Projected Area with Mach Number, Velocity and Dynamic Pressure - Hyperflo Type Parachutes

parachute averaged 104 percent subsonically and 108 percent during supersonic operation. The medium size parachute provided only subsonic data and attained an area ratio of 107 percent.

Because total porosities of all the Hyperflo type parachutes were nearly identical, effects on performance parameters due to porosity variation could not be evaluated for these configurations.

Investigation of the inflation characteristics of the Hyperflo type parachutes provided data from which only generalized trends could be noted. Inflation time and time to maximum opening force showed tendencies to decrease with increasing deployment velocity, but data was generally scattered. The opening shock factor, (X), also exhibited large and seemingly random variations in magnitude. The average value of 1.40 for supersonic speed inflations resulted from a range of values from 1.16 to 1.66. Corresponding values for subsonic speed inflation ranged from 1.00 to 1.45 and averaged 1.20.

Stability of Hyperflo type parachutes was generally excellent. Average angular displacements were rarely over 2-3 degrees in steady state operation.

One test was conducted with a triple cluster of 3.69 foot nominal diameter Hyperflo Type HY-143B parachutes. No supersonic cluster data was obtained during the test because of a delay in the inflation of two of the three parachutes. After all three parachutes were inflated, however, subsonic performance was essentially the same as with single parachutes. Parachute separation in the cluster configuration during subsonic steady state operation was approximately 1.5 parachute projected diameters between apex positions of adjacent parachutes.

4.3 HEMISFLO TYPE PARACHUTES

Three basic configurations of Hemisflo type parachutes were used during the seven tests conducted with this type of parachute. Five of the tests were conducted with the 20 gore, 6.77 foot nominal diameter type EHR-137 configuration and one test each was conducted with a 5.54 foot nominal diameter type EHR-138 parachute and a 4.12 foot nominal diameter type EHR-139 parachute, both of which incorporated 16 gores.

Major physical and geometric properties and average performance characteristics for the parachutes of this configuration group which exhibited satisfactory operating characteristics are presented in Table 4.3.1.

TABLE 4.3.1

AVERAGE PERFORMANCE CHARACTERISTICS
HEMISFLO TYPE PARACHUTES

Hemisflo Type	EHR-137	EHR-138	EHR-139
No. of Gores	20	16	16
Nominal Diameter, D_o (ft)	6.77	5.54	4.12
Nominal Area, S_o (ft^2)	36.0	24.0	13.33
Total Porosity, λ_T(%)	27.28	25.70	25.19
Weight (Canopy and Lines) (lb)	14.3-23.4	13.9	10.1
Drag Coefficient, C_{D_o}	.41/.41	.44/.49	.41/-
Opening Shock Factor, X	1.18/1.20	1.32/1.19	1.36/-
Area S_{p_i} (ft^2)	18.8/17.8	-	6.0/
Stability, ø (degrees)	0.5 ± 0.5	-	1.0 ± 1.0
Deployment Mach No. Range	1.10 - 1.47	1.30	1.29

Numbers separated by slant (/), indicates (supersonic/subsonic) values.

Five of the seven tests provided performance information through the operating range from deployment velocities in the Mach 1.1 to Mach 1.5 range to the mid-subsonic region. One of these tests, No. 8, the only test with the Type EHR-139B parachute, provided only limited information because of the eventual collapse of the parachute due to rotation and line twist. On the two tests in which performance information was not obtained, one parachute was not deployed because of a rocket motor malfunction, and one parachute suffered structural failure of the suspension lines during inflation. Data of all the individual tests conducted with the Hemisflo type parachute configurations are presented in detail in Section 5.2. of this report.

In the investigation of parametric variations with respect to Mach number, velocity and dynamic pressure, one characteristic in particular was noted. As shown in Figure 4.3.1, the variation of drag coefficient does not show a transition and decrease with increasing Mach number. The average drag coefficient variation indicated by the heavy solid line is the average of all test data except that of the Hemisflo Type EHR-138B from Test No. 6 and is essentially constant over the range indicated. The reason for the divergence of the Test No. 6 data is not known but it is sufficiently different from all the other data that it is considered to be of questionable accuracy.

Total porosities of the parachutes were approximately the same, ranging between 25.19 and 27.28 percent. Because of this similarity, no noticeable effect on performance parameters would be expected and no evaluations for such effects are attempted.

The variation of inflated or projected canopy areas as a function of Mach number, velocity and dynamic pressure are shown in Figure 4.3.2 for the two parachute configurations for which this data was available. This information was not obtained on the one test conducted with the Hemisflo Type EHR-138B parachute.

For the largest Hemisflo type parachute, the Type EHR-137 configuration, a projected canopy area variation is noted. The canopy area increases with Mach number and appears to be essentially linear over the indicated range. At the low end of the subsonic speed range, the area ratio is approximately 125 percent of the design projected canopy area. At the supersonic end of the data, the ratio is on the order of 135 percent.

The limited data available on the small, 4.12 foot nominal diameter Hemisflo Type EHR 139B parachute indicated an area ratio variation from approximately 120-125 percent at subsonic velocity to approximately 115 percent supersonically.

Inflation behavior of the Hemisflo type parachute, like that of the Hyperflo type, did not produce data from which performance characteristics could be determined. General trends indicated, as would be expected, that inflation time and time to maximum opening force decreased with increasing deployment velocity. The opening shock factor (X) varied somewhat in the tests but no excessive variations were noted. The average value for supersonic speed inflation was 1.26 and resulted from a range of values of from 1.12 to 1.36. Corresponding subsonic values ranged from 1.12 to 1.26 and averaged 1.20. The small variation between supersonic and subsonic values are expected because of the similarities in the respective steady state drag characteristics of the parachute.

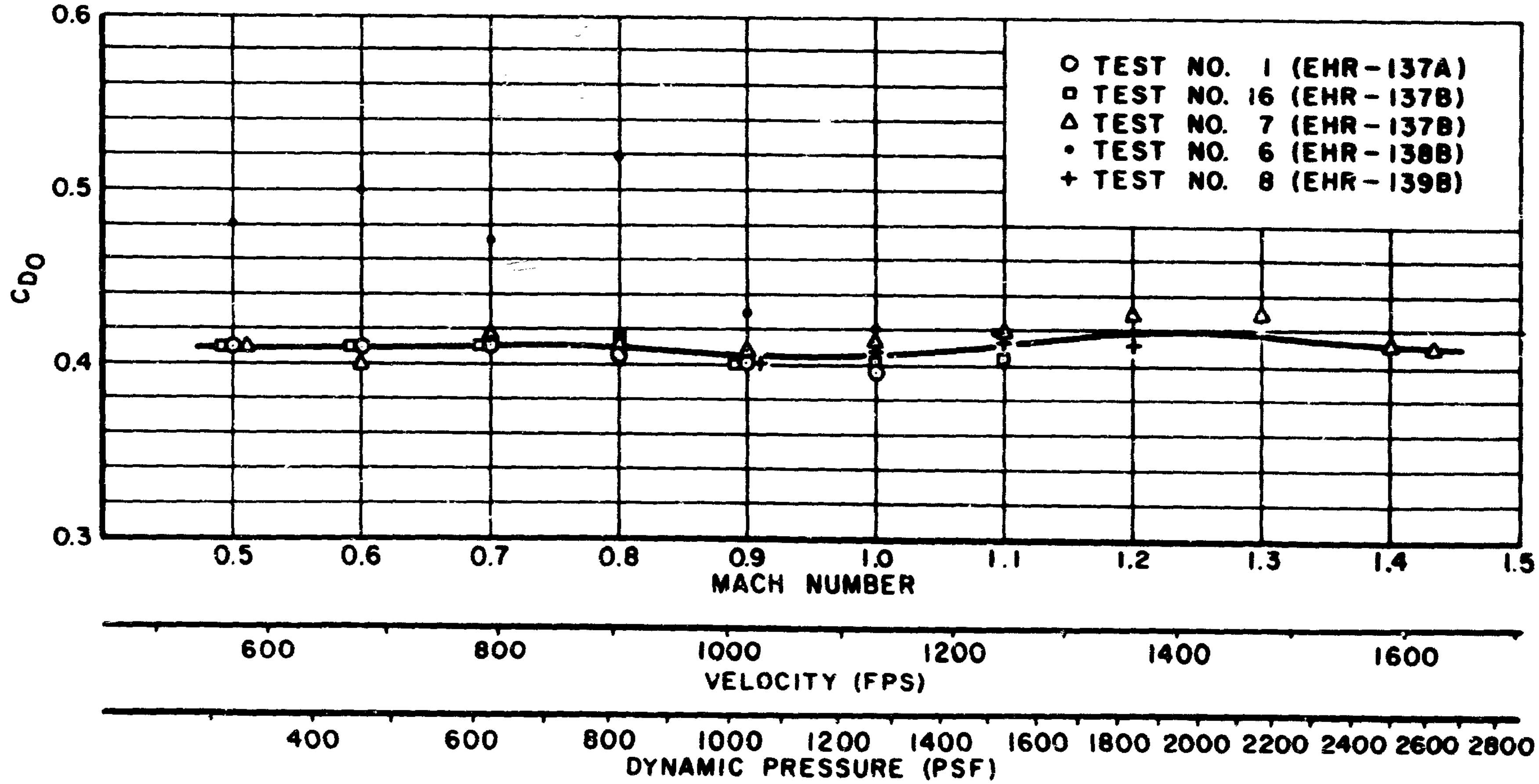

Figure 4.3.1. Variation of Drag Coefficient with Mach Number, Velocity and Dynamic Pressure - Hemisflo Type Parachutes

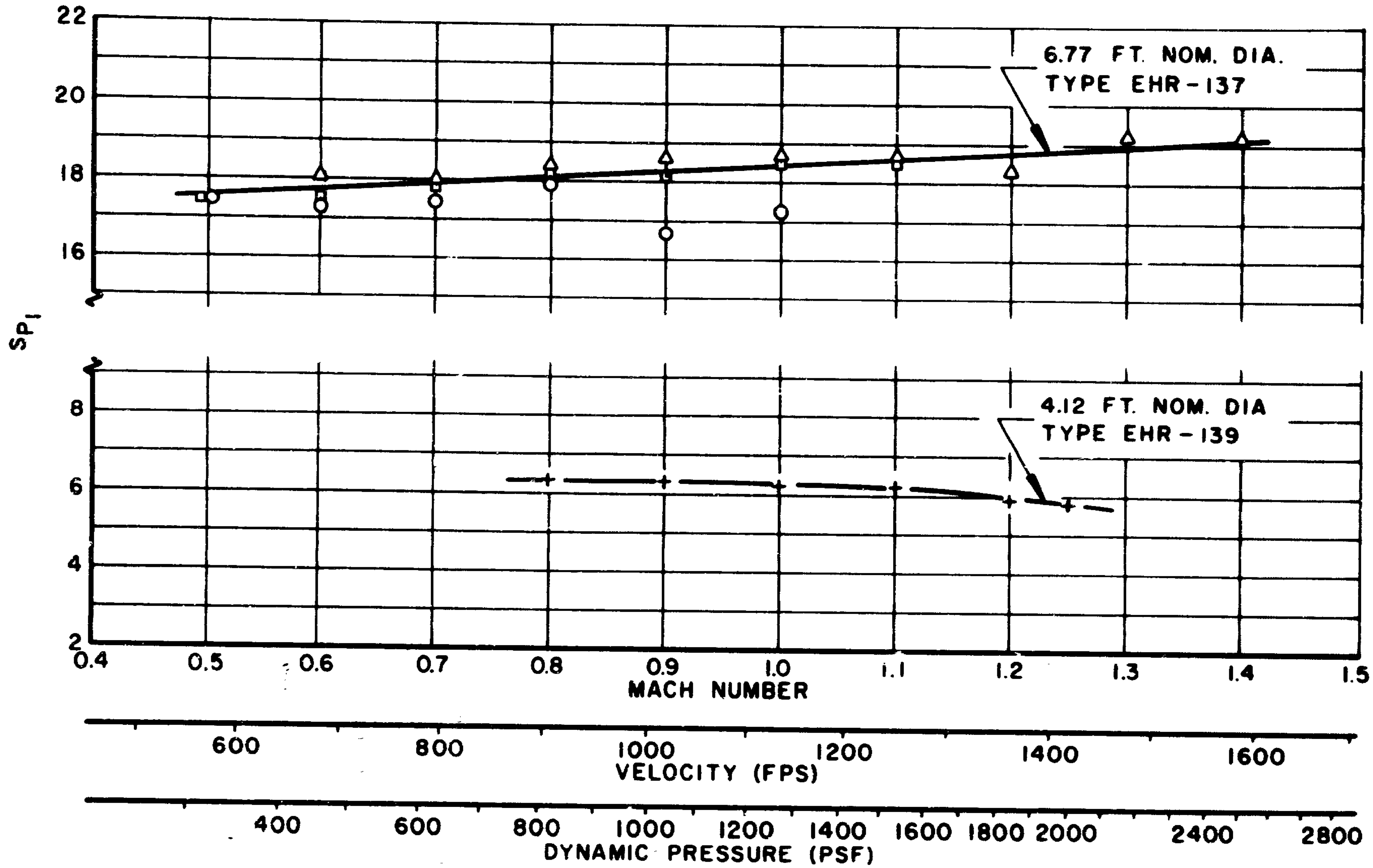

Figure 4.3.2. Variation of Projected Areas with Mach Number, Velocity and Dynamic Pressure - Hemisflo Type Parachutes

Excellent stability characteristics were noted on all tests of the Hemisflo type parachute. The average angular displacements were generally on the order of 0.5 to 1.0 degree and rarely had excursions that exceeded 2.0 degrees.

4.4 CONICAL RIBBON TYPE PARACHUTE (20 DEGREE)

One basic configuration of Conical Ribbon type parachute was tested during the program to study reefing and disreefing characteristics of this type of parachute at supersonic speeds. This configuration was an 8.44 foot nominal diameter, 20 degree Type 20CR150B design having 16 gores and a total porosity of 24.17 percent.

Of the three tests conducted with the reefed Conical Ribbon type parachute only one test provided complete performance information. This was a Mach 1.3 deployment with a one second reefing time on a parachute that was reefed to 30 percent of the subsonic canopy drag area. One test, in which the parachute was permanently reefed to 20 percent of the subsonic canopy drag area, provided data until the parachute collapsed. The other test, also with a 20 percent permanently reefed parachute, resulted in no data because of structural failure of the parachute during inflation. More detailed information on these individual tests with the reefed 20 degree Conical Ribbon parachutes can be found in Section 5.3 of this report.

Average performance characteristics and pertinent physical and geometric properties of the parachutes of this configuration are presented in Table 4.4.1. Figure 4.4.1 shows drag coefficient and projected canopy areas of the 20 and 30 percent reefed parachutes and of the disreefed parachute.

The drag coefficients for both of the reefed parachutes were approximately the magnitudes that would be expected for 20 and 30 percent reefing ratios. The reason for the collapse of the parachute that was reefed to 20 percent is not known, but it is possible that its geometric properties, i.e., porosity, distribution of porosity and reefed inlet shape, were such that a critical opening condition existed. This obviously was not the case with the parachute reefed to 30 percent of the subsonic drag area.

The reefed opening shock factors were quite similar for the two tests, being 1.10 and 1.20 for the 20 percent and 30 percent reefed parachutes, respectively. The opening shock factor during disreefing of the 30 percent reefed parachute, the only one on which a disreefing capability was used, was under 1.0

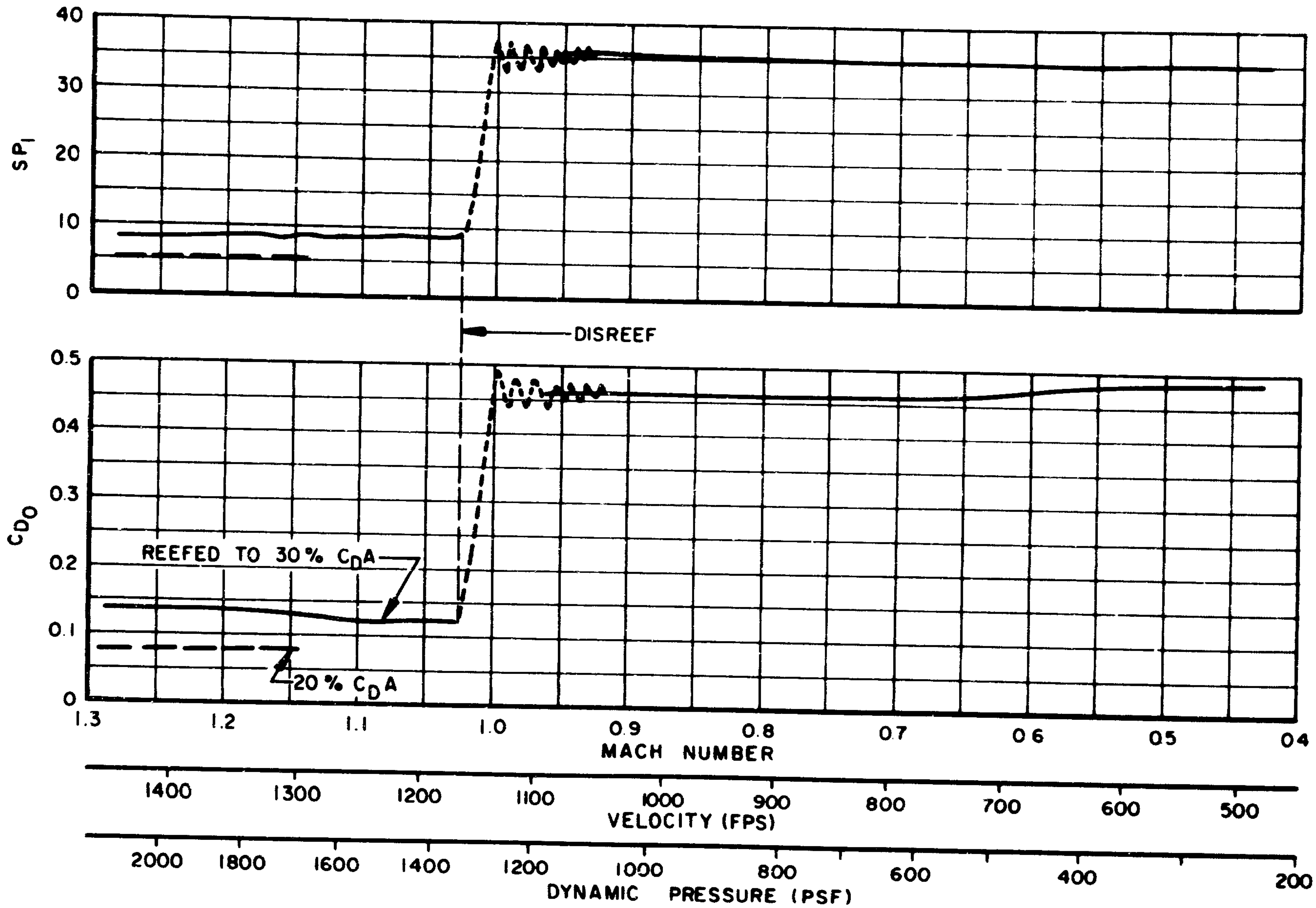

Figure 4.4.1. Variation of Drag Coefficient and Projected Area of Reefed and Disreefed 20 Degree Conical Ribbon Type Parachute

TABLE 4.4.1

AVERAGE PERFORMANCE CHARACTERISTICS
20 DEGREE CONICAL RIBBON TYPE PARACHUTE
(REEFED TO 30 PERCENT OF SUBSONIC CANOPY DRAG AREA)

No. of Gores	16	
Nominal Diameter, D_o (ft)	8.44	
Nominal Area, S_o (ft^2)	56.0	
Total Porosity, λ_T (%)	24.17	
Weight (canopy and lines) (lb)	18.0	
Performance	Reefed	Disreefed
Drag Coefficient, C_{D_o}	.14	.48
Opening Shock Factor, X	1.20	0.97
Area, S_{p_1} (ft^2)	8.5	35.5
Stability, ϕ (degrees)	4.0 ± 1.0	4.5 ± 1.0
Mach No.	1.34	1.01

4.5 SUPERSONIC GUIDE SURFACE (CONE-CUP) TYPE PARACHUTE

Of the three tests conducted with the one configuration of the Supersonic Guide Surface type parachute, a two foot projected diameter, 12 gore design, only one test provided limited performance data. In the other two tests, one parachute was not deployed and one parachute failed structurally during inflation.

In the Mach 1.1 test in which data was obtained, both drag coefficient and projected canopy area varied widely and irregularly throughout the test. On the basis of average steady state forces and design projected area of the parachute, the subsonic drag coefficient ranged from 0.3 to 0.8, the latter figure being obtained near the end of the test when the canopy area was becoming fairly steady and averaging about 80-90 percent inflation.

Over-all parachute stability was fair after steady state operation had been attained. Although there was considerable interaction between the cone and the cup portion of the canopy, the average angular displacement of the system varied between 4 and 6 degrees.

Additional information on the individual tests with the Supersonic Guide Surface type parachute is presented in Section 5.4 of this report.

4.6 TEMPERATURE ENVIRONMENT

A number of the parachutes which were tested had temperature detectors applied to various points of the parachute canopy in an attempt to determine the temperature environment and the effects, of any, on the canopy material.

Two types of temperature sensors were tried. The most frequently used was the Pyrodyne temp-plate, a small adhesive backed strip that contained a number of calibrated heat sensitive elements, hermetically sealed in laminated high temperature-resistant plastic. Temperature indications with these devices were obtained by noting change, from white to black, of the sensing elements. In the initial tests with these devices, it was found that the adhesive bond on some of the relatively rough parachute materials was not sufficient to keep the detector from being blown off. Subsequent tests with this unit were therefore made with the detector secured under a small piece of light ribbon material which had been sewn to the parachute. The other type of temperature detector that was used on a limited number of tests was the Curtiss-Wright Detecto-Temp crayons. These were applied in typical crayola fashion on various components of the parachute and indicated temperature level by color change.

Figure 4.6.1 shows the temperatures (°R) attained as a function of test Mach number and indicates by symbolic presentation the temperature sensor location on the parachute canopy.

Although the data does not show a distinct and progressive temperature rise between the Mach 1.3 and Mach 1.5 test conditions, it does substantiate that a significant temperature rise occurs in this general velocity range. Except for the data from Test No. 7, all of the test points, representative of those from which a full temperature indication was obtained, fall within a range that varied from 83 to 92 percent of the calculated recovery temperature as defined by:

$$T_R = T_\infty (1 + 0.2\, r\, M^2)$$

where r is the turbulent recovery factor = 0.9.

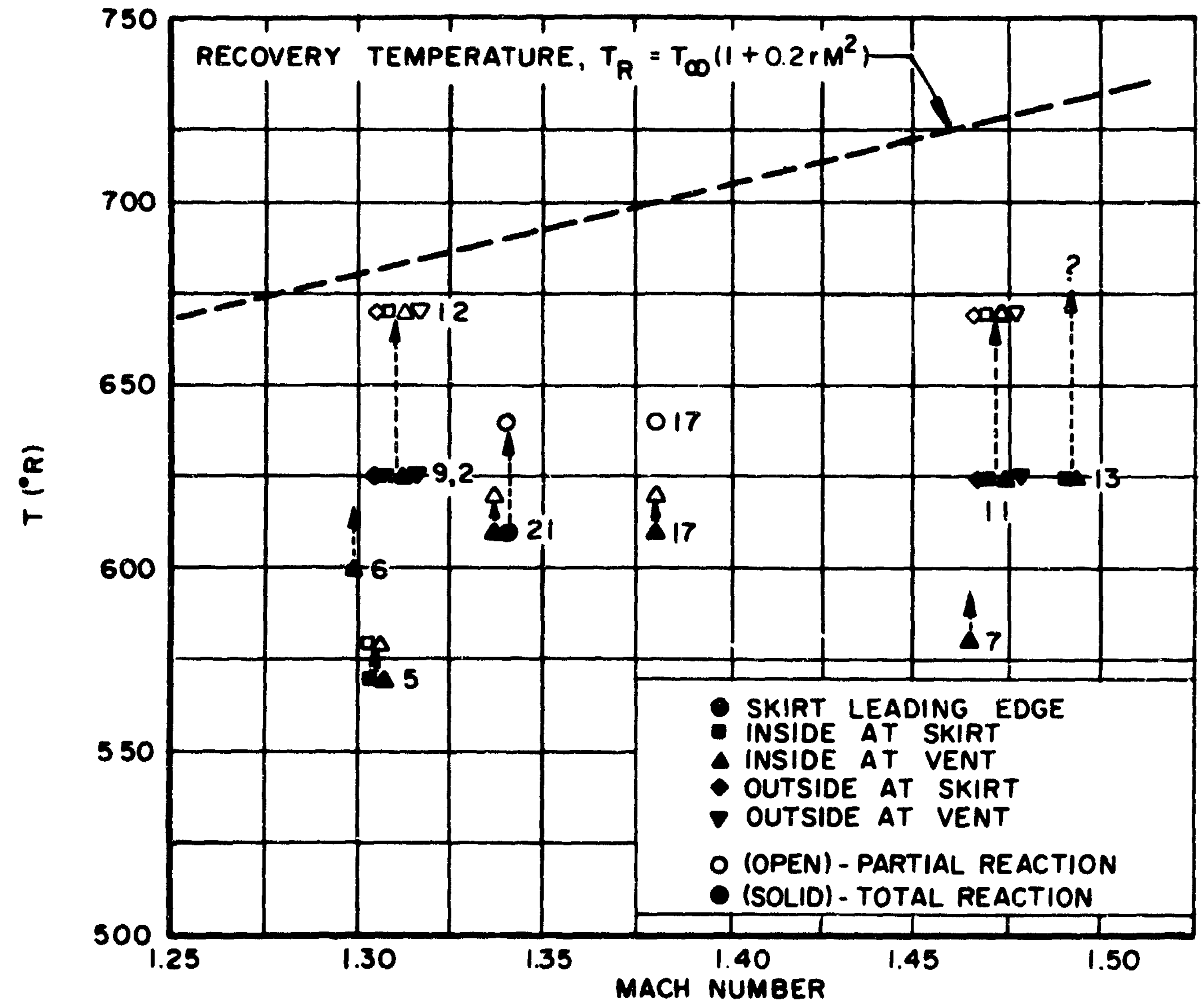

Figure 4.6.1. Temperatures Measured in Test Parachute Canopies as a Function of Deployment Mach Number

No explanation can be given for the exception indicated by Test No. 7.

In the tests where some of the heat sensitive elements indicated partial reaction to the temperature environment, it is probably safe to assume that the ultimate total temperature would have been somewhere between the two data points representing total and partial reaction.

There was no evidence of any significant temperature variation which could be attributed to sensor location on the parachute canopy. On the tests where sensors were placed both inside and outside, at skirt and vent locations on the canopy, the same total exposures were indicated.

SECTION 5

TEST RESULTS

5.1 HYPERFLO TYPE PARACHUTES

5.1.1 General

The Hyperflo type parachute is a shaped parachute with a design geometric shape like an inverted right regular conical frustum. The low porosity, conical inlet region has a cone angle limited to that corresponding to the local flow direction ahead of the plane of the canopy inlet. A relatively high porosity roof, of ribbon or mesh construction, gives the parachute a low exit-to-inlet area ratio and a low total porosity.

Figure 5.1.1 illustrates a schematic view of a typical Hyperflo parachute.

5.1.2 Test Program

Eleven tests were conducted with six configurations of Hyperflo type parachutes during the program. Eight of these tests were with parachutes having ribbon type of roof construction and three tests were with parachutes constructed with mesh roofs. Among the ribbon roof configurations tested, three tests were conducted with 6.06 foot nominal diameter, 20 gore type HY-140 and HY-141 designs, two tests each were made with 4.95 foot, 16 gore type HY-142 and 3.69 foot, 12 gore type HY-143 designs, and one test was conducted with the type HY-143 parachute in triple clustered configuration. Mesh roof configurations which were tested consisted of the types HY-144 and HY-145, the mesh roof equivalents of the HY-143 and HY-142, respectively. The type HY-144 was used in two tests and the type HY-145 was tested once.

Deployment velocities on these tests ranged from Mach number 1.03 to Mach number 1.49, with dynamic pressure equivalents of 1350 to 2840 psf.

All of the Hyperflo type parachutes were geometrically identical and total porosities of the designs varied only between 13.3 and 16.3 percent.

Major dimensional details and materials used in fabrication of the parachutes are listed in Table 5.1.1. A general list of materials and related material specifications are tabulated in Table 5.1.2.

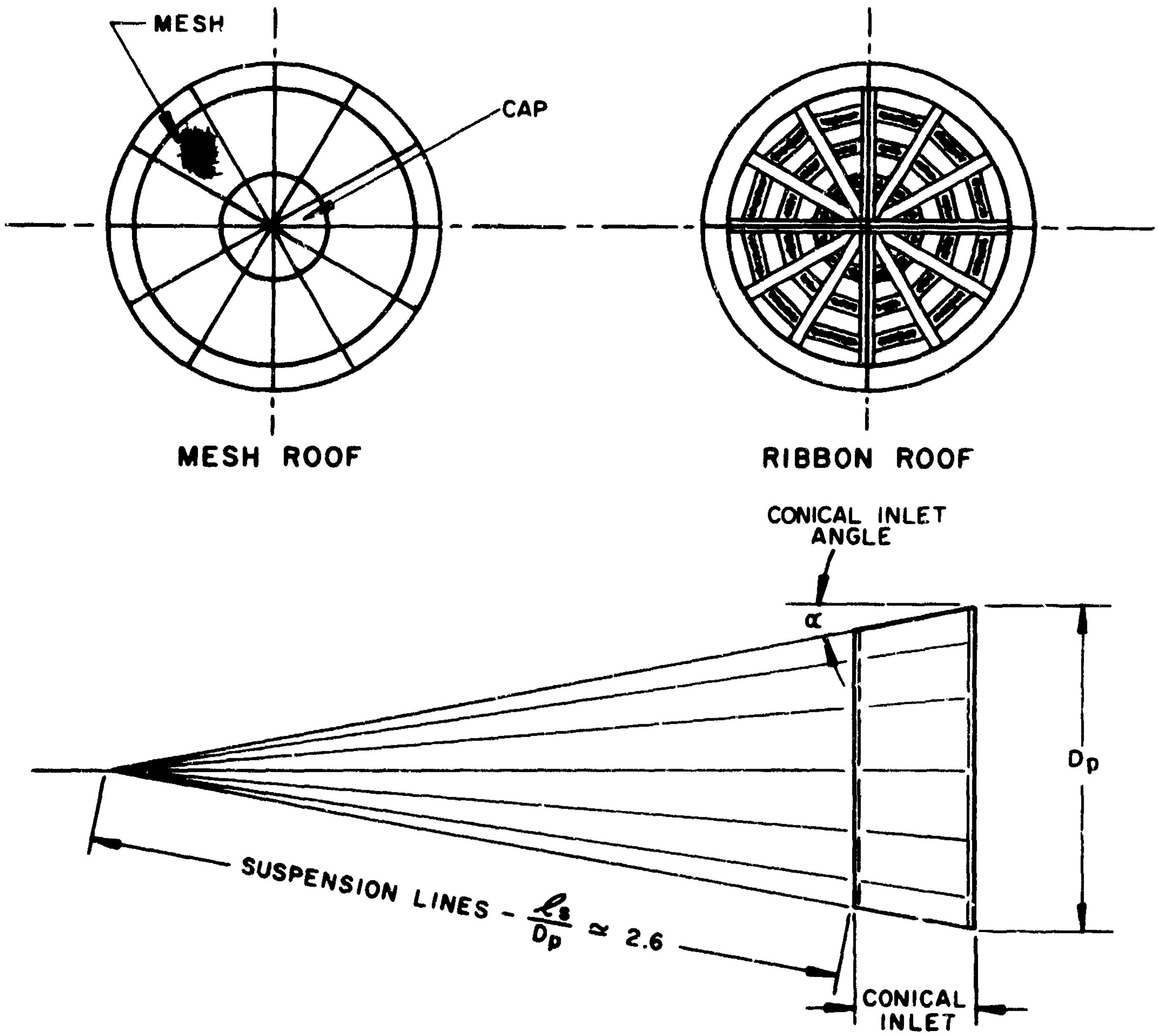

Figure 5.1.1. Typical Hyperflo Type Parachute

TABLE 5.1.1

PHYSICAL DETAILS AND DIMENSIONS OF HYPERFLO TYPE PARACHUTES

Hyperflo Type	HY-140A	HY-141B	HY-141C	HY-142B	HY-142C	HY-143B	HY-143C	HY-144A	HY-144B	HY-145A
Nominal Diameter, D_o (Ft)	6.06	6.06	6.06	4.95	4.95	3.69	3.69	3.69	3.69	4.95
Canopy Area, S_o (Ft^2)	28.84	28.84	28.84	19.22	19.22	10.67	10.67	10.67	10.67	19.22
Total Porosity, λ_t (Percent)	16.30	15.10	14.00	14.84	14.84	14.58	14.58	14.30	13.32	14.50
No. of Gores and Suspension Lines	20	20	20	16	16	12	12	12	12	16
Suspension Line Length (Ft)	10.85	10.85	10.85	8.86	8.86	6.60	6.60	6.60	6.60	8.86
Suspension Line Material	1 x 3000	1 x 6000	1 x 6000	1 x 6000	1 x 6000	1 x 6000	1 x 6000	1 x 3000	1 x 3000	1 x 3000
Roof Construction	Ribbon	Ribbon	Ribbon	Ribbon	Ribbon	Ribbon	Ribbon	Mesh	Mesh	Mesh
Horizontal Ribbon Material	2 x 2000	1 x 1000	1 x 2400	1 x 1000	1 x 2400	9/16x500	9/16x500	-	-	-
Vertical Ribbon Material (2 Ply)	9/16x500	1/2x250	9/16x500	9/16x500	9/16x500	1/2x250	1/2x250	1/2x250	1/2x250	1/2x250
Radial Band Material	1 x 1000	1 1/4x650	1 1/4x650	1 1/4x650	1 1/4x650	1 1/4x650	1 1/4x650	1 x 525	1 x 525	1 x 525
Mesh Material	-	-	-	-	-	-	-	Perlon	Perlon	Perlon
Concentric Roof Reinf. Material	-	-	-	-	-	-	6-9/16x500	-	1-9/16x500	-
Cone Material	3 x 1800 5 x 3000	2 x 2000	2 x 4000	600 (III)	600 (III)	600 (III)	600 (III)	600 (III)	600 (III)	600 (III)
Concentric Cone Reinf. Material	-	-	-	2-1x4500	2-1x4500	1 x 4500	1 x 4500	1 x 4500	1 x 4500	2-1x4500
Weight, Canopy and Lines (Lbs)	14.4	19.5	22.7	13.5	14.1	7.3	8.0	6.5	6.7	10.5
Cook T-CD Specification Number	596-8782	596-8987	596-8987A	596-9103	596-9103A	596-8990	596-8990A	596-9021	596-9021A	596-9027
Used on Test Number	2	5	11	12	17	9, 18	13	15	21	23

TABLE 5.1.2

MATERIALS USED IN HYPERFLO TYPE PARACHUTE

PART	MATERIAL	SIZE-STRENGTH	SPECIFICATION
Cone Material	Webbing, Nylon Webbing, Nylon Ribbon, Nylon Ribbon, Nylon Cloth, Nylon	3 In.-1800 Lb. 5 In.-3000 Lb. 2 In.-2000 Lb. 2 In.-4000 Lb. 600 Lb/In.	MIL-W-4088 (IV) MIL-W-4088 (V) MIL-R-5608 (EIV) MIL-R-5608 (EVI) MIL-C-8021A (III)
Horizontal Ribbon Material In Roof	Ribbon, Nylon Tape, Nylon Webbing, Nylon Webbing, Nylon	2 In.-2000 Lb. 1 In.-1000 Lb. 1 In.-2400 Lb. 9/16 In.-500 Lb.	MIL-R-5608 (EIV) MIL-T-5038 (IV) MIL-W-4088 (XI) MIL-W-4088 (I)
Vertical Ribbon Material In Roof	Webbing, Nylon Tape, Nylon	9/16 In.-500 Lb. 1/2 In.-250 Lb.	MIL-W-4088 (I) MIL-T-5038 (III)
Radial Band Material	Tape, Nylon Ribbon, Nylon Tape, Nylon	1 In.-1000 Lb. 1 1/4 In.-650 Lb. 1 In.-525 Lb.	MIL-T-5038 (IV) MIL-R-5608 (EI) MIL-T-5038 (III)
Mesh Material In Roof	Perlon 25/2/280	85 Lb/In.	-
Concentric Roof Reinf.	Webbing, Nylon	9/16 In.-500 Lb.	MIL-W-4088 (I)
Concentric Cone Reinf.	Webbing, Nylon	1 In.-4500 Lb.	MIL-W-4088 (XXV)
Suspension Lines	Webbing, Nylon Webbing, Nylon	1 In.-3000 Lb. 1 In.-6000 Lb.	MIL-W-5625 MIL-W-4088 (XVIII)
Thread	Thread, Nylon	Size E, F, FF 3 Cord, 5 Cord	MIL-T-7807 (I)

5.1.3 Parachute Performance

Hyperflo type parachute performance summary data for the six parachute configurations used in 11 test runs are presented in Table 5.1.3.

Performance details, and summary curves showing performance characteristics, of the parachutes in the tests of each Hyperflo type parachute configuration group are presented in the following paragraphs.

5.1.3.1 Hyperflo Type HY-140 Parachute

The Hyperflo Type HY-140A parachute was a 6.06 foot nominal diameter, 20 gore ribbon roof design having a total porosity of 16.3 percent.

Only one test, No. 2, was conducted with this configuration. This was a M 1.058 deployment and resulted in failure in the ribbon roof portion of the canopy. Precisely when and how the failure occurred could not be determined because of the absence of usable film data; however, inspection of the parachute at the end of the test revealed that the damage to the roof portion of the canopy had progressed during the test run to a state of total destruction.

TABLE 5.1.2

5.1.3.2 Hyperflo Type HY-141 Parachute

The Hyperflo Type HY-141, a modified version of the type HY-140 design, was like the type HY-140, a 6.06 foot nominal diameter parachute of 20 gore construction. Two strength variations of this parachute were produced; the type HY-141B, a Mach 1.3 design, and the type HY-141C, a Mach 1.5 design. Two tests, Numbers 5 and 11, were conducted with these parachutes. The parachute in Test No. 5, a Hyperflo Type HY-141B, was deployed at Mach number 1.302 and a dynamic pressure of 2205 psf. In the initial second of operation, this test appeared to be progressing normally. After about one second of operation, the parachute started to rotate and twist the lines and at approximately 3.0 seconds, the parachute started to collapse. Recovery from this collapsed state did not occur during the remainder of the test. Figure 5.1.2 shows this parachute in operation in the early portion of the test.

On Test No. 11, the Hyperflo Type HY-141C parachute was deployed at Mach 1.466 and a dynamic pressure of 2723 psf. Figure 5.1.3 shows this parachute in operation shortly after deployment and inflation. Performance curves for this test are shown in Figure 5.1.4.

TABLE 5.1.3

PERFORMANCE SUMMARY DATA - HYPERFLO TYPE PARACHUTES

Parachute Type Number		HY-140A	HY-141B	HY-141C	HY-142B	HY-142C	HY-143B	HY-143C	HY-143B Cluster	HY-144A	HY-144B	HY-145A
Test Number		2	5	11	12	17	9	13	18	15	21	23
Velocity, V_s (Ft/Sec)		1164	1436	1626	1451	1592	1469	1653	1524	1219	1510	1169
Mach Number, M		1.058	1.302	1.466	1.308	1.378	1.310	1.491	1.355	1.078	1.336	1.026
Dynamic Pressure, q (Lb/Ft^2)		1367	2205	2723	2200	2435	2205	2839	2346	1482	2300	1351
Deployment Time, t_d (Sec)		0.232	0.214	0.229	0.232	0.202	0.183	0.178	0.149	0.213	0.186	0.230
Time To Max. Opening Force, t_{s_o} (Sec)		-	0.080	0.057	0.158	0.109	0.062	0.085	0.142	0.075	0.188	0.094
Snatch Force, F_s (Lbs)		-	23,000	15,340	15,072	25,020	17,575	21,300	45,000	11,337	12,768	12,700
Maximum Opening Force, F_o (Lbs)		-	35,600	51,330	18,768	24,210	12,400	13,600	16,100*	9,443	11,571	11,195
Avg. Drag Coefficient, C_{D_o}		-	-	.47/.44	.38/.42	.36/.42	.33/.43	.36/.42	-/.42	.36/.43	.34/.43	-/.42
Opening Shock Factor, X		-	-	1.36/1.45	1.16/1.05	1.44/1.24	1.60/1.23	1.25/1.07	-	1.66/1.39	1.38/1.09	-/1.04
Area, S_p (Sq. Ft.)		-	-	17.5/15.6	11.3/10.5	11.5/10.7	6.2/5.9	6.2/5.7	-/17.0	5.4/5.2	5.5/5.4	-/9.8
Stability, ϕ (Degrees)		-	-	8.0±2.0	1.5±1.0	1.5±1.0	6.0±2.0	1.7±0.5	1.0±0.8	0.5±0.5	2.0±0.8	1.0±0.5
Parachute Damage	Canopy	Severe All Roof Panels	None	Strain At Line Attach	None	None	None	None	None	Minor Roof Damage	Minor Roof Damage	Minor Roof Damage
	Lines	None	None	One Line Severed 4.0 ft. From Canopy	None	None	None	None	None	None	None	None

Numbers Separated By Slant (/), Indicates (Supersonic/Subsonic) Values; * See Text

Figure 5.1.2. Hyperflo Type HY-141B Parachute in Operation on Test No. 5

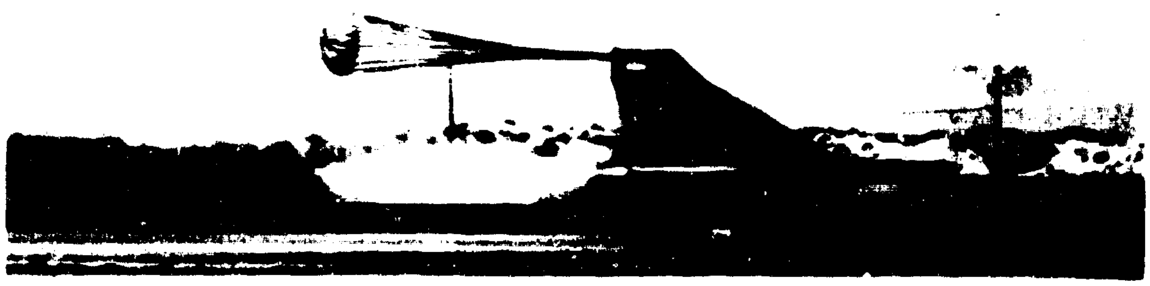

Figure 5.1.3. Hyperflo Type HY-141C Parachute in Operation on Test No. 11

The average supersonic drag coefficient of approximately 0.47 as recorded during this test was somewhat higher than that obtained on other tests of the Hyperflo type parachute. Being higher than the average subsonic value of 0.44, it was in fact, a reverse of the indicated trend for this parachute type, as compared to other tests in this series. This should not necessarily suggest that these data are therefore erroneous. There is information to be found in the steady state inflation characteristics of this parachute that seems to verify the trend toward the higher drag coefficient in the supersonic region. The instantaneous areas, as measured from photographic data, are on the order of 17-18 square feet in the supersonic speed region while the average in the subsonic speed region is more like 15.5 square feet. Although this area difference is not sufficient to account for all of the deviation from the expected supersonic drag coefficient, it is the only apparent parameter from which some substantiation can be obtained.

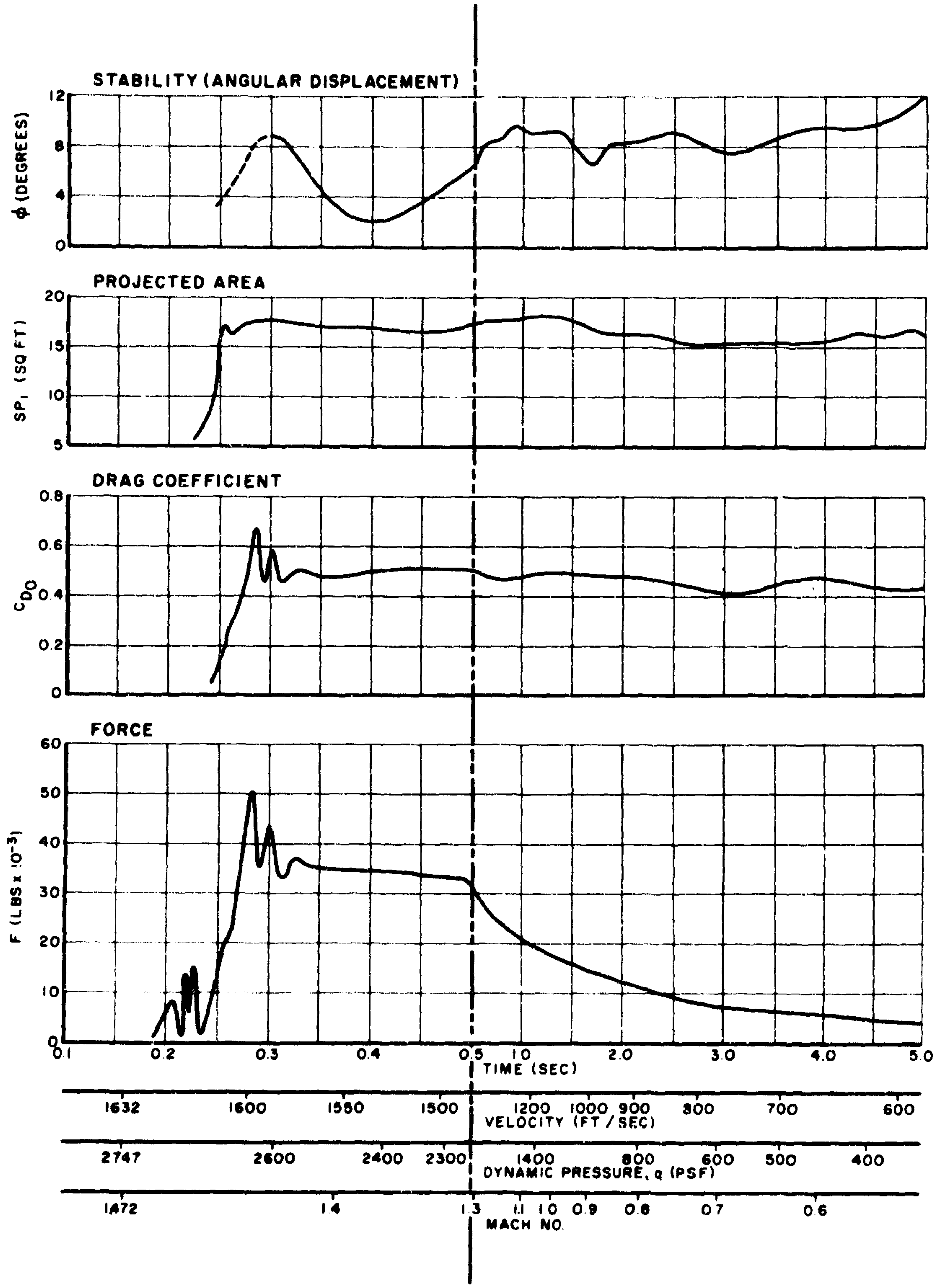

Figure 5.1.4. Performance Curves - Hyperflo Type HY-141C Parachute, Test No. 11

There is also information on the stability of this parachute which is not apparent from the performance curves in Figure 5. 1. 4. The initial impression is that stability was, in general, rather poor. It was in fact quite good, even though one suspension line was severed near the canopy at or near the time of maximum parachute opening force. This caused the parachute to become sufficiently unsymmetrical to induce a slow circular drift but with little or no oscillatory motion. So although a rather large average angular oscillation is indicated in the performance curves, it is not truly indicative of the stability of this parachute design.

Generally, the Mach 1. 5 Hyperflo Type HY-141C parachute design exhibited good performance characteristics.

5. 1. 3. 3 Hyperflo Type HY-142 Parachute

The Hyperflo Type HY-142 parachute was a 4. 95 foot nominal diameter, 16 gore ribbon roof design having a total porosity of 14. 84 percent. Two strength variations of this parachute were produced for the two tests conducted with this configuration. The type HY-142B, a Mach 1. 3 design, was used in Test No. 12 and the Type HY-142C, a Mach 1. 5 design, was used in Test No. 17.

Good deployments and inflations were obtained during both tests.

The parachute on Test No. 12 was deployed at a Mach number of 1. 308 and a dynamic pressure of 2200 psf. This parachute is shown in operation in the photograph in Figure 5. 1. 5.

On Test No. 17, a scheduled Mach 1. 5 test, a rocket motor malfunction caused a reduction in deployment velocity to Mach number 1. 378 with a corresponding deployment dynamic pressure of 2435 psf. Although this malfunction prevented the acquisition of the higher velocity data on this parachute, sufficient information was obtained to provide both supersonic and subsonic data points.

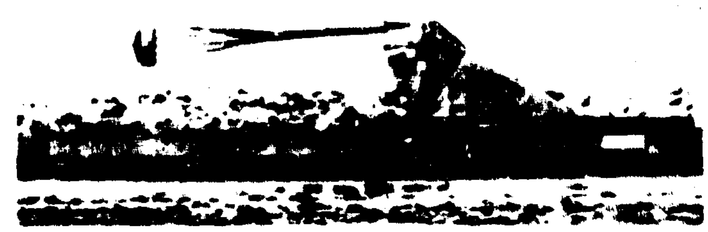

Figure 5. 1. 5. Hyperflo Type HY-142B Parachute in Operation on Test No. 12

Performance curves for these two tests are shown in the graphs in Figures 5.1.6 and 5.1.7. Average performance characteristics of the two Hyperflo Type HY-142 parachutes tested in the program are given in Table 5.1.4.

TABLE 5.1.4

AVERAGE PERFORMANCE CHARACTERISTICS
HYPERFLO TYPE HY-142 PARACHUTES

Test No.	Deploy. Mach No.	C_{D_o}	X	S_{P_1}	ϕ
12	1.308	.38/.42	1.16/1.05	11.3/10.5	1.5 ± 1.0
17	1.378	.36/.42	1.44/1.24	11.5/10.7	1.5 ± 1.0
Average	-	.37/.42	1.30/1.15	11.4/10.6	1.5 ± 1.0

(supersonic/subsonic)

Average supersonic drag coefficients of 0.38 and 0.36 were recorded on the two tests. Subsonic drag coefficients averaged 0.42 on both tests. These averages were without significant variation throughout the steady state portions of each test and appear to be quite consistent with values obtained in other tests in the series. The opening shock factors varied somewhat on the two tests. Both, however, were within respective maximum and minimum ranges experienced during this test series. Steady state inflation characteristics were nearly identical in both tests. The average inflated areas varied between 11.0 and 12.0 square feet in the supersonic speed regimes to approximately 10.0 - 11.0 square feet in subsonic operation. These represent area ratios, based on the design projected area, of approximately 130 percent and 120 percent, respectively. Similar stability characteristics were also exhibited by the parachutes on these two tests. Sufficient time is not available during supersonic operation to obtain stabilized oscillation characteristics, and the parachutes on both tests reacted with rather violent oscillatory motions during transition from supersonic to subsonic velocities. Average steady state subsonic stability was good on both tests with average oscillations not exceeding 3.5 degrees.

No structural damage was incurred to the test parachutes during either test.

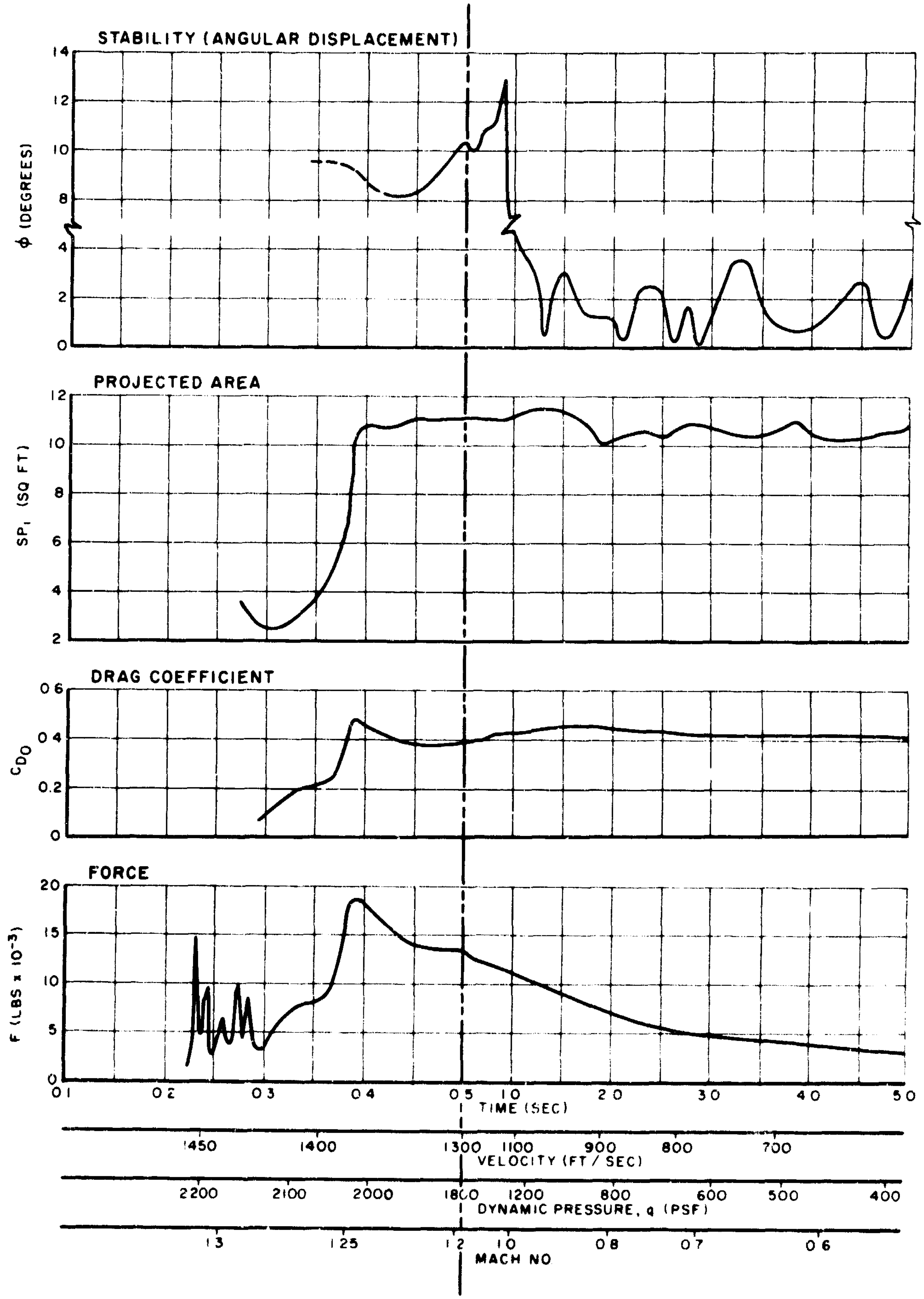

Figure 5.1.6. Performance Curves - Hyperflo Type HY-142B Parachute, Test No. 12

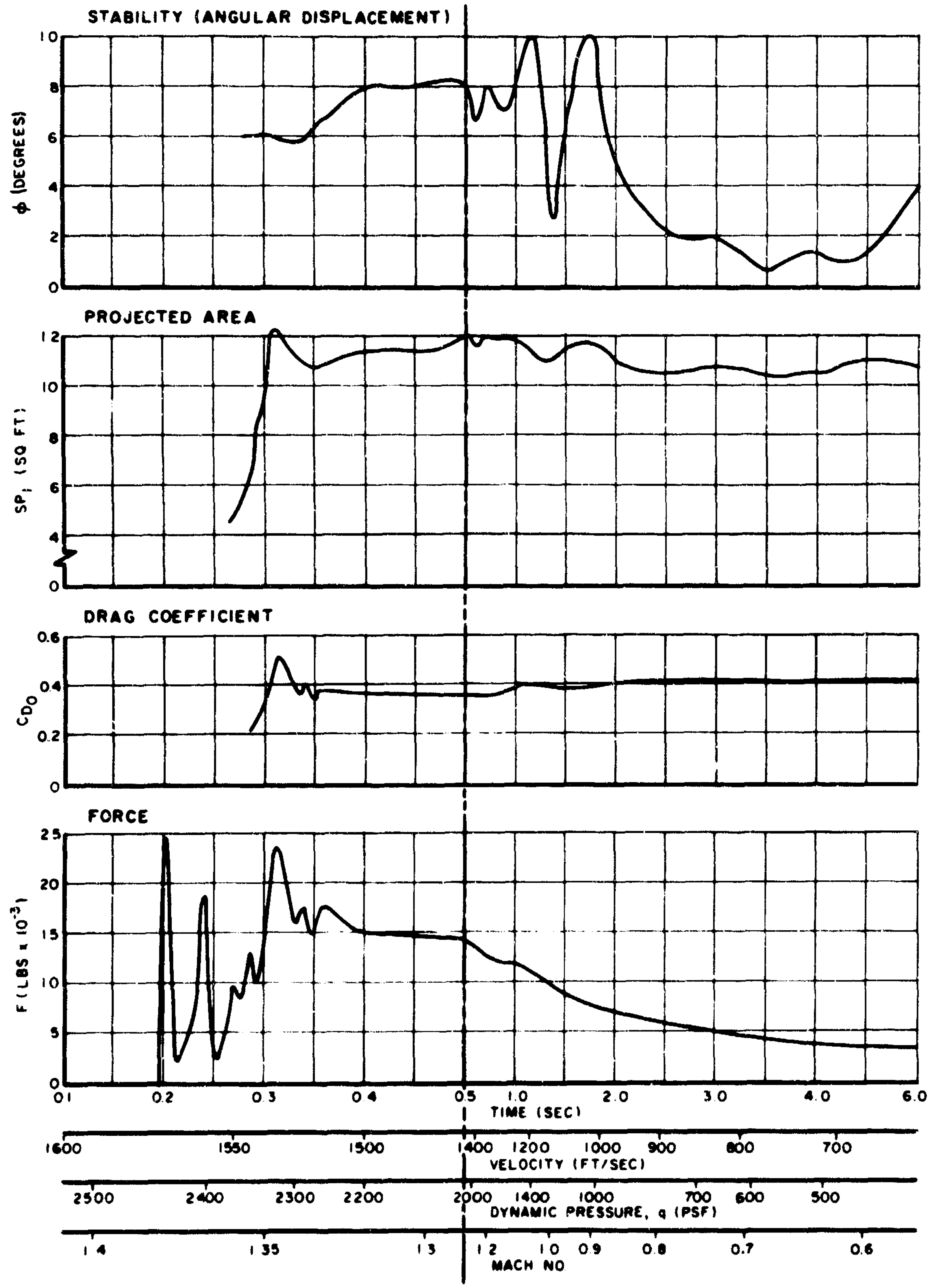

Figure 5.1.7. Performance Curves - Hyperflo Type HY-142C Parachute, Test No. 17

Generally good performance characteristics were exhibited by the Hyperflo type HY-142 parachutes.

5.1.3.4 Hyperflo Type HY-143 Parachute

The Hyperflo Type HY-143 parachute was a 3.69 foot nominal diameter, 12 gore ribbon roof design having a total porosity of 14.58 percent. Two strength variations of this parachute were produced for the three tests conducted. The type HY-143B, a Mach 1.3 design, was used in Test No. 9 and the type HY-143C, a Mach 1.5 design, was used on Test No. 13. The type HY-143B was also tested in triple cluster configuration in Test No. 18.

Good deployments and inflations were obtained on both of the single parachute tests of the type HY-143 configuration. The type HY-143B parachute on Test No. 9 was deployed at Mach number 1.31 with a corresponding dynamic pressure of 2205psf. On Test No. 13, the type HY-143C parachute was deployed at a Mach number of 1.491. This was the highest velocity attained in this series of tests and corresponded to a deployment dynamic pressure of 2839 psf. Both of these tests yielded performance information in the supersonic and subsonic ranges. Figures 5.1.8 and 5.1.9 illustrate these parachutes in operation on Tests Nos. 9 and 13, respectively.

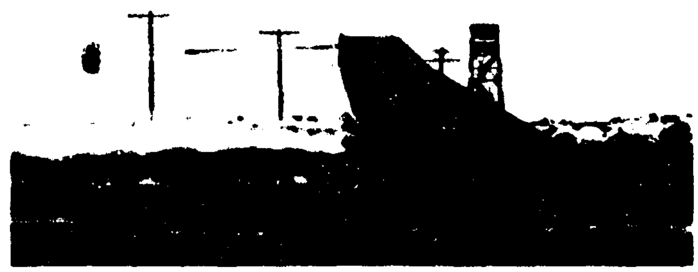

Figure 5.1.8. Hyperflo Type HY-143B Parachute in Operation on Test No. 9

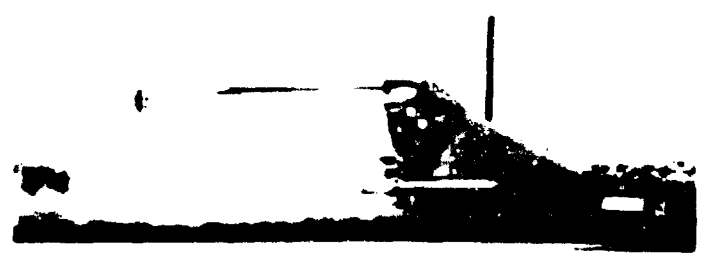

Figure 5.1.9. Hyperflo Type HY-143C Parachute in Operation on Test No. 13

Performance data for the two tests conducted with the single type HY-143 parachutes are shown in Figures 5.1.10 and 5.1.11. Average performance characteristics for the parachutes of this configuration are given in Table 5.1.5.

The supersonic drag coefficient of 0.35 represents the average of a 0.33 as obtained on Test No. 9 and a value of 0.36 as obtained on Test No. 13. Because of the extended range of supersonic data obtained

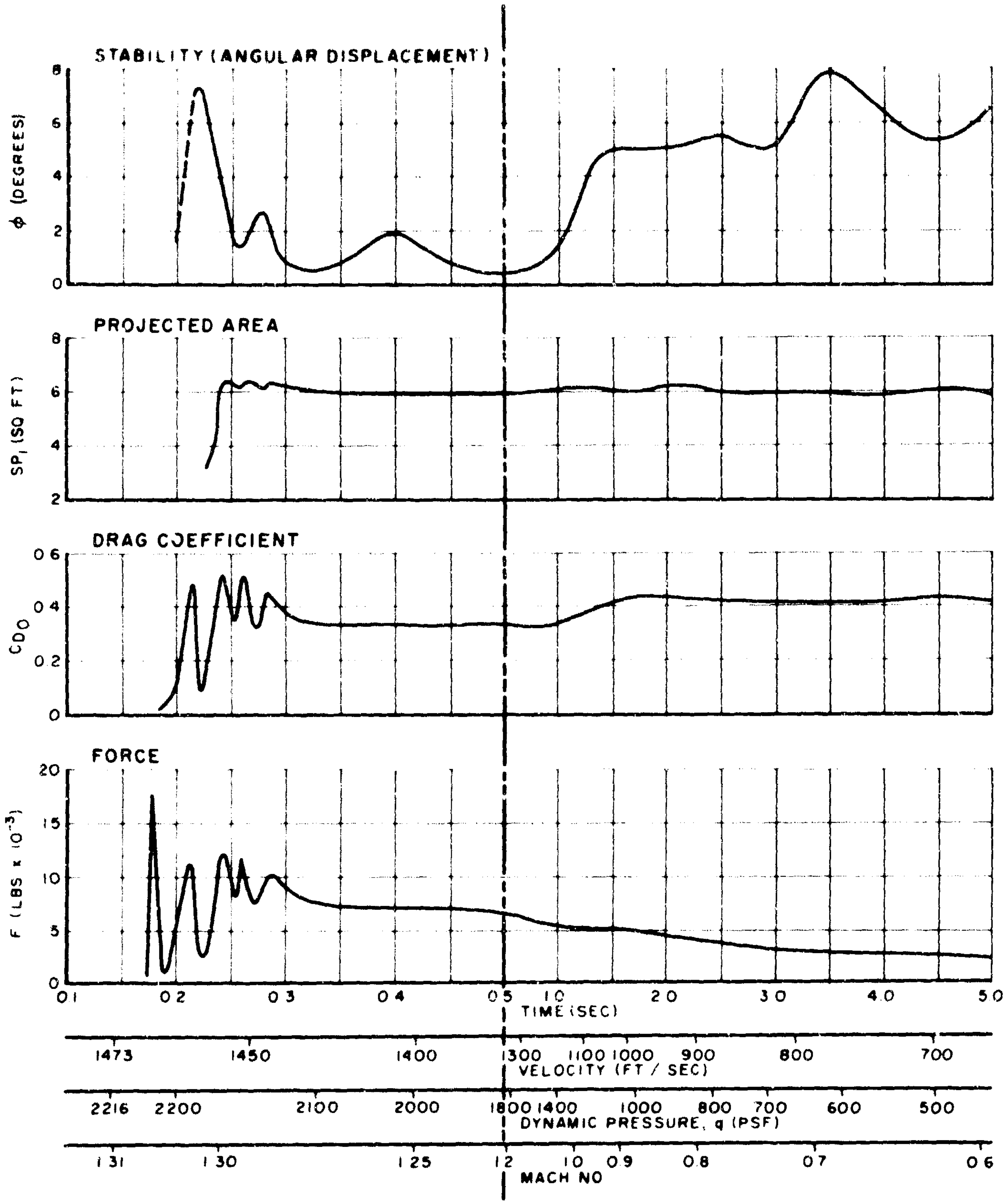

Figure 5.1.10. Performance Curves - Hyperflo Type HY-143B Parachute, Test No. 9

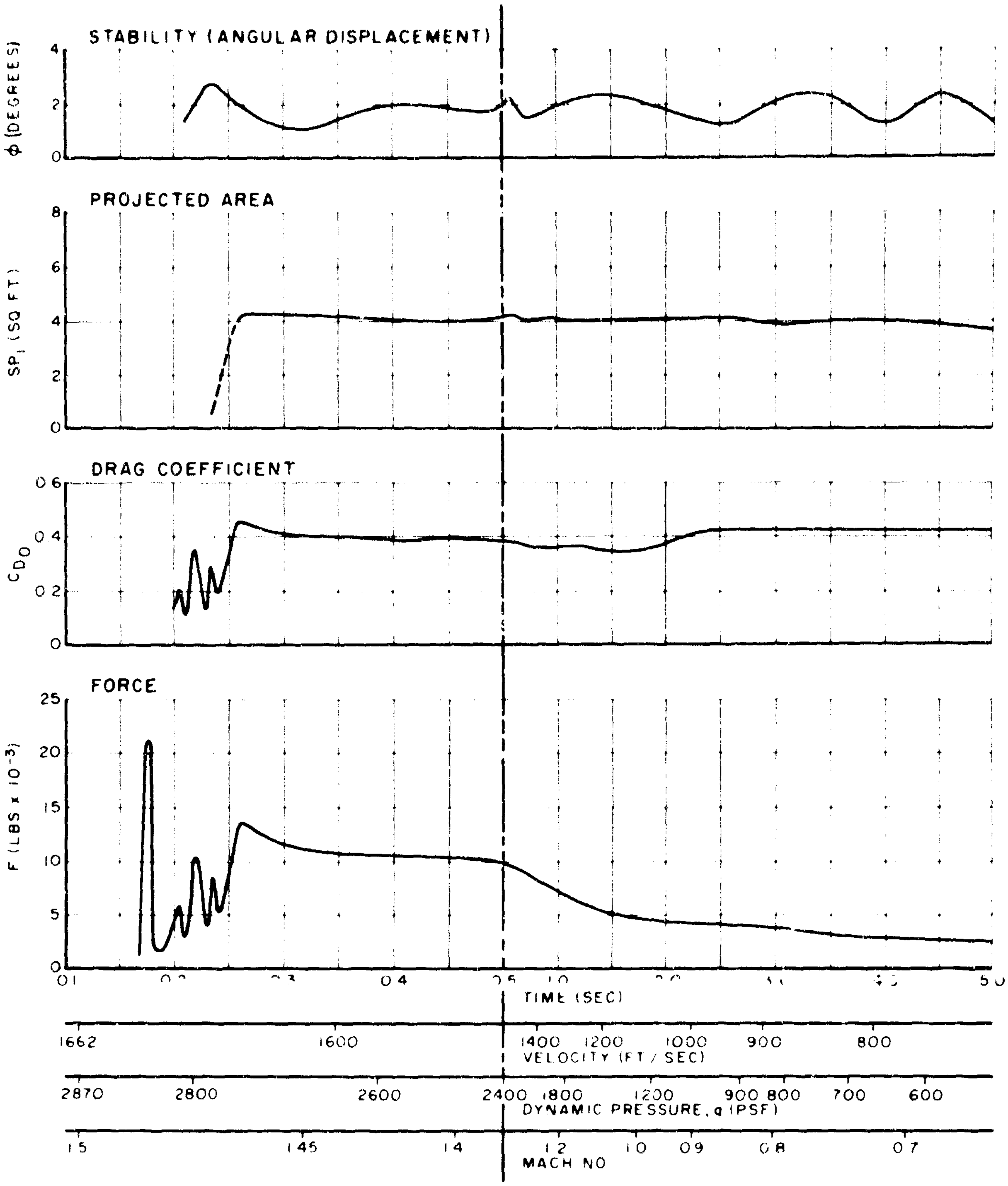

Figure 5.1.11. Performance Curves - Hyperflo Type HY-143C Parachute, Test No. 15

TABLE 5.1.5

AVERAGE PERFORMANCE CHARACTERISTICS
HYPERFLO TYPE HY-143 PARACHUTES

Test No.	Deploy. Mach No.	C_{D_o}	X	S_{p_1}	ϕ
9	1.310	.33/.43	1.60/1.23	6.2/5.9	6.0 ± 2.0
13	1.491	.36/.42	1.25/1.07	6.2/5.7	1.7 ± 0.5
Average	-	.35/.42	1.42/1.15	6.2/5.8	-

(supersonic/subsonic)

on Test No. 13, the average coefficient tends toward the higher of the two average values. The subsonic drag coefficient averaged 0.42 - 0.43, with no significant variation throughout the steady state subsonic portion of each test. This appears to be in quite good agreement with similar data obtained on other tests in the series.

Opening shock factors for this parachute varied sufficiently on the two tests that they could not be considered to be indicative of average characteristics. Both however, were within the over-all range of values experienced in all tests in the series.

Very consistent steady state projected canopy areas were recorded on the tests. The average inflated area of approximately 6.0 square feet was the result of less than one-half square foot over-all area variation in either test or less than one-quarter square foot variation from the indicated average. Neither of the parachutes in these two tests exhibited significantly different inflated characteristics in the supersonic regime than in the subsonic ranges. Based on the design projected area of this parachute, the average area ratio obtained on these tests was approximately 120 percent.

Although the parachute on Test No. 9 tended to wander or drift slowly in subsonic operation, over-all stability of the type HY-143 design was quite good. In the Mach 1.5 deployment in Test No. 13, oscillatory deviations of the parachute were limited to within 2.5 degrees throughout the test.

There was no structural damage to either of the parachutes of this configuration during the tests.

In Test No. 18, a triple cluster of Hyperflo Type HY-143B parachutes was deployed at Mach number 1.355 and a dynamic pressure of 2346 psf. The triple cluster configuration consisted of three single type HY-143B parachutes and line systems assembled to a common confluence point on the riser. Figure 5.1.12 shows the geometry of the triple cluster configuration as used on the test in this program.

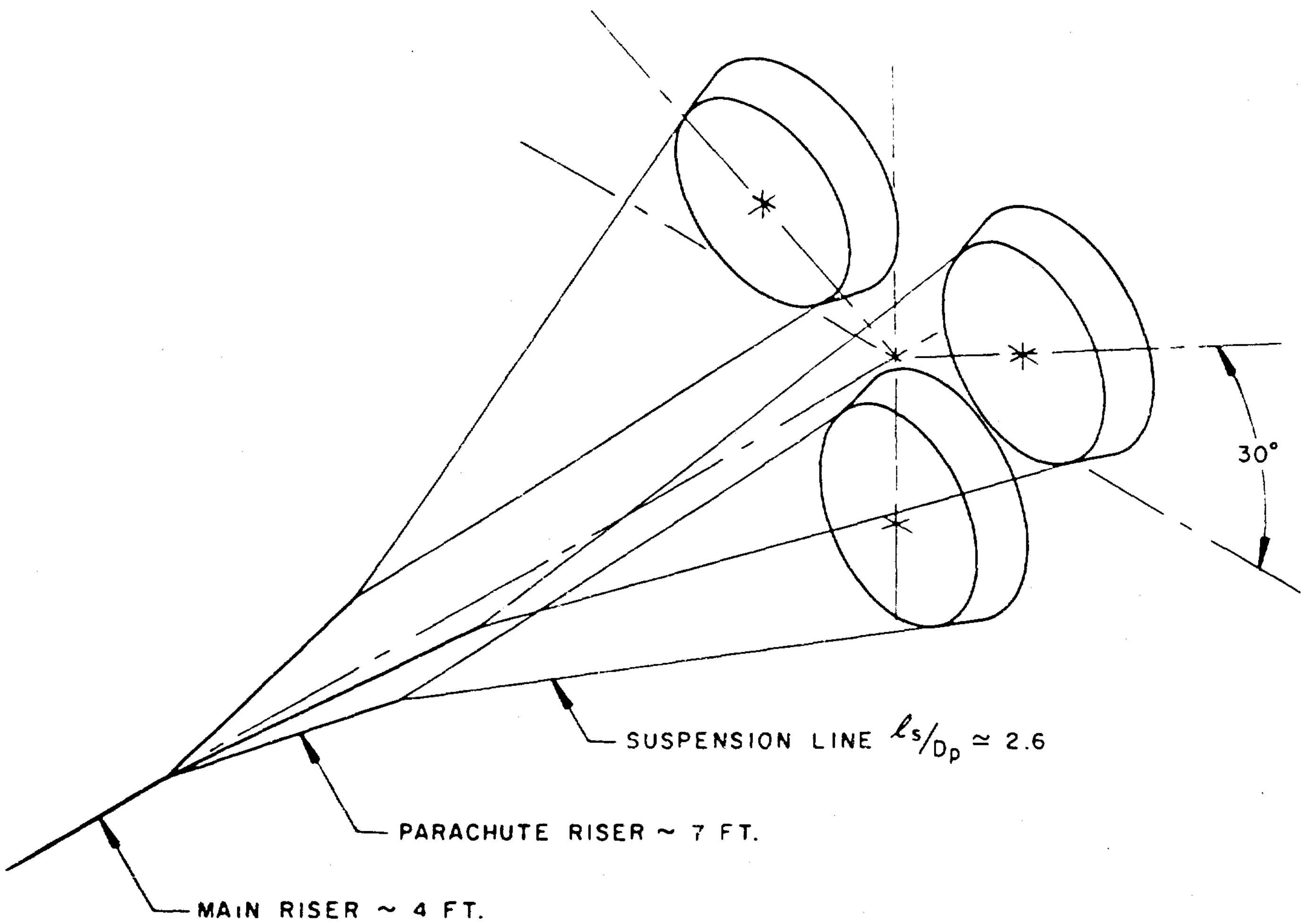

Figure 5.1.12. Geometry of Triple Cluster Configuration

Although a normal deployment appears to have occurred only one of the parachutes in the three parachute cluster inflated immediately after deployment. This operational state is illustrated in the photograph in Figure 5.1.13. The other two parachutes inflated nearly together approximately 2-1/2 seconds later. Performance curves for this test are shown in Figure 5.1.14.

Because of the unusual behavior of the clustered configuration on this test, supersonic data are not available. The subsonic drag coefficient of about 0. 42 was essentially the same as on the tests with single parachutes.

BEST AVAILABLE COPY

Figure 5. 1. 13. Partial Inflation of Three Cluster Configuration of Hyperflo Type HY-143B Parachutes on Test No. 18

The opening shock factor cannot be obtained on the test because only one of the clustered parachutes opened at the time normally associated with maximum opening force.

The late inflation of two of the parachutes in the cluster is much more dramatically illustrated in the canopy area relationship than in the force relationship. Prior to the time when the two parachutes inflate, the area relationship for the three parachutes total up to only approximately 9-1/2 square feet. Immediately after all parachutes are inflated, this total has risen suddenly to approximately 17 square feet.

Stability of the parachutes, when considered as a system, was not bad at any time during the test. Throughout the test, the center of the system never exceeds 2 degrees. After all three parachutes have inflated, the three maintain quite steady positions which average approximately 6-1/2 degrees from the cluster centerline at the test vehicle attachment. This angle, when referenced to the design projected diameter of the parachutes, positions them at 1. 4 to 1. 5 diameters relative to each other's apex.

None of the three parachutes in the cluster were damaged on this test.

5. 1. 3. 5 Hyperflo Type HY-144 Parachutes

The Hyperflo Type HY-144 parachute was a 3. 69 foot nominal diameter, 12 gore parachute having a roof constructed of Perlon monofilament mesh. Two strength variations of this configuration were produced for the two tests conducted. The type HY-144A was a Mach 1. 1 design having a total porosity of 14. 3 percent. This parachute was tested on Test No. 15. The type HY-144B, a Mach 1. 3 design, had a total porosity of 13. 32 percent. This parachute was used on Test No. 21. The difference in porosity in the two parachutes resulted from an additional reinforcing that was put on the type HY-144B to permit the higher deployment velocity to be attained with essentially the same design as the type HY-144A.

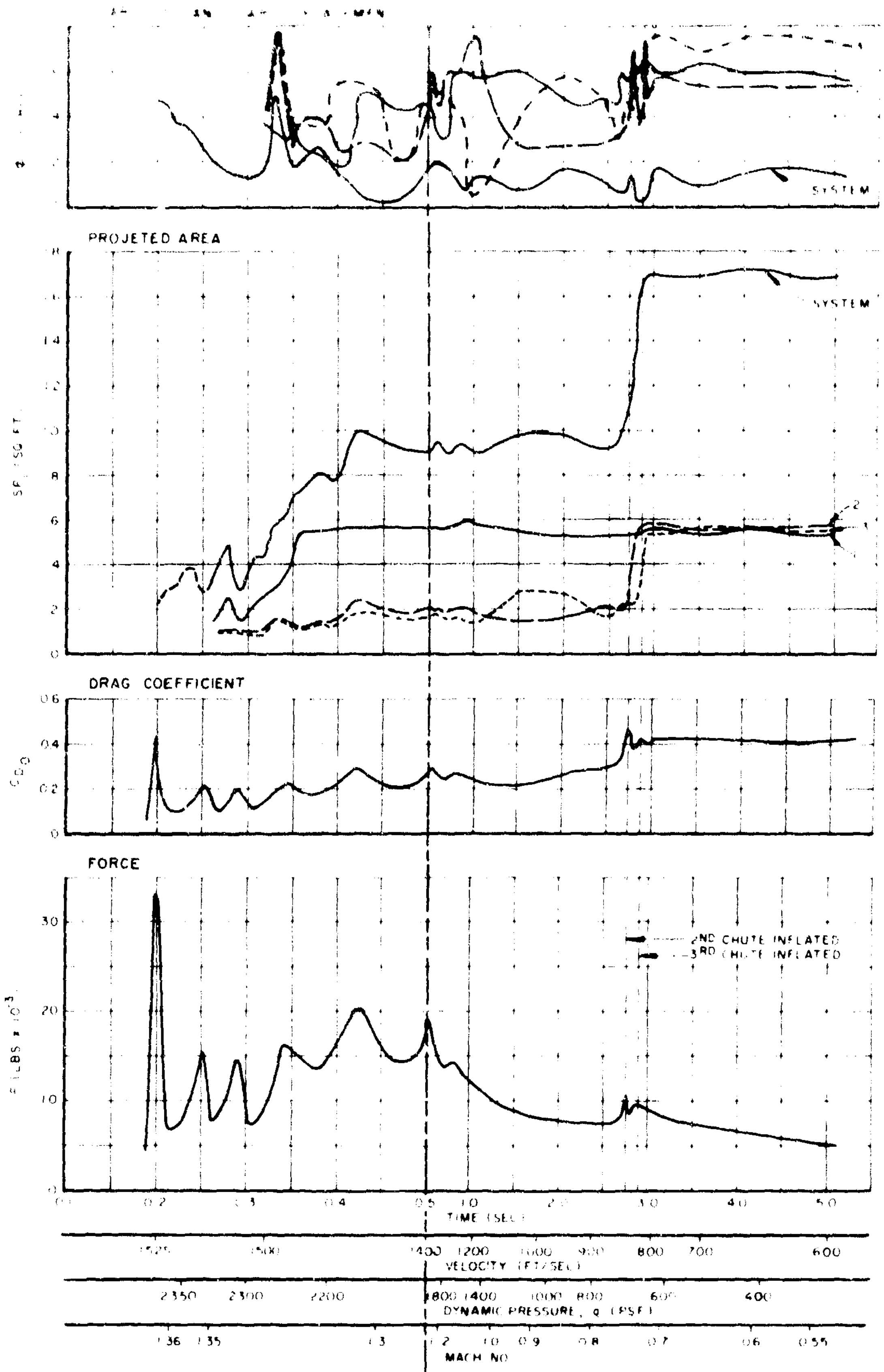

Figure 5.1.14. Performance Curves - Triple Cluster, Hyperflo Type 143B Parachute, Test No. 18

Good deployments and inflations were obtained in both tests with the Hyperflo Type HY-144 parachutes. The type HY-144A parachute used on Test No. 15 was deployed at a Mach number of 1.078 and a dynamic pressure of 1482 psf. On Test No. 21, the type HY-144B parachute was deployed at a Mach number of 1.336. This corresponded to a dynamic pressure of 2300 psf. Photographs of these parachutes in operation on Tests Nos. 15 and 21 are shown in Figures 5.1.15 and 5.1.16, respectively.

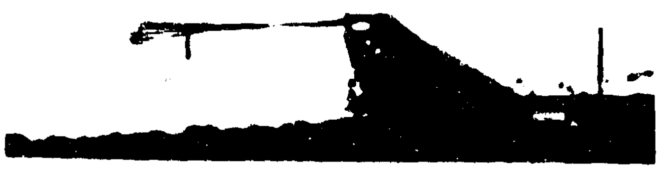

Figure 5.1.15. Hyperflo Type HY-144A Parachute in Operation on Test No. 15

Figure 5.1.16. Hyperflo Type HY-144A Parachute in Operation on Test No. 16

Performance data for these two tests are shown in Figures 5.1.17 and 5.1.18, and average performance characteristics for the parachutes of this configuration are given in Table 5.1.6.

TABLE 5.1.6

AVERAGE PERFORMANCE CHARACTERISTICS
HYPERFLO TYPE HY-144 PARACHUTE

Test No.	Deploy. Mach No.	C_{D_o}	X	S_{P_1}	Ø
15	1.078	.36/.43	1.66/1.39	5.4/5.2	0.5 ± 0.5
21	1.336	.34/.43	1.38/1.09	5.5/5.4	2.0 ± 0.8
Average	-	.35/.43	1.52/1.24	5.5/5.3	-

(supersonic/subsonic)

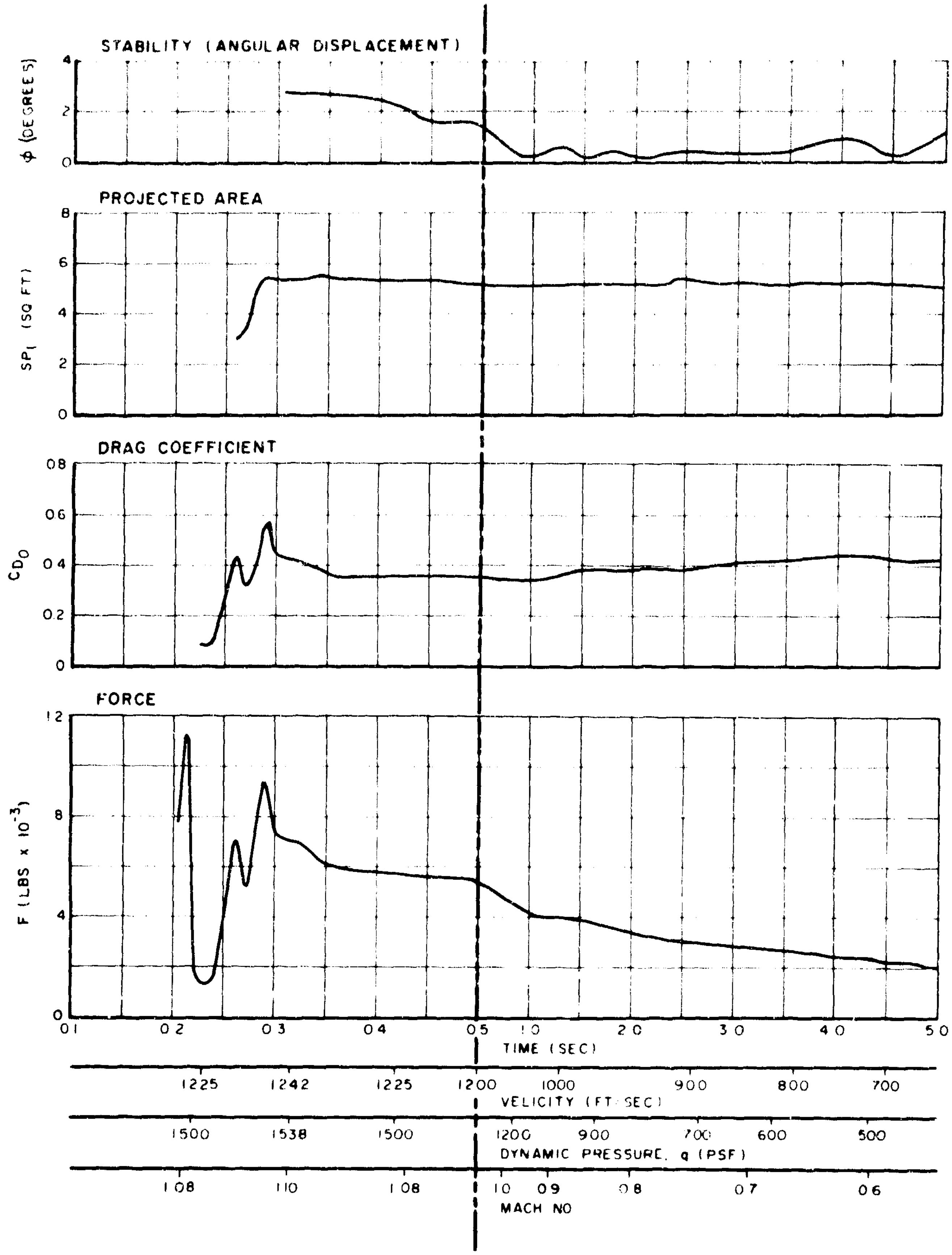

Figure 5.1.17. Performance Curves - Hyperflo Type HY-144A Parachute, Test No. 15

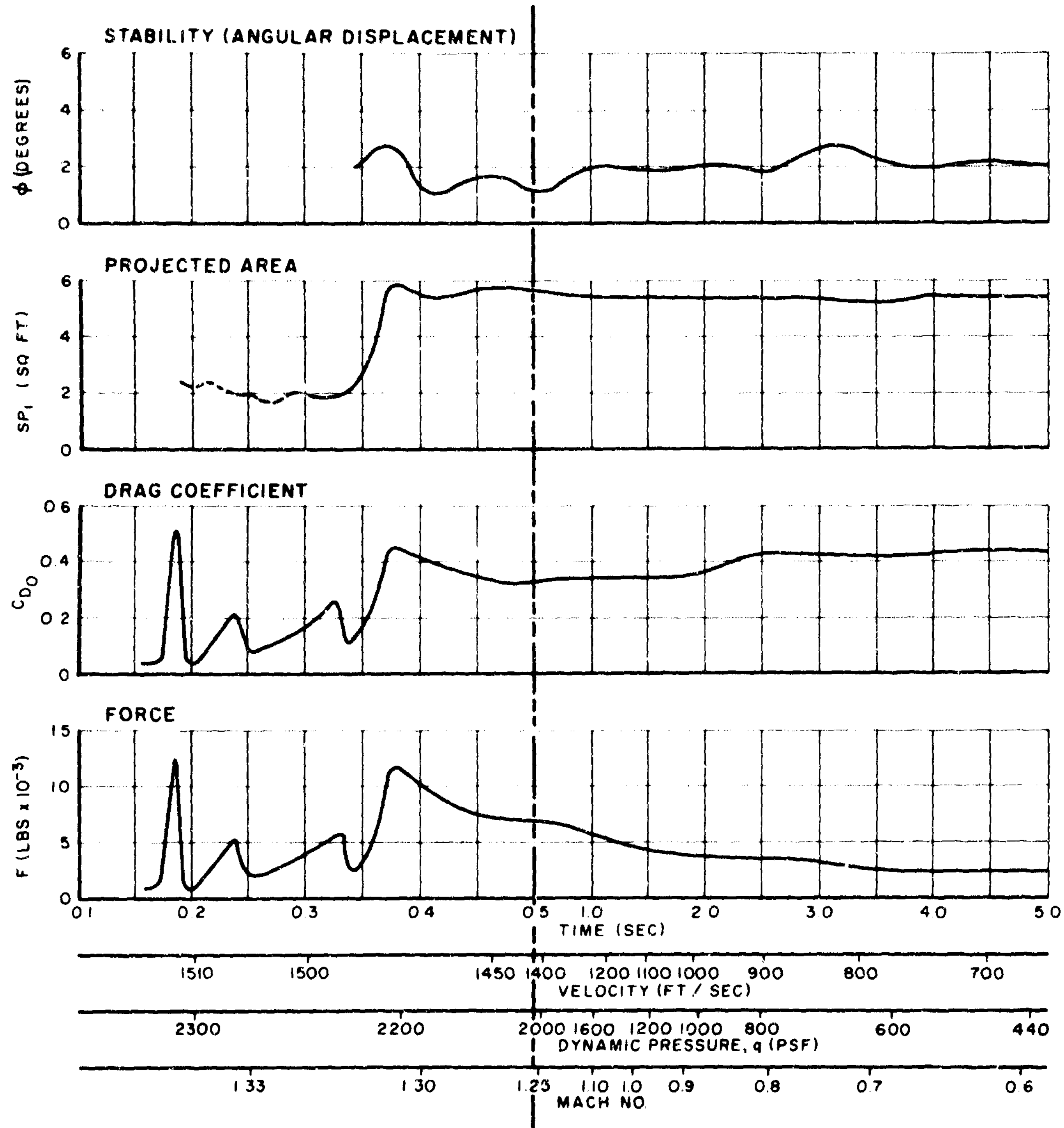

Figure 5.1.18. Performance Curves - Hyperflo Type HY-144B Parachute, Test No. 21

Both supersonic and subsonic drag coefficients on these two tests with mesh roof designs were similar to the data obtained with the ribbon roof parachutes. The supersonic drag coefficient of 0.35 is the average of the variation between a 0.36 value obtained on Test No. 15 and a 0.34 value obtained on Test No. 21. If a tendency toward one or the other value should be noted, the lower value would take precedent by virtue of the greater velocity range. Test 15 was not truly indicative of supersonic operations since the deployment was transonic. The subsonic drag coefficient averaged 0.43 with variations between 0.42 and 0.44 on both tests.

An average indication of the opening shock factor for this parachute could not be obtained from the data because of the wide variation on the two tests. This factor, on Test No. 15, was 1.66 on the basis of supersonic comparison while on Test No. 21, the factor was 1.38. On the basis of subsonic steady state data, the respective values for the two tests were 1.39 and 1.09.

Inflated canopy area relationships on the two tests were nearly identical. An average inflated area of approximately 5.4 square feet was obtained from data which varied only between 5.5 and 5.2 square feet in both tests in supersonic and subsonic operation, respectively. Based on the design projected area of this parachute, the average area ratio obtained on these tests was approximately 105 percent. This was significantly less than the area ratio which was obtained on the comparable ribbon roof parachute.

Excellent stability was apparent on both tests with the type HY-144 parachute. On Test No. 15, there were no excursions in excess of one degree after the parachute had gone through transonic and steadied out in subsonic operation. On Test No. 21, oscillations in both the supersonic and subsonic speed regimes were within one degree of an average angular displacement of two degrees.

Both of the parachutes on the two tests suffered minor damage to the mesh roof portion of the canopies. In each case, the damage was found to have been caused by impact with foreign material, such as bits of tape and wire, from the test vehicle propulsion section. In neither case however, was the damage thought to have significantly affected the performance of the parachutes.

Generally, the Hyperflo Type HY-144 parachutes exhibited very good performance characteristics.

5.1.3.6 Hyperflo Type HY-145 Parachute

The Hyperflo Type HY-145 parachute was a 4.95 foot nominal diameter, 16 gore parachute having a total porosity of 14.5 percent. This parachute, like the type HY-144 configuration, was constructed with a Perlon monofilament mesh roof.

Only one parachute, the type HY-145A, a Mach 1.1 design, was tested on the program on Test No. 23.

Good deployment and inflation was obtained on this test at a Mach number of 1.026 and a dynamic pressure of 1351 psf. Figure 5.1.19 shows the parachute in operation just after inflation.

Performance curves for this test are shown in Figure 5.1.20

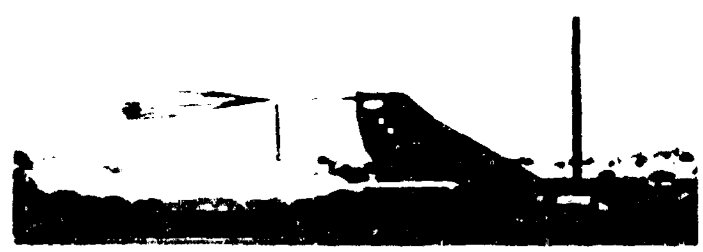

Figure 5.1.19. Hyperflo Type HY-145A Parachute in Operation on Test No. 23

Because of the low deployment velocity on this test, only subsonic data is available. The drag coefficient averaged approximately 0.42 after attaining steady state operation. Immediately after inflation, the projected canopy area was approximately 10.0 - 10.2 square feet. As the parachute settled into steady state subsonic operation, this value decreased and stabilized at between 9.7 - 9.8 square feet. This steady state value is approximately 106 percent of the design projected area of this parachute.

On the basis of subsonic steady state data, the opening shock factor on this test was 1.04. Although this was the lowest subsonic factor recorded in the series of Hyperflo tests, it was not significantly lower than those observed in several of the other tests. On the basis of the transonic data available on this test, and comparable tests in which supersonic data are available, the supersonic factor for this test would be on the order of 1.20 - 1.30.

Quite good stability of the parachute was noted on the test. Oscillation information showed that after inflation and transition through the transonic region, the average oscillations were within approximately one-half degree of an average angular displacement of one degree.

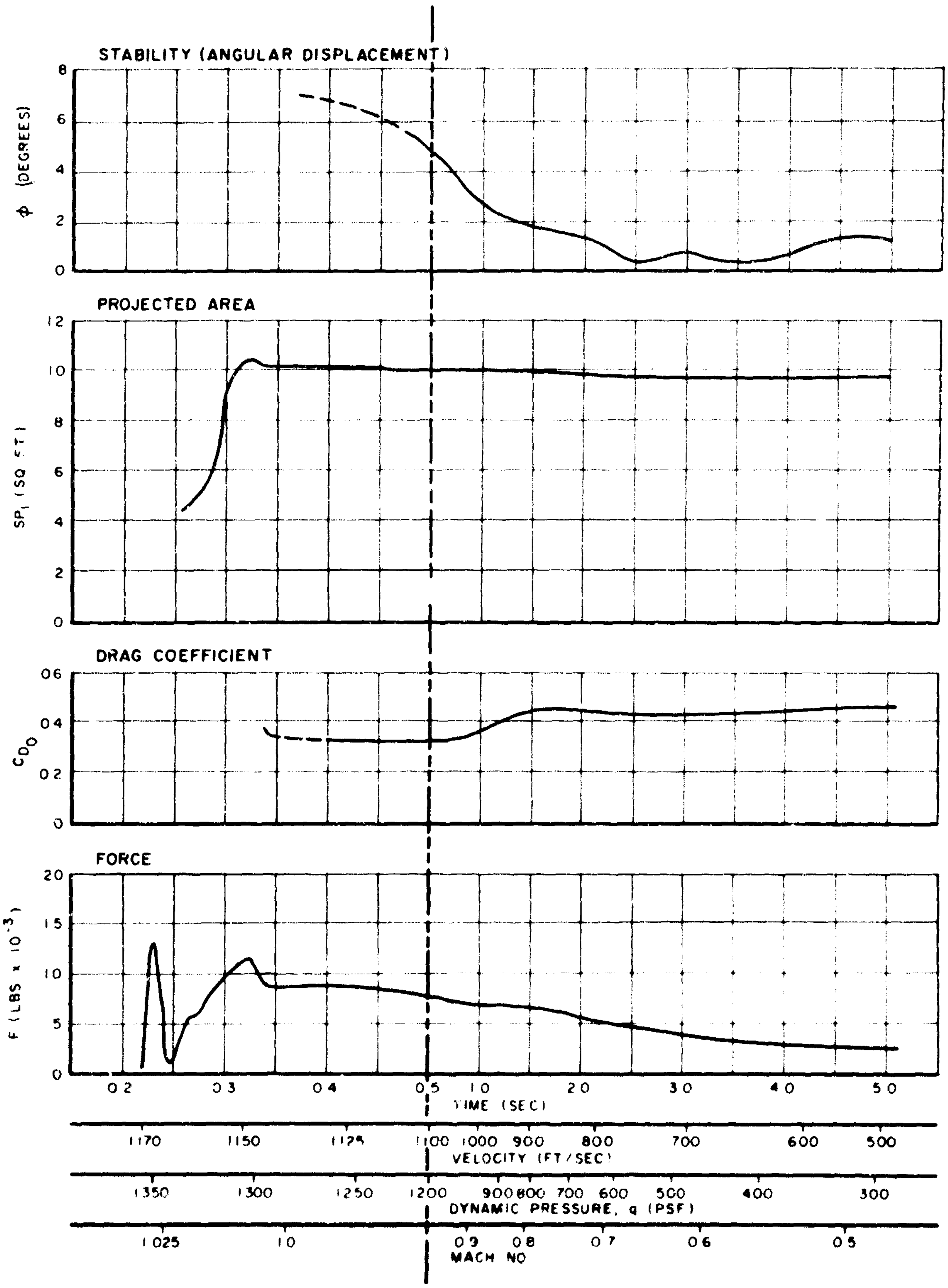

Figure 5.1.20. Performance Curves - Hyperflo Type HY-145A Parachute, Test No. 23

Considerable damage was incurred to the Perlon mesh roof portion of two gores of the parachute. This damage was found to have been caused by impact with foreign material, such as bits of tape and wire from the rocket propulsion section and parachute disconnect on the test vehicle. No apparent effect on the performance of the parachute was noted because of the damage.

5.2 HEMISFLO TYPE PARACHUTE

5.2.1 General

The Hemisflo type parachute is a ribbon type full extended skirt design with a hemispherical shape above the equator of the parachute and a skirt extension added to the areas between adjacent suspension lines below the equator. The skirt extensions are expressed in percent of the basic constructed diameter, which is the circumferential distance of the hemispherical portion, measured from equator to equator over the apex of the parachute. Suspension line length is also related to this diameter.

The individual gore of the Hemisflo type parachute is best constructed as a continuous flat assembly from dimensional characteristics of the shaped gore. Because of the flexibility of materials used in parachute construction, little error is introduced by utilization of this technique. Based on standard flat circular ribbon construction, each gore is a grid of horizontal ribbons spaced and retained at regular intervals by one or more vertical ribbons. Radial bands extend from the vent to the skirt at each side of the gore. These bands join the gores together in the canopy assembly and transfer the aerodynamic forces developed in the canopy to the suspension lines.

Figure 5.2.1 shows a typical Hemisflo type parachute gore assembly.

5.2.2 Test Program

Seven tests were conducted with three basic configurations of Hemisflo type parachutes during the program. Five of these tests were performed with 6.77 foot nominal diameter, 20 gore, type EHR-137 parachutes and one test each was conducted with a 5.54 foot nominal diameter, 16 gore, type EHR-138 parachute and a 4.12 foot nominal diameter, 16 gore, type EHR-139 parachute.

Deployment velocities on the tests with the type EHR-137 parachutes ranged from Mach numbers 1.10 to 1.465. The type EHR-138 and type EHR-139 were each deployed at approximately Mach number 1.3.

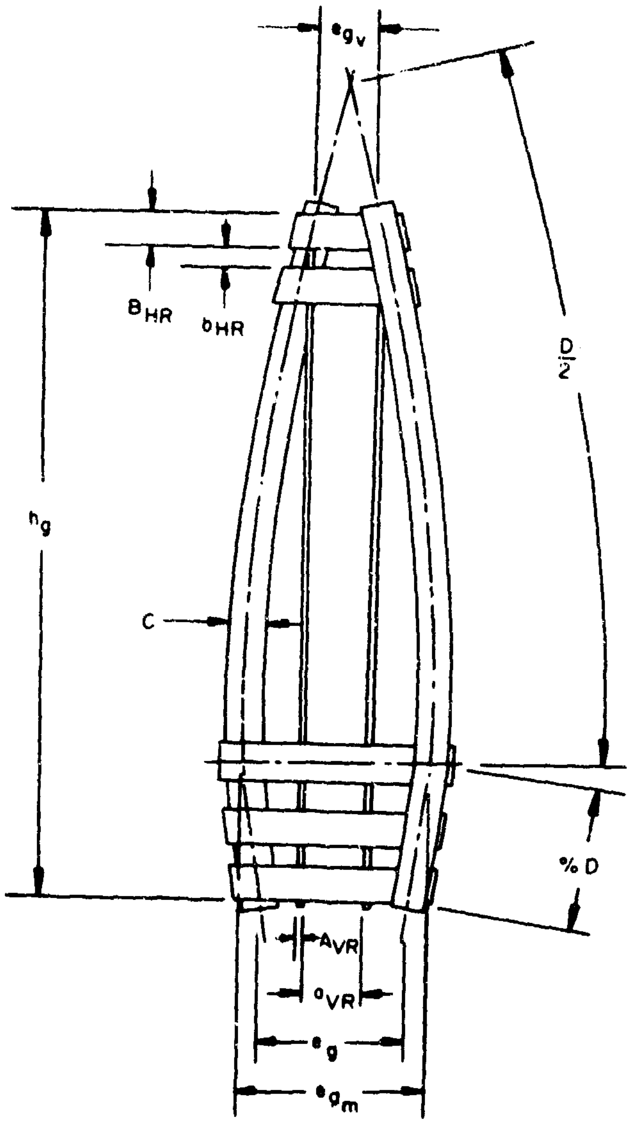

Figure 5. 2. 1. Typical Gore Assembly-Hemisflo Type Parachute

Total porosities of all of the Hemisflo type parachutes tested were approximately 25-27 percent.

Major dimensional details and materials used infabrication of the parachutes are listed in Table 5. 2. 1. A general list of materials and related material specifications are tabulated in Table 5. 2. 2.

5. 2. 3 Parachute Performance

Parachute performance summary data for the three basic Hemisflo type parachute configurations used in the six (6) tests in which parachute deployment was obtained, are presented in Table 5. 2. 3. Details of the performance of these parachutes in the tests of each configuration group are presented in the following paragraphs.

5. 2. 3. 1 Hemisflo Type EHR-137 Parachute

The Hemisflo Type EHR-137 parachute was a 6. 77 foot nominal diameter, 20 gore configuration having a 10 percent fully extended skirt and a total porosity of 27. 28 percent.

Three strength variations of this configuration were produced for the five (5) tests conducted. The type EHR-137A, a Mach 1. 1 design was used in Test No. 1.

The type EHR-137B, the original Mach 1.3 design, was used on Test No. 3. A modified Mach 1.3 version, the type EHR-137B-A1, was used on Tests 14 and 16. The Mach 1. 5 design, the type EHR-137C, was used on Test No. 7.

TABLE 5.2.1

PHYSICAL DETAILS AND DIMENSIONS OF HEMISFLO TYPE PARACHUTES

Hemisflo Type	EHR-137A	EHR-137B	EHR-137B-A1	EHR-137C	EHR-139B	EHR-139B
Nominal Diameter, D_o (Ft.)	6.77	6.77	6.77	6.77	5.54	4.12
Canopy Area, S_o (Ft.^{2})	36	36	36	36	24	13.33
Total Porosity, λ_t (Percent)	27.28	27.28	27.28	27.28	25.70	25.19
No. of Gores and Suspension Lines	20	20	20	20	16	16
No. of Horizontal Ribbons	13	13	13	13	15	15
No. of Vertical Ribbons	1	1	1	1	1	1
Suspension Line Length (Ft.)	13.27	13.27	13.27	13.27	10.86	6.08
Length of Gore, h_g (In.)	40.01	40.01	40.01	40.01	32.60	23.65
Width of Gore At Skirt, e_g (In.)	7.50	7.50	7.50	7.50	7.70	5.74
Width of Gore At Vent, e_{g_v} (In.)	2.54	2.54	2.54	2.54	2.58	2.20
Max. Width of Gore, e_{g_m}, At Equator (In.)	7.90	7.90	7.90	7.90	8.10	6.04
Spacing Between Horizontal Ribbons, b_{HR} (In.)	1.17	1.17	1.17	1.17	0.72	0.61
Spacing Between Vertical Ribbons, a_{HR} (In.)	-	-	-	-	-	-
Suspension Line Material	1x3000	1x4500	1x6000	1x6000	1x6000	1x6000
Horizontal Ribbon Material	2x1500	2x2000	2x2000	2x3000	1 1/2x1500	1x1000
Vertical Ribbon Material (2 Ply)	9/16x500	9/16x500	9/16x500	9/16x500	1/2x250	1/2x250
Radial Band Material	1 1/4x650	1 1/4x800	1 1/4x800	1 1/4x800	1 1/4x650	1 1/4x650
Horizontal Reinforcing Band Material	2x1500	2x2000	2x2000	2x3000	-	-
Reinforcing Band On Ribbon No's.	4,7	4,7	4,7	4,7	-	-
Weight, Canopy and Lines (Lbs)	14.3	17.7	22.7	23.4	13.9	10.1
Cook TCD Specification Number	596-8593A	596-8593B	596-8593D	596-8593C	596-8988	596-8989
Used On Test Number	1	3	14.16	7	6	8

TABLE 5.2.2

MATERIALS USED IN HEMISFLO TYPE PARACHUTES

PART	MATERIAL	SIZE-STRENGTH	SPECIFICATION
Horizontal Ribbons	Ribbon, Nylon	2 In.-1500 Lb. 2 In.-2000 Lb. 2 In.-3000 Lb.	MIL-R-5608-E III MIL-R-5608-E IV MIL-R-5608-E V
	Tape, Nylon	1 1/2 In.-1500 Lb. 1 In.-1000 Lb.	MIL-T-5038- IV MIL-T-5038- IV
Vertical Ribbons	Tape, Nylon	9/16 In.-500 Lb. 1/2 In.-250 Lb.	MIL-T-5038- V MIL-T-5038- III
Radial Ribbons	Ribbon, Nylon Webbing, Nylon	1 1/4 In.-650 Lb. 1 1/4 In.-800 Lb.	MIL-R-5608- E I MIL-W-4088- III
Horizontal Reinforcing	Ribbon, Nylon	2 In.-1500 Lb. 2 In.-2000 Lb. 2 In.-3000 Lb.	MIL-R-5608-E III MIL-R-5608-E IV MIL-R-5608-E V
Skirt Reinforcing	Webbing, Nylon Tape, Nylon	1 3/4 In.-3600 Lb. 1 1/2 In.-1500 Lb.	MIL-W-4088- VIII MIL-T-5038- IV
Vent Reinforcing	Webbing, Nylon	1 In.-6000 Lb.	MIL-W-4088- XVIII
Suspension Lines	Webbing, Nylon	1 In.-3000 Lb. 1 In.-4500 Lb. 1 In.-6000 Lb.	MIL-W-5625 MIL-W-4088- XXV MIL-W-4088- XVIII
Thread	Nylon	Size E, F, FF 3 Cord, 5 Cord	MIL-T-7807

TABLE 5.2.1

TABLE 5.2.3

PERFORMANCE SUMMARY DATA - HEMISFLO TYPE PARACHUTES

Parachute Type Number		EHR-137A	EHR-137B	EHR-137B-A1	EHR-137C	EHR-138B	EHR-139B
Test Number		1	3	16	7	6	8
Velocity, V_s (Ft/Sec)		1235	1462	1491	1597	1454	1457
Mach Number, M		1.100	1.316	1.314	1.465	1.295	1.288
Dynamic Pressure, q (Lb/Ft^2)		1520	2220	2217	2764	2142	2131
Deployment Time, t_d (Sec)		0.210	0.187	0.206	0.198	0.172	0.190
Time To Max. Opening Force, t_{s_o} (Sec)		0.111	0.102	0.104	0.076	0.100	0.118
Snatch Force, F_s (Lbs)		13,300	14,150	26,050	27,900	20,800	20,130
Maximum Opening Force, F_o (Lbs)		28,230	> 45,000	36,700	52,200	30,440	15,900
Avg. Drag Coefficient, C_{D_o}		-/.41	-	~.41/.41	.42/.41	.44/.48	.41/-
Opening Shock Factor, X		-/1.22	-	1.12/1.12	1.23/1.26	1.32/1.19	1.36/-
Area, S_{p_i} (Ft^2)		-/17.5	-	18.5/17.7	19.0/18.0	-	6.0/-
Stability, ϕ (Degrees)		0-0.5	-	0-1.5	0.1.0	-	0-2.0
Parachute Damage	Canopy	None	None	None	None	None	None
	Lines	None	All Lines Severed At Skirt	None	None	None	None

Numbers Separated By Slant (/), Indicate (Supersonic/Subsonic) Values

Good deployments and inflations were obtained on three tests, one each with each parachute design. On Test No. 1, a type EHR-137A was deployed at Mach number 1.10 and a dynamic pressure of 1520 psf. On Test No. 16, a type EHR-137B-A1 was deployed at Mach number 1.314 and a dynamic pressure of 2217 psf and, a type EHR-137C was deployed on Test No. 7 at a Mach number of 1.465 with a corresponding dynamic pressure of 2764 psf. Figure 5.2.2 shows the type EHR-137B-A1 parachute in operation on Test No. 16.

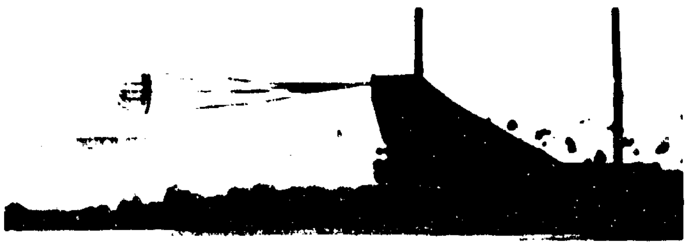

Figure 5.2.2. Hemisflo Type EHR-137B-A1 Parachute in Operation on Test No. 16

Performance data for these three tests conducted with the three type EHR-137 designs, are shown in Figures 5.2.3, 5.2.4, and 5.2.5. Average performance characteristics for the parachute of this configuration are given in Table 5.2.4.

Little difference is noted in the supersonic and subsonic drag coefficients for this parachute. Both supersonic and subsonic values averaged between 0.40 and 0.43 on all tests with no significant variation throughout the steady state portion of the test.

TABLE 5.2.4

AVERAGE PERFORMANCE CHARACTERISTICS
HEMISFLO TYPE EHR-137 PARACHUTES

Test No.	Deploy. Mach No.	C_{D_o}	X	S_{P_1}	Ø
1	1.100	-/.41	-/1.22	-/17.5	0.3 ± 0.2
16	1.314	.41/.41	1.12/1.12	18.5/17.8	0.8 ± 0.7
7	1.465	.42/.41	1.23/1.26	19.0/18.0	0.5 ± 0.5
Average	-	.41/.41	1.18/1.20	18.8/17.8	0.5 ± 0.5

(supersonic/subsonic)

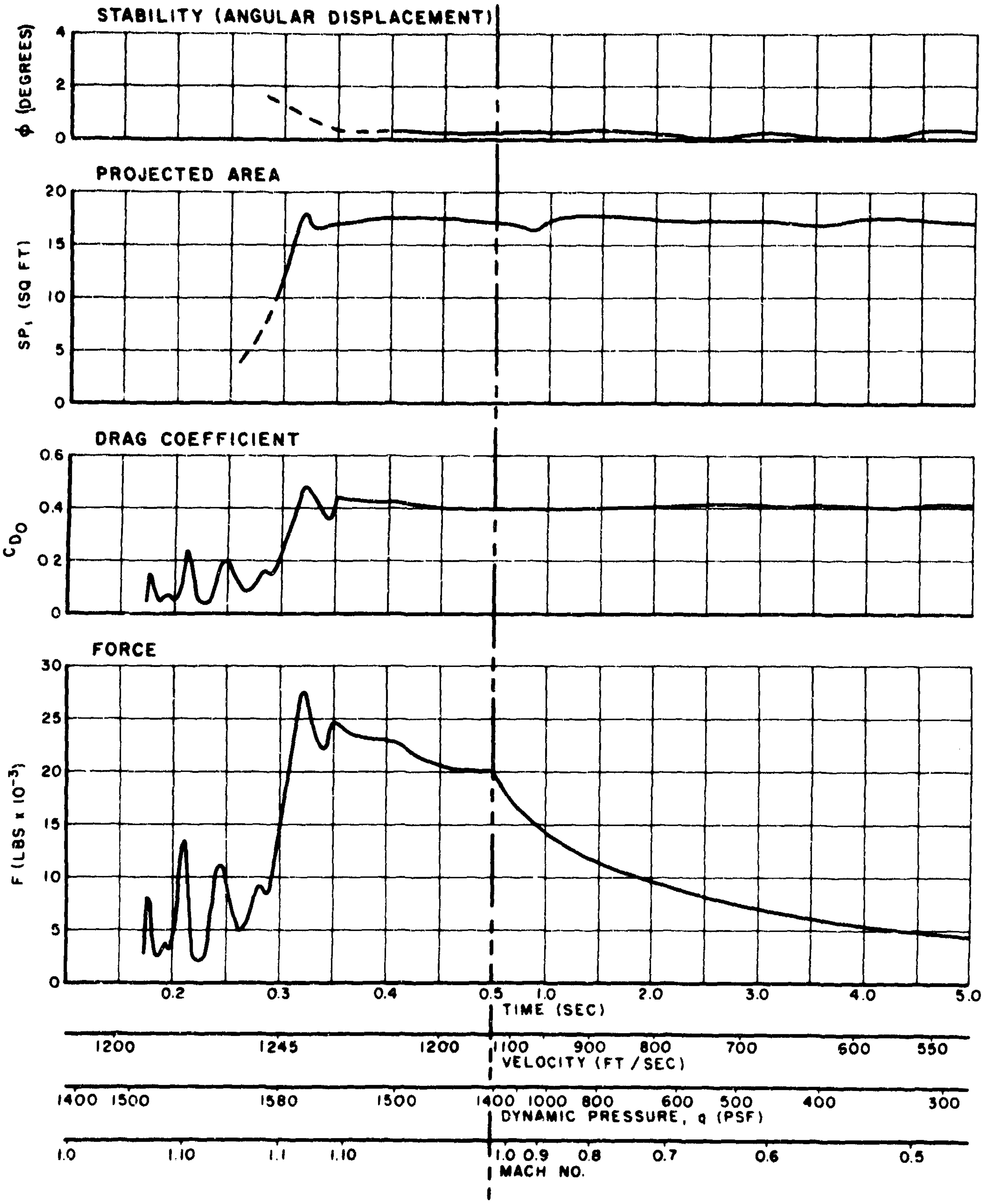

Figure 5.2.3. Performance Curves - Hemisflo Type EHR-137A Parachute, Test No. 1

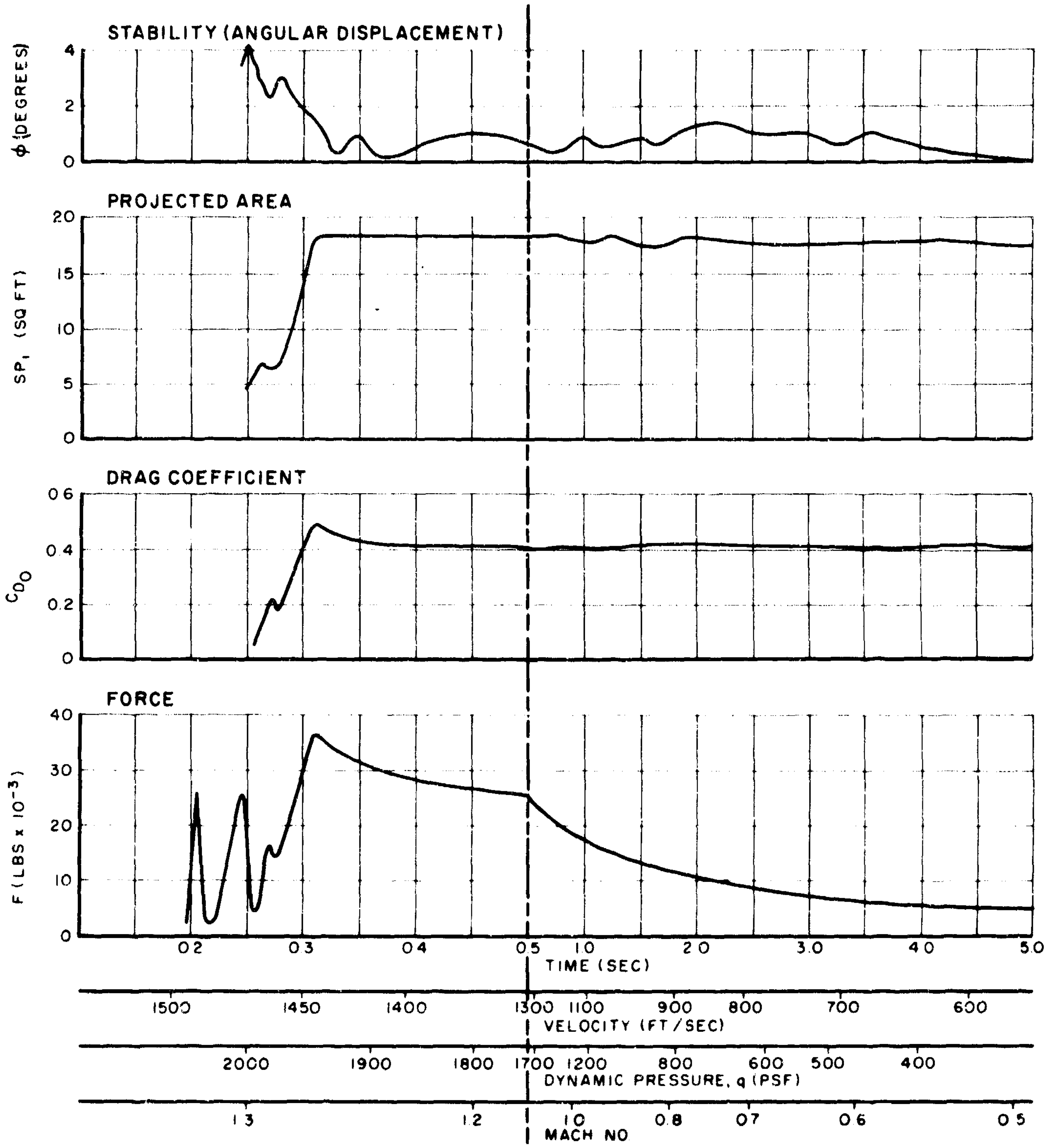

Figure 5.2.4. Performance Curves - Hemisflo Type EHR-137B-A1 Parachute, Test No. 16

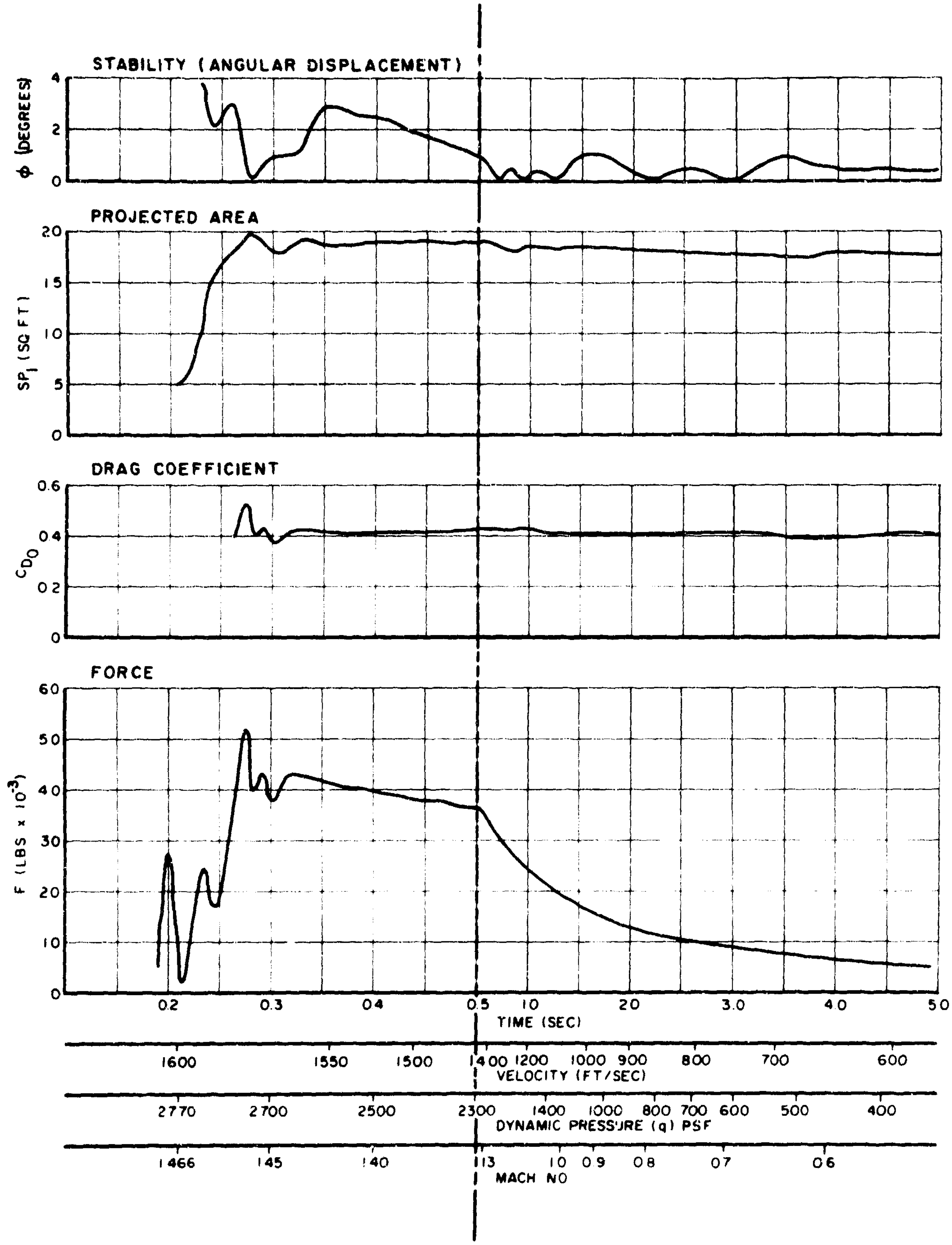

Figure 5.2.5. Performance Curves - Hemisflo Type EHR-137C Parachute, Test No. 7

The average opening shock factor of 1.20 represents two tests in which slightly higher values were obtained and one test in which a lower value was obtained. Because of the similarities in the steady state drag characteristics in both supersonic and subsonic operation, no effect upon the opening shock factor can be shown.

Steady state projected canopy areas were very similar on the three tests. Supersonic values were noted to be slightly greater than subsonic values although the effect may be one of dynamic pressure rather than a supersonic characteristic. Projected canopy area values for the supersonic speed region averaged between 18-19 square feet, and for the subsonic speed region these values averaged between 17 and 18.5 square feet. Based on the design projected area of this parachute, the steady state canopy area ratio variation obtained on these tests was between 125-135 percent.

Excellent stability was apparent on all tests with this parachute. Average angular displacement did not exceed 2.0 degrees at any time during steady state operation.

No structural damage was incurred during any of the tests.

Two Mach 1.3 tests were conducted with type EHR-137B designs from which little or no data resulted. On Test No. 3 with the original type EHR-137B design, all suspension lines severed at the skirt of the parachute during inflation (see Figure 5.2.6). Exact values of parachute force at the time of failure could not be determined because of extremely bad data. The best estimate from available information indicates that the force was 45,000 pounds or greater. Although this is a significantly larger force than would normally be expected, it should not have been sufficient to fail twenty 4500 pound lines. A possible explanation lies in the fact that the 1 inch 4500 pound webbing that was used, although specified as a new MIL-W-4088 webbing, did not have weave characteristics similar to other MIL-W-4088 webbings and therefore different elongation and response behavior.

No other significant canopy damage resulted from the test.

On Test No. 14, a modified version of the type EHR-137B parachute was to have been tested. This parachute, type EHR-137B-A1, was the same design as the original parachute but had 1 inch-6000 pound suspension lines rather than the 1 inch-4500 pound line.

The parachute however was not deployed on this test. Shortly after rocket ignition, one of the rocket motors malfunctioned and damaged the deployment circuitry so that deployment could not be initiated.

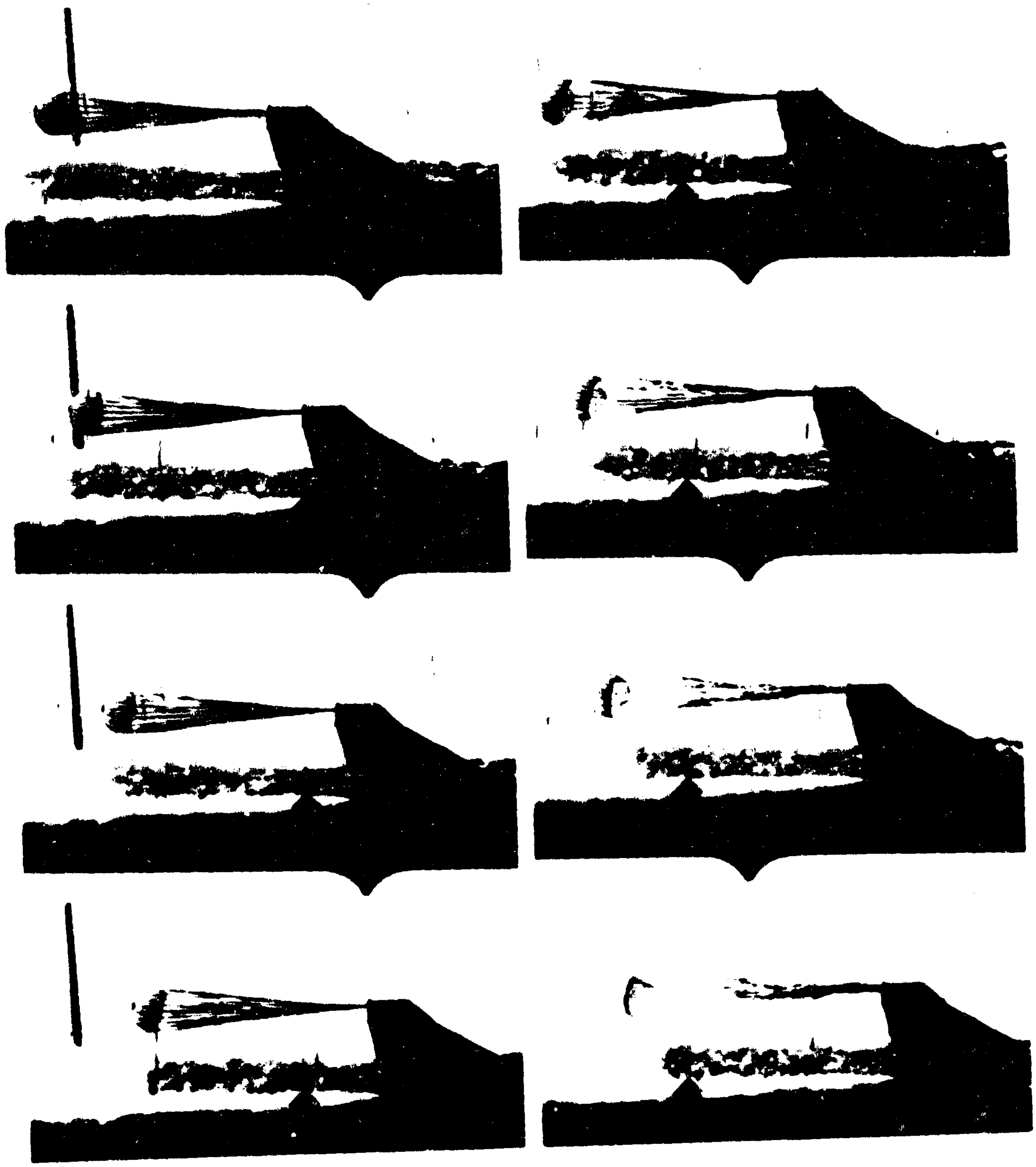

Figure 5.2.6. Sequence Showing Suspension Line Failure of Hemisflo Type EHR-137B Parachute on Test No. 3

As discussed earlier in this section, this parachute was subsequently tested successfully on Test No. 16.

5.2.3.2 Hemisflo Type EHR-138 Parachute

The Hemisflo Type EHR-138 parachute was a 5.54 foot nominal diameter, 16 gore configuration having a 10 percent fully extended skirt and a total porosity of 25.70 percent.

Only one strength version of this parachute, a Mach 1.3 type EHR-138B was tested on the program on Test No. 6.

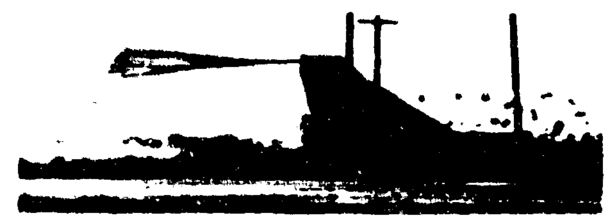

Figure 5.2.7. Hemisflo Type EHR-138B Parachute in Operation on Test No. 6

A good deployment and inflation was obtained on this test at a Mach number of 1.295 and a dynamic pressure of 2142 psf. Figure 5.2.7 shows the parachute in operation.

Performance curves for the test are shown in Figure 5.2.8.

This test was the only one of the Hemisflo type parachute tests in which a difference was noted between the supersonic and subsonic drag coefficients. There was also a marked increase of drag coefficients over those experienced on other tests. In the supersonic regime, the drag coefficient varied between 0.42 and 0.47. This is 10 to 15 percent over the average of the other tests. Subsonically, the drag coefficient varied between 0.46 and 0.52, a variation as high as 25 percent from the expected average.

It is unfortunate that photographic data was not obtained on this test. Lack of this data prevented the acquisition of inflation information necessary to substantiate the increase in drag coefficients obtained on the test. The small porosity difference in the design is obviously not sufficient to account for the change.

Stability data, also measured photographically, was not obtained on the test because of the failure of the on-board photo instrumentation.

On the basis of the steady state drag information obtained the opening shock factors measured were 1.32 and 1.19 for supersonic and subsonic conditions, respectively.

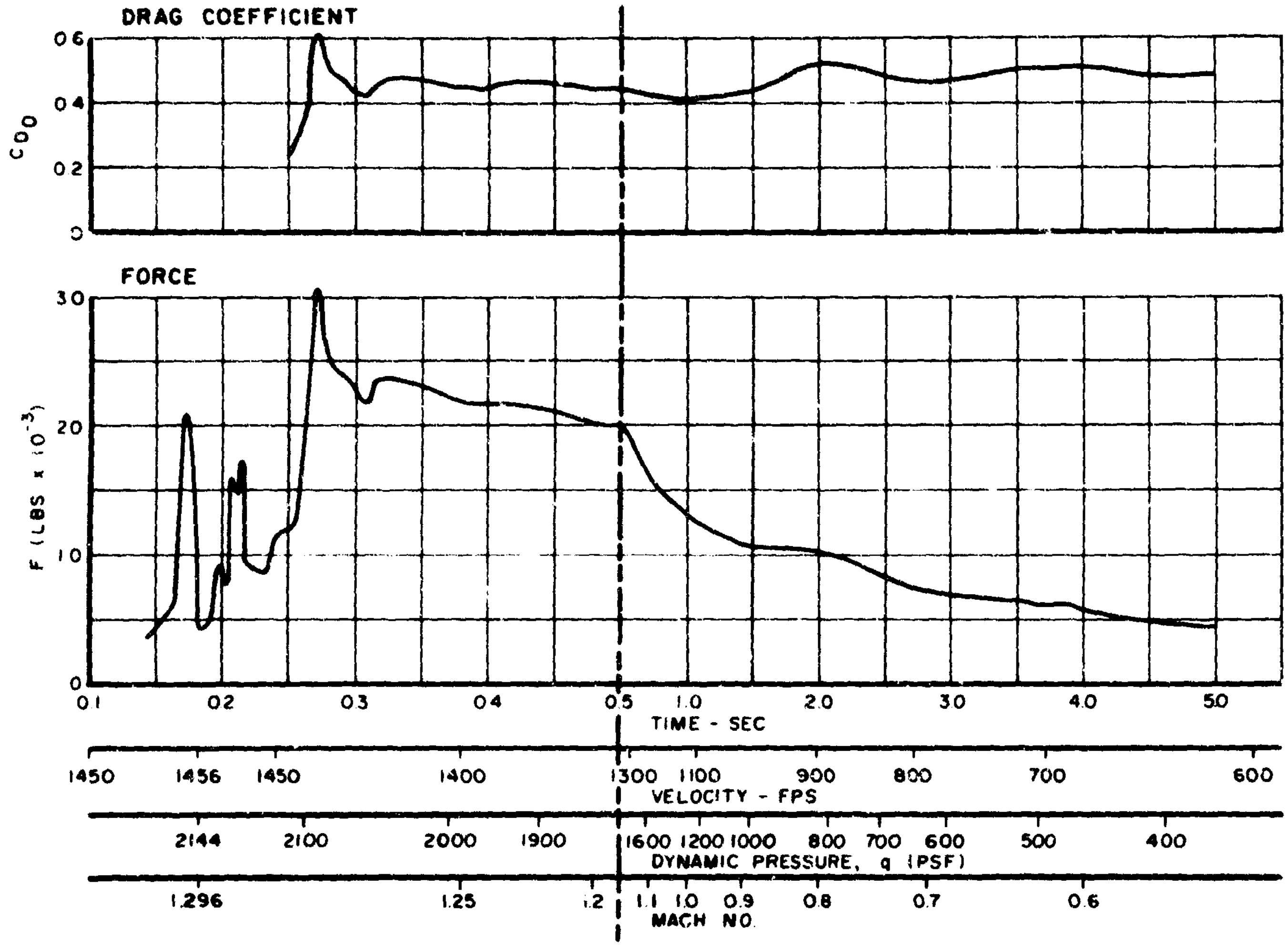

Figure 5.2.8. Performance Curves-Hemisflo Type EHR-138B, Parachute, Test No. 6

There was no operational canopy or line damage to the parachute as a result of the test.

5.2.3.3 Hemisflo Type EHR-139 Parachute

The Hemisflo Type EHR-139 parachute was a 4.12 foot nominal diameter, 16 gore configuration having a 10 percent fully extended skirt and a total porosity of 25.19 percent.

Only one parachute, the type EHR-139B, a Mach 1.3 design, was tested on the program on Test No. 8.

Except for an excessively high snatch force, a good deployment and inflation was obtained. Deployment occurred at Mach No. 1.288

and a dynamic pressure of 2131 psf. Immediately after inflation, however, the parachute system started to rotate. Rotation continued until, at approximately 3.0 seconds, the parachute collapsed. In the collapsed state, the parachute unwound sufficiently to become reinflated at approximately 4.8 seconds. At approximately 6.0 seconds, the parachute had again rotated itself into a collapsed state. Recovery from this condition was not attained by the time of parachute cutoff. Figure 5.2.9 shows the parachute in operation immediately after deployment and inflation.

Figure 5.2.9. Hemisflo Type EHR-139B Parachute in Operation on Test No. 8

In the three seconds of operation before the initial collapse of the parachute, sufficient information was obtained to provide drag, inflation and stability data. Although this portion of information is primarily supersonic data, the available transonic and subsonic data indicate that there is essentially no change indicated in average performance characteristics through the range tested. This also agrees with the behavior encountered on the majority of other Hemisflo type parachute tests.

Performance curves showing the unusual behavior of the type EHR-139B parachute on Test No. 8, is shown in Figure 5.2.10.

The drag coefficient averaged 0.39 to 0.42 after attaining steady state operation and prior to collapse of the parachute. Canopy areas, during this same period of time, varied between 5.8 and 6.3 square feet, the average area being approximately 6.1 square feet. On the basis of the design projected canopy area of the parachute, the area ratio was approximately 120 percent.

The parachute exhibited good stability on the test. Oscillation data indicated maximum angular displacements of approximately 2.0 degrees, with the average being well under 1.0 degree during the major part of the test.

No structural damage was incurred to the test parachute during the test.

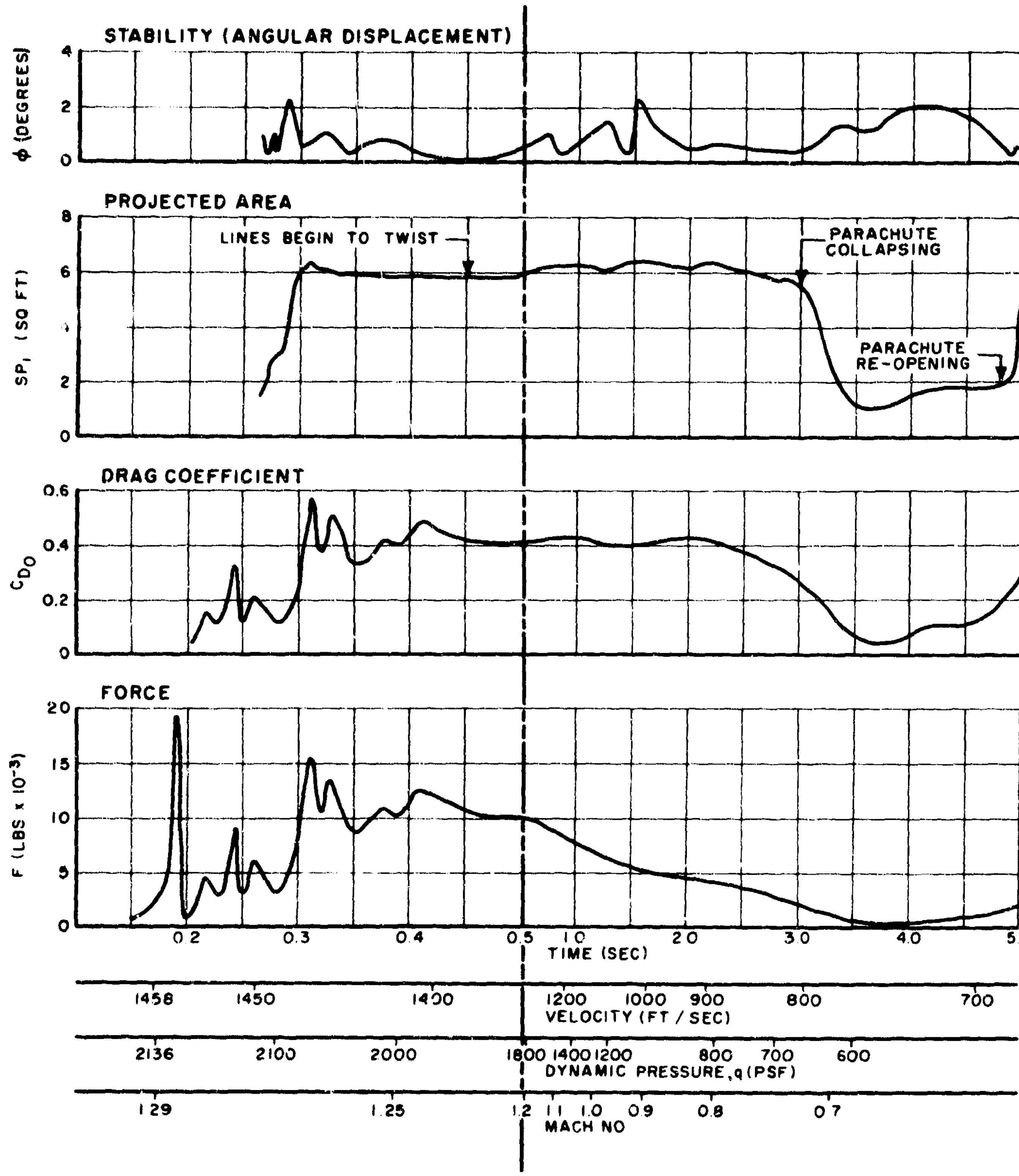

Figure 5.2.10. Performance Curves - Hemisflo Type EHR-139B Parachute, Test No. 8

5.3 20 DEGREE CONICAL RIBBON TYPE PARACHUTES - REEFING TESTS

5.3.1 General

The basic conical ribbon type parachute is a shaped parachute with a design geometric configuration equivalent to a right regular pyramid. The gores of the parachute, represented by the sides of the pyramid are, like in the familiar flat circular ribbon type parachute design, composed of a grid of horizontal ribbons spaced and retained at close intervals by one or more vertical ribbons. Radial bands extend from the vent or apex of the pyramid to the skirt or base, at the sides of each gore. These bands join adjacent gores together along the edges formed by the intersection of the faces of the pyramid and transfer the aerodynamic forces developed in the canopy to the attached suspension lines.

Figure 5.3.1 illustrates the geometry of a typical conical ribbon type parachute and shows a typical gore assembly. For the 20 degree conical ribbon type parachute used on the tests in this series the angle, α, was 20 degrees. The design apex angle was therefore 140 degrees.

Construction of the 20 degree conical ribbon type parachute was based on standard flat circular ribbon type parachute procedure as found in the applicable Military Specification (Reference 6).

5.3.2 Test Program

Three tests were conducted with the basic 20 Degree Conical Ribbon Type 20CR150B parachute, a 16 gore design having a total porosity of approximately 24 percent. Two of the tests were made with 20 percent reefing and one test was made with 30 percent reefing. Percent reefing, as referred to here, is the same as the reefing ratio and is defined as the ratio of drag area of the reefed parachute canopy to the drag area of the fully inflated canopy (Reference 1). All parachutes were designed for deployment at Mach 1.3 test conditions and all three tests conducted had deployments in this general area.

Major dimensional details and materials used in fabrication of the parachutes are listed in Table 5.3.1. Applicable materials and related material specification are tabulated in Table 5.3.2.

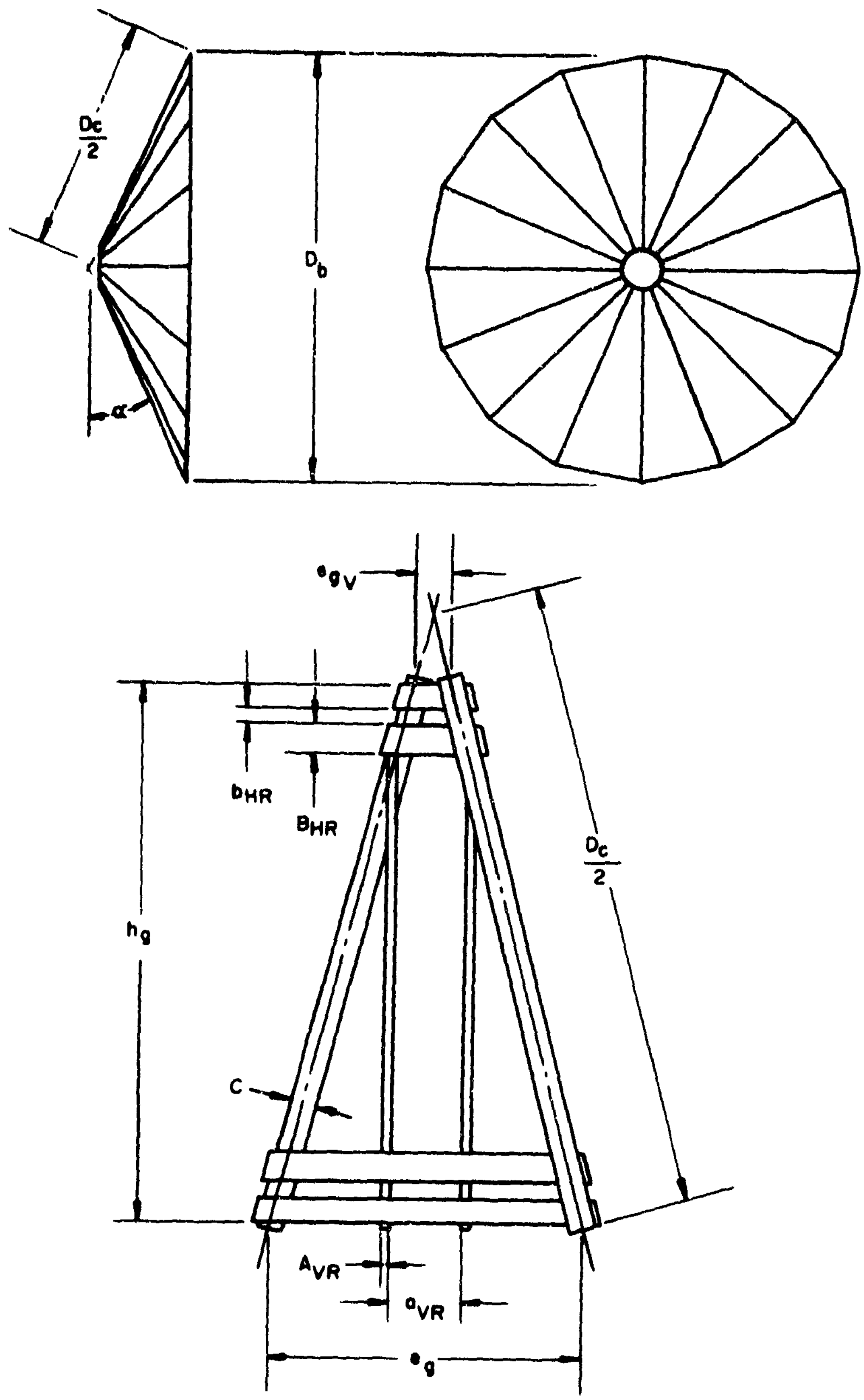

Figure 5.3.1. Geometry and Gore Layout - Conical Ribbon Type Parachute

TABLE 5.3.1

PHYSICAL DETAILS AND DIMENSIONS OF 20 DEGREE CONICAL RIBBON TYPE PARACHUTES

Parachute Type Number	20CR150B	20CR150B-A1	20CR150B-A2
Nominal Diameter, D_o (Ft.)	8.44	8.44	8.44
Canopy Area, S_o (Sq. Ft.)	56	56	56
Reefing, Percent Drag Area	20	20	30
Porosity, Total, λ_t (Percent)	24.17	24.17	23.76
No. of Gores and Suspension Lines	16	16	16
No. of Horizontal Ribbons	15	15	15
No. of Vertical Ribbons	4	4	4
Suspension Line Length (Ft.)	8.44	8.44	8.44
Length of Gore, h_g (In.)	44.9	44.9	44.9
Width of Gore at Skirt, e_g (In.)	19.25	19.25	19.25
Width of Gore at Vent, e_{g_v} (In.)	2.82	2.82	2.82
Reefing Line Length (Ft.)	4.38	4.38	5.96
Spacing Between Vertical Ribbons, a_{VR} (In.)	3.0	3.0	3.0
Spacing Between Horizontal Ribbons, b_{HR} (In.)	1.06	1.06	1.06
Suspension Line Material	9/16-1500	1x3000	1x6000
Horizontal Ribbon Material	2x1000	2x1000	2x1000
Vertical Ribbon Material (2 Ply)	9/16-500	9/16-500	9/16-500
Radial Band Material (2 Ply)	2x1000	2x1000	2x1000
Reefing Line Material	Cord 750	3/4-2250	1x6000
Weight, Parachute and Lines (Lbs)	9.1	14.3	18.0
Cook TCD Specification Number	596-8923	596-8923A	596-8923B
Used On Test Number	4	10	20

BEST AVAILABLE COPY

TABLE 5.3.2

MATERIALS USED IN 20 DEGREE CONICAL RIBBON TYPE PARACHUTES

PART	MATERIAL	SIZE-STRENGTH	SPECIFICATION
Horizontal Ribbons	Ribbon, Nylon	2 In. - 1000 Lb.	MIL-R-5608-E II
Vertical Ribbons	Ribbon, Nylon	9/16 In. - 500 Lb.	MIL-W-4088-I
Radial Ribbons	Ribbon, Nylon	2 In. -1000 Lb.	MIL-R-5608-E II
Suspension Lines	Webbing, Nylon	9/16 In. -1500 Lb. 1 In. -3000 Lb. 1 In. -6000 Lb.	MIL-W-5625 MIL-W-5625 MIL-W-4088-XVIII
Skirt Reinforcing	Ribbon, Nylon	2 In. - 2000 Lb.	MIL-R-5608-IV
Vent Reinforcing	Webbing, Nylon	1 In. - 3000 Lb.	MIL-W-5625
Reefing Line	Cord, Nylon Webbing, Nylon Webbing, Nylon	750 Lb. 3/4 In. - 2250 Lb. 1 In. - 6000 Lb.	MIL-C-7215-III MIL-W-5625 MIL-W-4088-XVIII
Pocket Bands	Webbing, Nylon	1 3/4 In. -3600 Lb.	MIL-W-4088-VIII
Butterflies	Webbing, Nylon	3/4 In. -2250 Lb.	Mil-W-5625
Thread	Nylon	Sizes E, F, FF, 3 Cord, 5 Cord	MIL-T-7807

5.3.3 Parachute Performance

Performance summary data for the 20 degree conical ribbon type parachutes used on the three tests conducted in this series are presented in Table 5.3.3. Details of the performance of the parachute in each of the tests conducted are presented in the following paragraphs.

5.3.3.1 20 Degree Conical Ribbon Type 20CR150B Parachute

The Conical Ribbon Type 20CR150B parachute was a 8.44 foot nominal diameter, 16 gore parachute having a geometric porosity of 24.17 percent. This parachute was permanently reefed to a reefing ratio of 20 percent by installation of a fixed reefing line at the canopy skirt.

Only one test, No. 4, was conducted with this particular design because of the failure of all suspension lines at or near the canopy attachment. The failure occurred at a time estimated to be at the point of maximum opening force. This information is based on photographic data since reliable parachute force data was not obtained on the test. As a result, neither the times involved nor the forces which caused the failure can be determined accurately.

5.3.3.2 20 Degree Conical Ribbon Type 20CR150B-A1 Parachute

The -A1 revision of the type 20CR150B parachute was, like the original design, an 8.44 foot nominal diameter, 16 gore parachute. Modification to the parachute, which consisted mainly of the application of stronger suspension lines, altered the total porosity slightly to 23.76 percent. Like the original parachute, the modified version was permanently reefed to a reefing ratio of 20 percent by installation of a fixed reefing line.

On Test No. 10, this parachute was deployed at a Mach number of 1.337 and a dynamic pressure of 2301 psf. A good deployment was observed and the parachute appeared to attempt to inflate immediately after deployment. At approximately one-half second, during the transition through transonic velocity, the parachute collapsed and never re-inflated to the fully reefed drag area. Figure 5.3.2 shows this parachute in operation just after deployment and prior to collapse.

Performance curves for this test are shown in Figure 5.3.3.

The average drag coefficient just before collapse of the parachute was approximately 0.078. The drag coefficient after collapse was approximately 0.05.

TABLE 5.3.3

PERFORMANCE SUMMARY DATA
20 DEGREE CONICAL RIBBON TYPE PARACHUTES

Test Number		4	10	20
Velocity, V_s (Ft/Sec)		~1400	1468	1516
Mach Number, M		1.27	1.337	1.340
Dynamic Pressure, q (Lb/Ft^2)		2070	2301	2297
Deployment Time, t_d (Sec)		-	0.191	0.172
Time To Reefed Max. Opening Force $(t_{so})_R$		-	0.067	0.070
Snatch Force, F_s (Lbs)		-	14,034	24,350
Maximum Opening Force, Reefed, F_{o_R} (Lbs)		-	11,086	24,500
Maximum Opening Force, Disreef, F_{o_D} (Lbs)		-	-	33.800
Avg. Reefed Drag Coefficient, $C_{D_{o\,R}}$		-	0.078	0.16
Avg. Disreef Drag Coefficient, C_{D_o}		-	-	0.47
Opening Shock Factor, X_R (Reefed)		-	1.10	1.19
Opening Shock Factor, X (Disreefed)		-	-	0.97
Area, Reefed (Sq. Ft.)		-	~5.25	8.8-9.3
Area, Disreefed (Sq. Ft.)		-	-	35-36
Stability, Reefed, ϕ (Degrees)		-	0-1.5	3-5
Stability, Disreefed, ϕ (Degrees)		-	-	4.5.5
Parachute Damage	Canopy	-	None	Minor
	Lines	All Failed	None	None

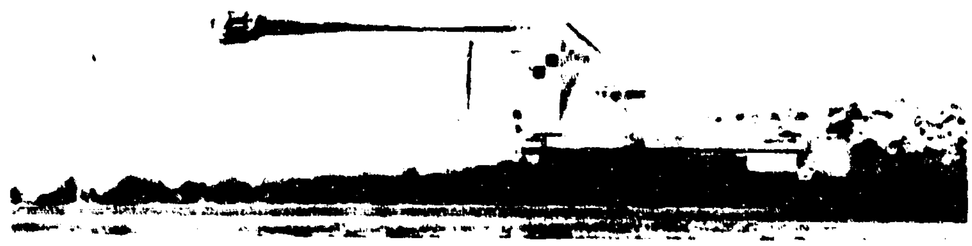

Figure 5.3.2. 20 Percent Reefed 20 Degree Conical Ribbon Type 20CR150B-A1 Parachute in Operation on Test No. 10

The opening shock factor of the reefed parachute, based on the steady state conditions just prior to collapse, was 1.10.

Effects of the collapse of the parachute are also evident in the measured inflated canopy areas. The areas varied between five and six square feet immediately after inflation and prior to collapse. After the transition point, the areas had decreased to between three and four square feet. Although the curve in Figure 5.3.3 shows the canopy area increasing slightly with time after the parachute had collapsed, the indicated increase included areas of the trailing parachute as it whipped back and forth. A more realistic indication of the true projected area is shown as a dotted line in the curve.

Parachute stability was very good throughout the entire test. The maximum oscillation reached 1.5 degrees at one point in the test. For the most part, however, oscillations were under 1.0 degree.

There was no major operational damage to the parachute as a result of the test. The first 4-5 horizontal ribbons near the skirt showed evidence of flutter strain, a condition which might well be expected in a reefed test condition.

5.3.3.3 20 Degree Conical Ribbon Type 20CR150B-A2 Parachute

The -A2 version of the type 20CR150B parachute was geometrically identical to the -A1 design except that this parachute was fitted with a reefing line giving a 30 percent reefing ratio and a reef-disreef capability after a one second time delay. The suspension lines were also strengthened to allow for the higher forces in both reef and disreef operation.

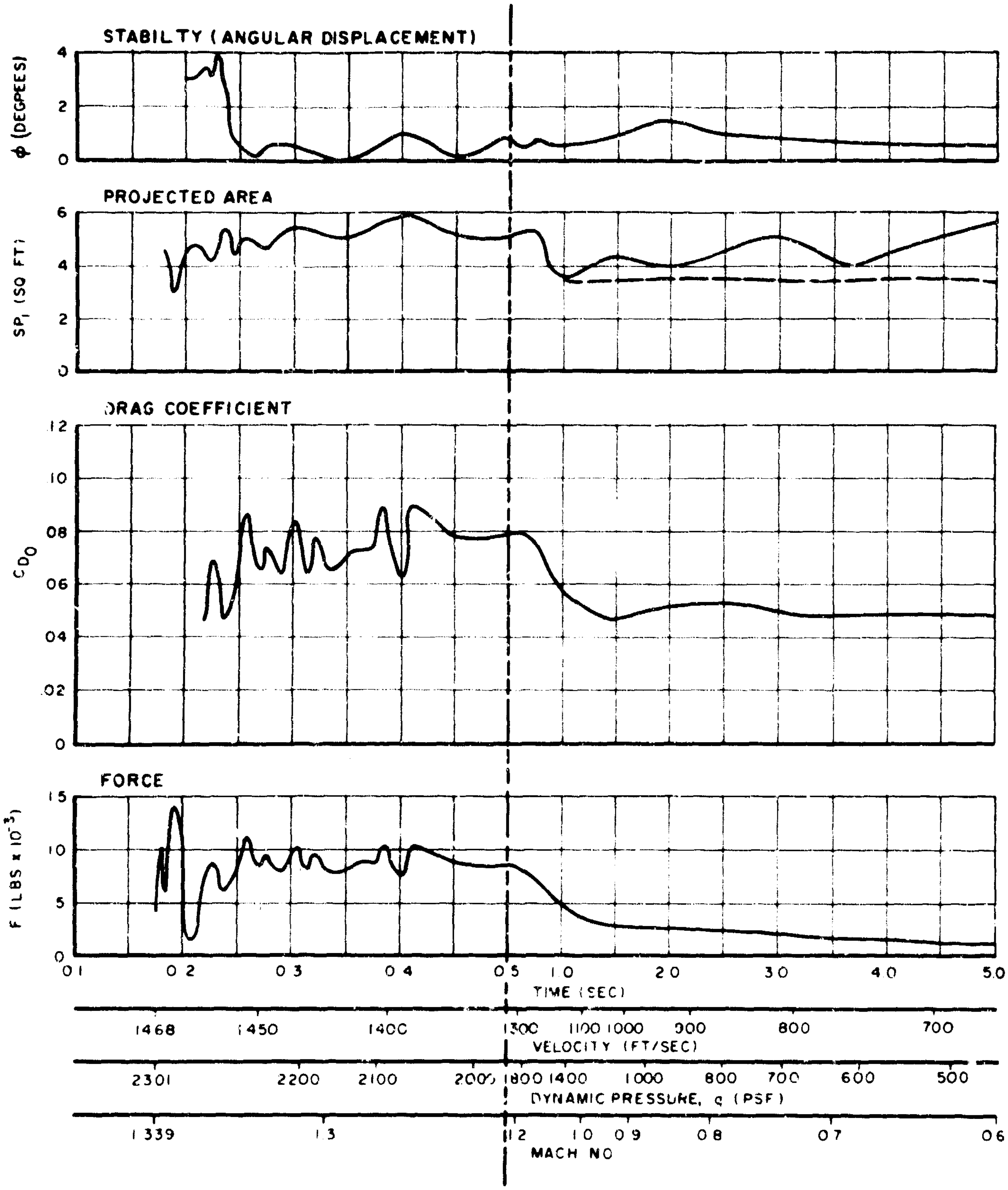

Figure 5.3.3. Performance Curves - 20 Degree Conical Ribbon Type 20CR150B-A1 Parachute, Test No. 10

This parachute was deployed, on Test No. 20, at a Mach number of 1.34 and a dynamic pressure of 2297 psf.

Performance curves for this test are shown in Figure 5.3.4.

Figure 5.3.5. 30 Percent Reefed 20 Degree Conical Ribbon Type 20CR150B-A2 Parachute in Operation on Test No. 20

A good deployment and reefed inflation was obtained. Immediately after the opening shock transients, the parachute attained an inflated area of approximately 9 square feet. This remained essentially constant until parachute disreef approximately one second later. The reefed drag coefficient during the same time interval was 0.12 to 0.14. Figure 5.3.5 shows the parachute in reefed operation.

Disreef occurred precisely at the intended time. At disreef, the maximum opening force peaked to approximately 140 percent of the reefed opening force. Although this is not optimum, it is not as severe as might be indicated since disreef opening shock factor was only 0.97 whereas reefed opening shock factor was 1.20.

After steady state operation had been attained in the disreef condition, the average drag coefficient was 0.46 to 0.48. The inflated canopy area corresponding to this was steady at 35 to 36 square feet.

Parachute stability was relatively good with no large oscillatory excursions during the test except during the disreefing process. During the reefed phase of the test, the average angular displacement was about 3 to 5 degrees. After disreef, the parachute drifted around at an average angular displacement of approximately 4.5 to 5.5 degrees. No rapid oscillatory displacements were evident in either the reefed or disreefed steady state portion of the test.

There was no major structural damage to the test parachute as a result of the test. Some flutter damage was evident, however, in the attachments of the horizontal ribbons to the two center vertical ribbons near the skirt of the canopy and slight stitching strain was observed in the vent ribbon attachments.

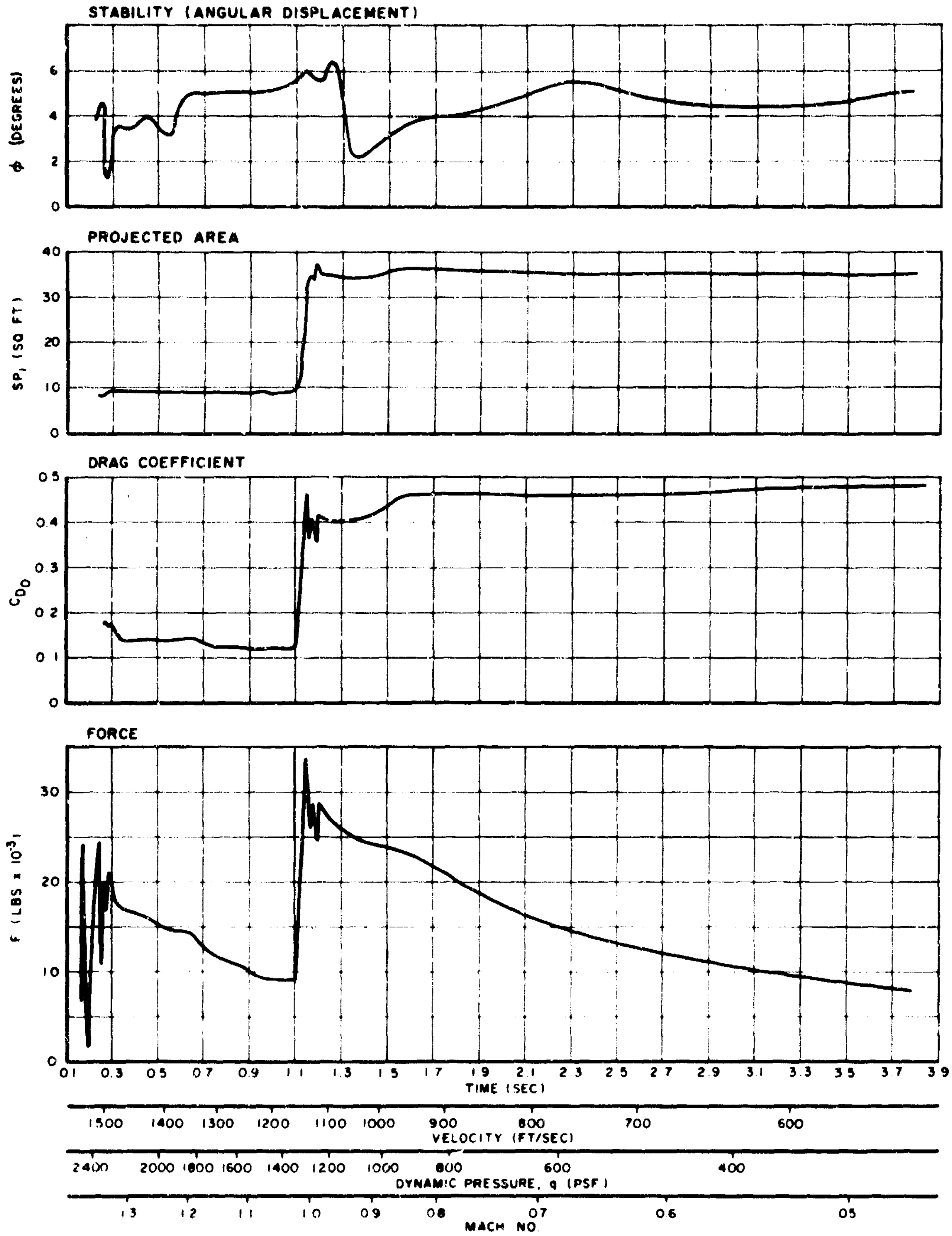

Figure 5.3.4. Performance Curves - 20 Degree Conical Ribbon Type 20CR150B-A2 Parachute, Test No. 20

5.4 SUPERSONIC GUIDE SURFACE (CONE-CUP) TYPE PARACHUTE

5.4.1 General

The Supersonic Guide Surface, or Cone-Cup Type Parachute, a flexible drag device configuration proposed by Dr. H. Heinrich of the University of Minnesota, consists of a textile type "cup" forming in its inflated state a body of revolution having the shape of a divergent conical frustum joined at its maximum diameter by a combination of torroidal segments which forms a convergent nozzle with an inflection near the trailing edge, and a cone made of polystrene foam molded within a thin spun aluminum conical form into which a nylon cone and suspension line system had previously been assembled. The cone is oriented along the longitudinal axis, and with respect to the cup portion of the device, by means of a suspension system consisting of suspension lines, radial lines and back lines.

An illustration of this parachute concept and the geometry of the parachute design tested in the program are shown in Figures 5.4.1 and 5.4.2.

5.4.2 Test Program

Three tests were conducted with the Supersonic Guide Surface Type parachute during the program. All of these tests were performed with 2.0 foot projected diameter, 12 gore designs having theoretical Mach 1.3 deployment capabilities. Construction of the parachutes was in accordance with design and fabrication information furnished by Dr. Heinrich, University of Minnesota. Major dimensional details of the parachute and materials used in its construction are shown in Table 5.4.1. A general listing of materials and the corresponding specifications are tabulated in Table 5.4.2.

5.4.3 Parachute Performance

Of the three tests, Numbers 19, 22 and 24, conducted with the Supersonic Guide Surface Type parachute, only one test, No. 22, provided a measure of performance and design information for this particular parachute type.

In Test No. 19, a Mach 1.1 test, the parachute was not deployed from the parachute compartment although all aspects of the deployment system operation apparently functioned normally.

Test No. 22, a repeat of Test No. 19, was another scheduled Mach 1.1 test with the same parachute as was used, but not tested, on Test No. 19. Deployment on this test, though not entirely normal, occurred at approximately Mach 1.04. Immediately after deployment, a portion of the deployment bag was noted to have remained on the lines of the parachute ahead of the inflated canopy. The bag proceeded to slide aft along the lines until it reached the

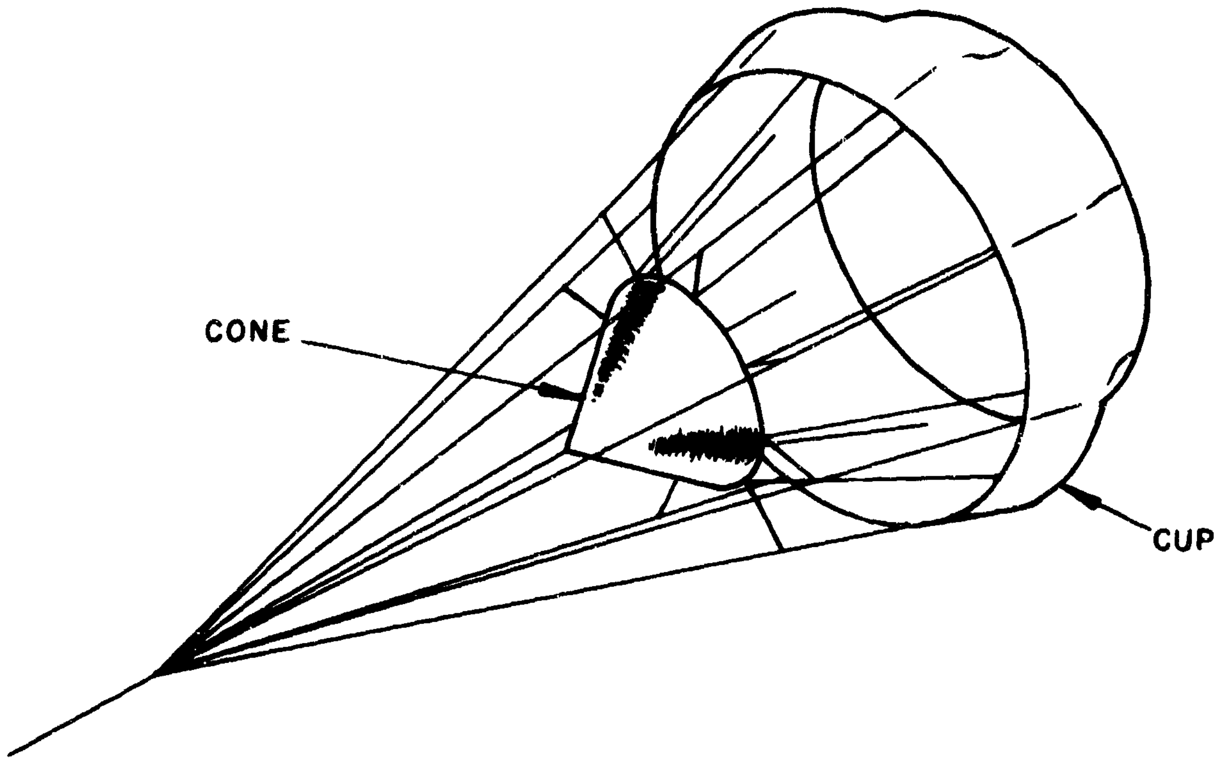

Figure 5.4.1. Typical Supersonic Guide Surface Type Parachute Concept

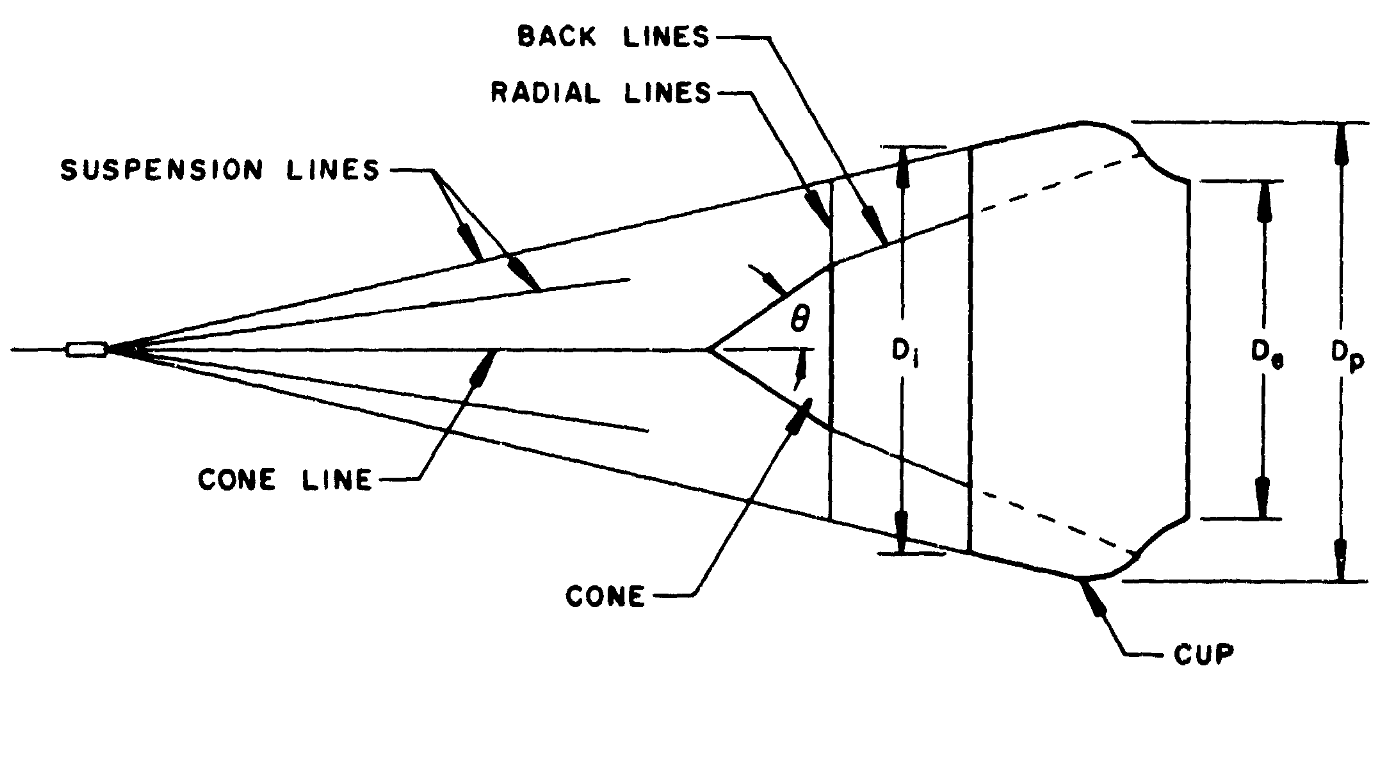

Figure 5.4.2. Geometry of Supersonic Guide Surface Type Parachute

TABLE 5.4.1

PHYSICAL DETAILS AND DIMENSIONS OF SUPERSONIC GUIDE SURFACE TYPE PARACHUTE

Design Diameter, D_p (Ft.)	2.0
Design Projected Area, S_p (Sq. Ft.)	3.14
No. of Gores and Suspension Lines	12
Suspension Line Length, L_s (Ft.)	5.08
Cone Line Length, L_C (Ft.)	3.92
Radial Line Length, L_r (Ft.)	0.386
Back Line Length, L_b (Ft.)	1.40
Cone Stand Off Distance, H (Ft.)	1.07
Cone Height, h_c (Ft.)	0.624
Cone Half Angle, θ (Degrees)	34
Exit/Inlet Area Ratio	0.49
Inlet Diameter, D_i (Ft.)	1.784
Exit Diameter, D_e (Ft.)	1.248
Weight (Lbs)	4.4
Used On Test Number	19, 22, 24
Cook TCD Specification Number	596-9025

TABLE 5.4.2

MATERIALS USED IN SUPERSONIC GUIDE SURFACE TYPE PARACHUTE

PART	MATERIAL	SIZE-STRENGTH	SPECIFICATION
Canopy (Cup)	Cloth, Nylon	14 Oz. -600 Lb.	MIL-C-8021-III
Suspension Lines	Webbing, Nylon	9/16 In. -1500 Lb.	MIL-W-5625
Cone Line	Webbing, Nylon	9/16 In. -1500 Lb.	MIL-W-5625
Radial Line	Cord, Nylon	750 Lb.	MIL-C-5040-III
Back Line	Webbing, Nylon	9/16 In. -1500 Lb.	MIL-W-5625
Canopy Reinforcing	Webbing, Nylon	1 In. - 3000 Lb.	MIL-W-5625
Cone	Cloth, Nylon *	14 Oz. -600 Lb.	MIL-C-8021-III
Thread	Nylon	E, FF, 3, 5	MIL-T-7807

* Cloth Cone Was Fitted With A Spun Aluminum Cone and Assembly Was Potted With "Aerothane" Foamed Polystyrene

canopy, collapsed the canopy, and then slid over the canopy assembly and freed itself from the parachute system. The collapsed canopy then reinflated. All of this occurred within the first two tenths seconds after initial inflation of the canopy. A photographic sequence illustrating this operation is shown in Figure 5.4.3.

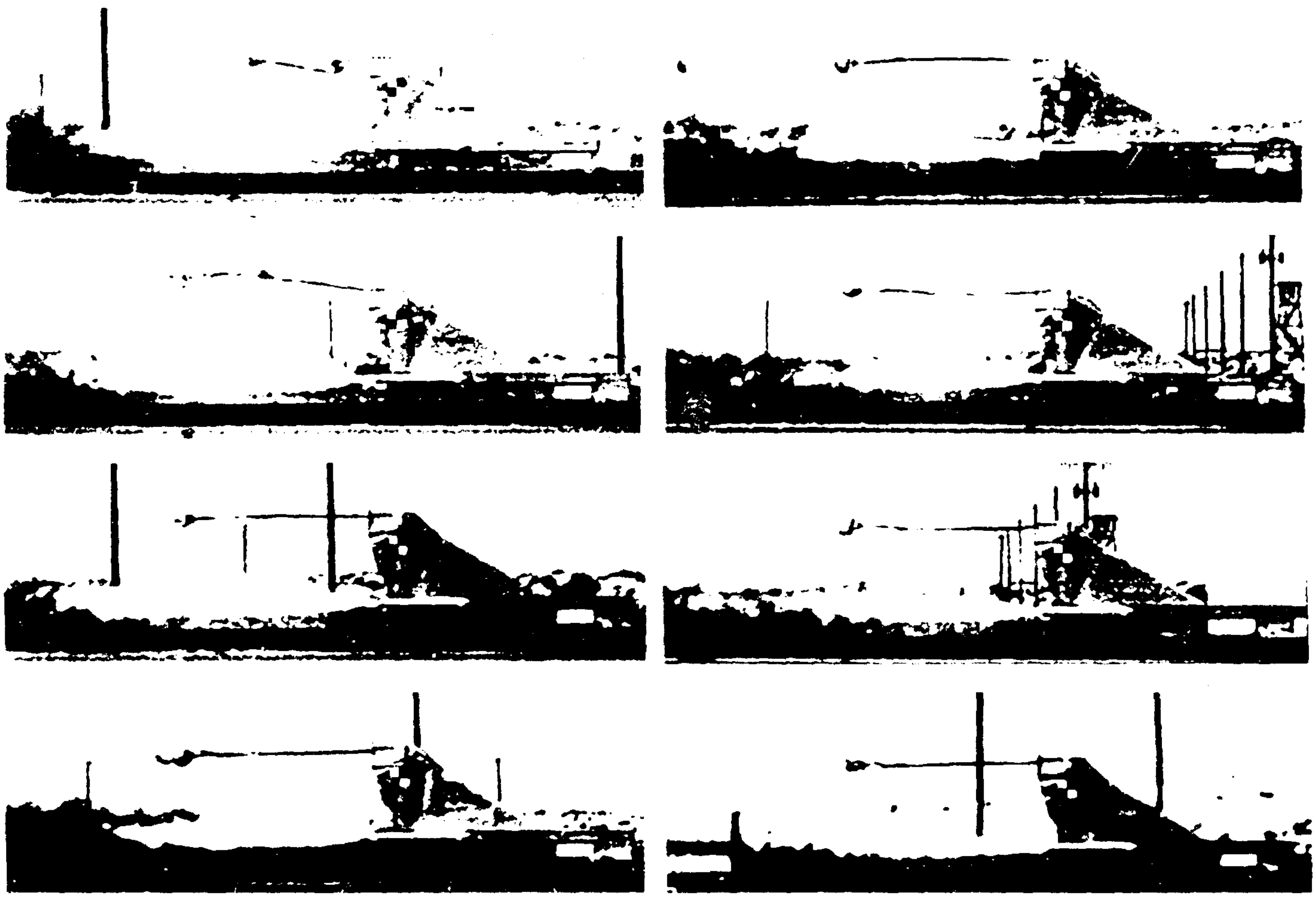

Figure 5.4.3. Sequence Showing Deployment Bag Entanglement and Partial Inflation of Supersonic Guide Surface Type Parachute on Test No. 22

On the basis of the theoretical inflated projected area of this parachute, average steady state inflation was approximately 80-90 percent. Variation from this ranged as low as 40 percent and as high as 120 percent and all areas were subject to rapid and irregular fluctuations in shape. The steady state subsonic drag coefficient, based on average steady state forces and design projected area, ranged from 0.3 at a time during the test when the areas were fluctuating widely, to about 0.8 near the end of the test when the areas were fairly steady and averaging about 80-90 percent inflation.

The parachute appeared to be fairly stable after steady state operation was attained. Although there was considerable relative movement between the cone and the rest of the canopy, the average angular displacement of the parachute was between 4 and 6 degrees.

On the basis of the performance of the parachute on Test No. 22, this design was again used on Test No. 24. This test was a Mach 1.3 deployment and resulted in severance of the canopy from the lines at or near full line stretch or peak force. This structural failure is illustrated in the sequence in Figure 5.4.4.

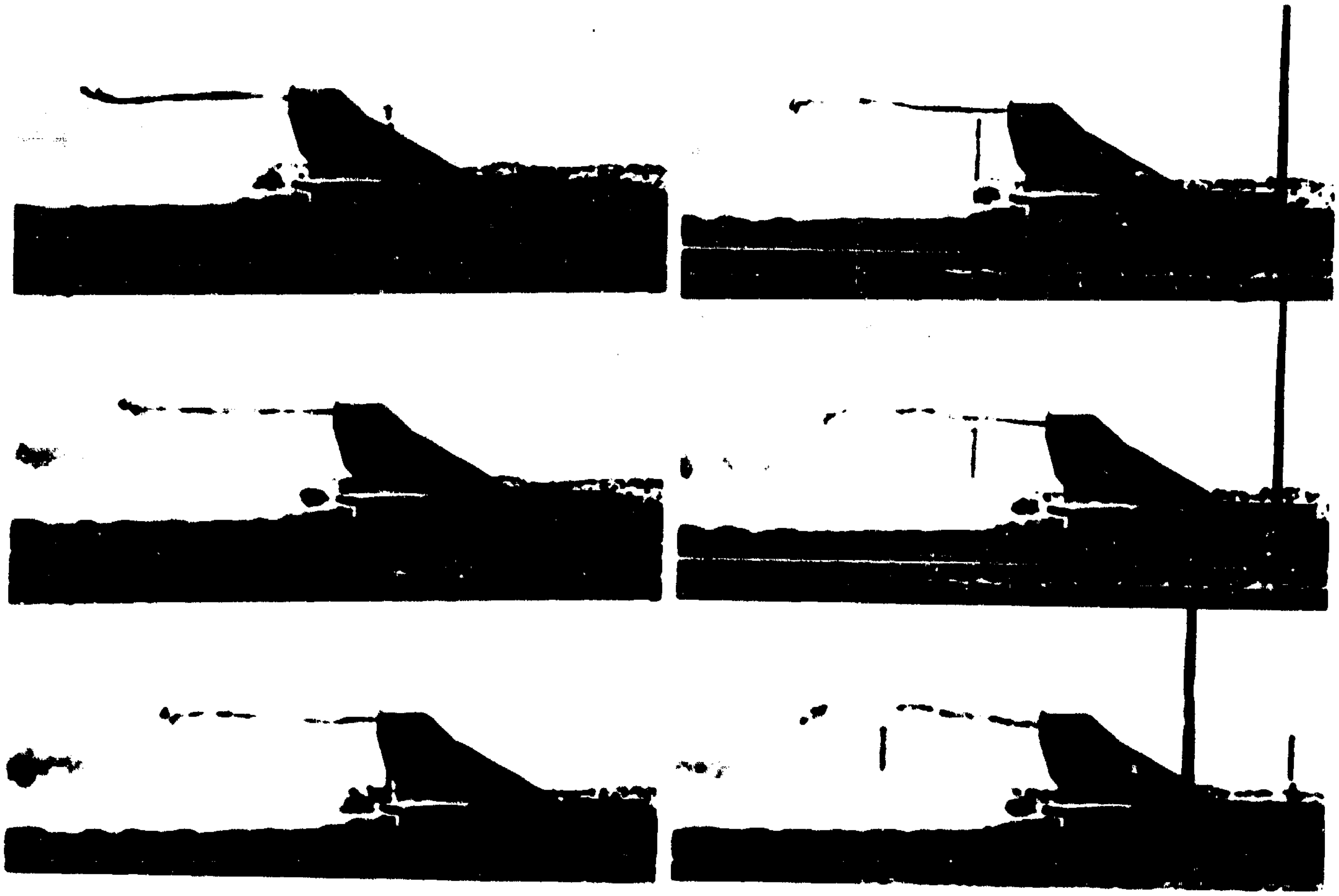

Figure 5.4.4. Sequence Showing Structural Failure of Supersonic Guide Surface Type Parachute on Test No. 24

SECTION 6

TEST VEHICLE SYSTEMS

6.1 TEST VEHICLE

All of the tests that were conducted on the program were conducted with the Tomahawk sled, a solid fuel rocket powered parachute test vehicle capable of operation in both single stage configuration and, with the addition of a noncaptive pusher vehicle, as a multiple stage vehicle. With a full complement of eight Aerojet 2.2 KS-11,000 rockets, the sled, in single stage configuration, developed approximately 90,000 pounds of thrust for a duration of 2.2 seconds. In this configuration, the sled could be accelerated to approximately Mach 1.2 at rocket engine burnout.

Originally designed and fabricated by Cook Electric Company for operation on the Air Force Flight Test Center High Speed Track Facility at Edwards Air Force Base, California, the Tomahawk sled was modified by the Track Test Division at the Air Force Missile Development Center, Holloman Air Force Base, New Mexico, for operation at that facility in the conduct of the current series of tests. Major modifications which were made to adapt the vehicle to the AFMDC installation included alterations to the slipper beams and fairings to accommodate the wider track gage, mounting of pull-away fixtures, knife blades and parachute release door, and installation of telemetry, cameras and space time equipment (Velocity Measuring System).

Another modification which was made to the Tomahawk vehicle consisted of the installation of adapters along each side of the main beam of the vehicle to accept two Javelin type rocket motors. This enhanced the economic use and versatility of the vehicle by extending single stage performance capability to the Mach 1.5 program requirements.

The sled is now identified as the AFMDC IDS 6301 Tomahawk sled.

A pusher stage was also used on a number of the test runs which were conducted on the program. This vehicle, identified as the IDS-5802-1, was an existing AFMDC vehicle which was modified to mate with the Tomahawk sled. Propulsion on the pusher consisted of four Aerojet 2.2 KS-11,000 rockets. The two-stage test vehicle-pusher combination was used on all Mach 1.3 tests.

Table 6.1.1 lists the propulsion units used on the test vehicle and shows the Mach numbers attained on each test.

Figures 6.1.1 and 6.1.2 show two views of the test vehicle as used in single stage and double stage operations.

Deceleration of the test vehicle at the end of the test was accomplished by air drag alone. The pusher vehicle, when used, was decelerated by water braking.

On two separate tests, Numbers 14 and 17, the igniter safety diaphragm failed on one of the 2.2 KS-11,000 rocket located in the left outboard position in the wedge fairing. These malfunctions caused the rockets to expel a large portion of the burning propellant gases forward into the fairing, and resulted in major sheet metal damage to the fairing. Rebuilding of the fairing was necessary after each of these malfunctions. After the second occurrence, modifications were made in the wedge fairing to permit operation of the vehicle without some portions of the upper and lower skin sections, thereby avoiding a pressure buildup within the fairing in the event of another malfunction. To further alleviate the possibility of another failure, the rocket complement was altered to include two Javelin rockets for five of the 2.2 KS-11,000 rockets on the Mach 1.1 and Mach 1.3 profiles. Delays to the program caused by the two rocket motor malfunctions were made up by accelerating the test schedule near the end of the test phase.

6.2 PARACHUTE DEPLOYMENT SYSTEM

All of the parachutes which were tested on this program were deployed directly aft from the test vehicle with a cover initiated pilot parachute deployment system. A piston bolt was used to remove the compartment cover and eject it into the airstream around the compartment. After its initial rearward movement, the cover assembly pulled the pilot parachute bag away from the negative pressure region immediately behind the parachute compartment and into the airstream aft of the vehicle. As the rearward travel was stopped, the inertia of the cover assembly removed the bag from the pilot parachute allowing it to inflate. At the same time, an acceleration lock, attached to the pilot parachute riser, was released from the harness assembly holding the test parachute pack in the compartment. The pilot parachute riser, now attached directly to the parachute pack through a bridle of heavy webbing, pulled the test parachute pack from the compartment and aft from the vehicle. To assure an orderly, lines first deployment, the test parachute riser and suspension lines were secured by break lines to a tray, or flap, external of the main stowage compartment of the pack. The test parachute was also secured to the inside of the parachute pack by closure stows, a combination of locking loops and line stows for the suspension lines

TABLE 6.1.1

TEST VEHICLES, PROPULSION AND PERFORMANCE

Test No.	AFMDC Sled Run No.	No. of Rockets On Test Vehicle	No. of Rockets On Pusher Vehicle	Burnout Mach Number
1	33-1A1	8 AJ	-	1.112
2	33-1B2	8 AJ	-	1.080
3	33-2A1	8 AJ	4 AJ	1.346
4	33-2B1	8 AJ	4 AJ	1.270
5	33-2D1	8 AJ	4 AJ	1.320
6	33-2E1	8 AJ	4 AJ	1.296
7	33-3A1	8 AJ & 2 JV	–	1.467
8	33-2F2	8 AJ	4 AJ	1.289
9	33-2G2	8 AJ	4 AJ	1.313
10	33-2H2	8 AJ	4 AJ	1.338
11	33-3B1	8 AJ & 2 JV	-	1.472
12	33-2I2	8 AJ	4 AJ	1.399
13	33-3C2	8 AJ & 2 JV	-	1.500
14	33-2J2	8 AJ	4 AJ	1.280
15	33-1C2	8 AJ	-	1.098
16	33-2K2	8 AJ	4 AJ	1.335
17	33-3D2	8 AJ & 2 JV	-	1.423
18	33-2L2	3 AJ & 2 JV	4 AJ	1.357
19	33-1D2	2 JV	4 AJ	1.080
20	33-2M2	3 AJ & 2 JV	4 AJ	1.343
21	33-2N2	3 AJ & 2 JV	4 AJ	1.336
22	33-1E2	2 JV	4 AJ	1.046
23	33-1F2	2JV	4 AJ	1.033
24	33-2O2	3 AJ & 2 JV	4 AJ	1.334

Notes: AJ - Aerojet-2.2 KS-11,000 Rocket
JV - Lockheed (GCR) Javelin Rocket

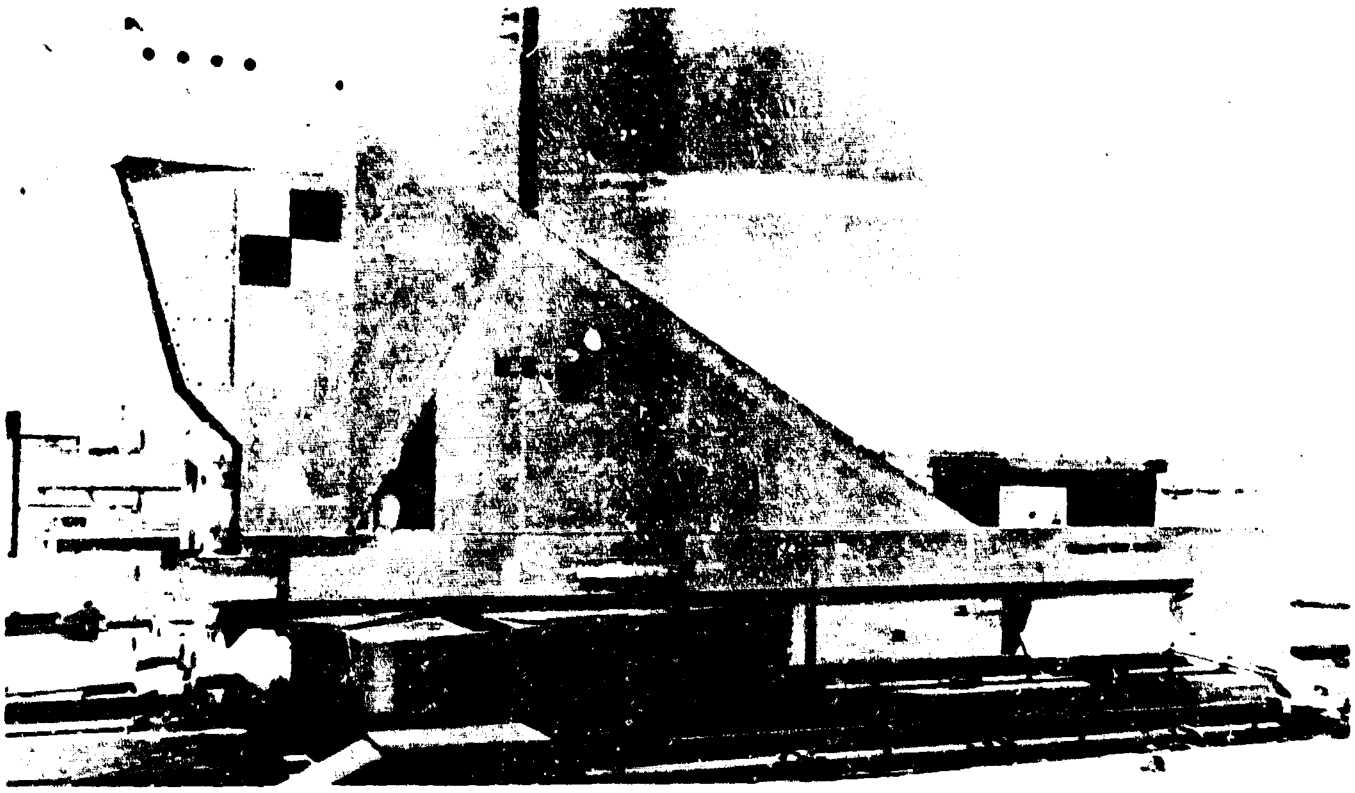

Figure 6.1.1. Tomahawk Parachute Test Vehicle

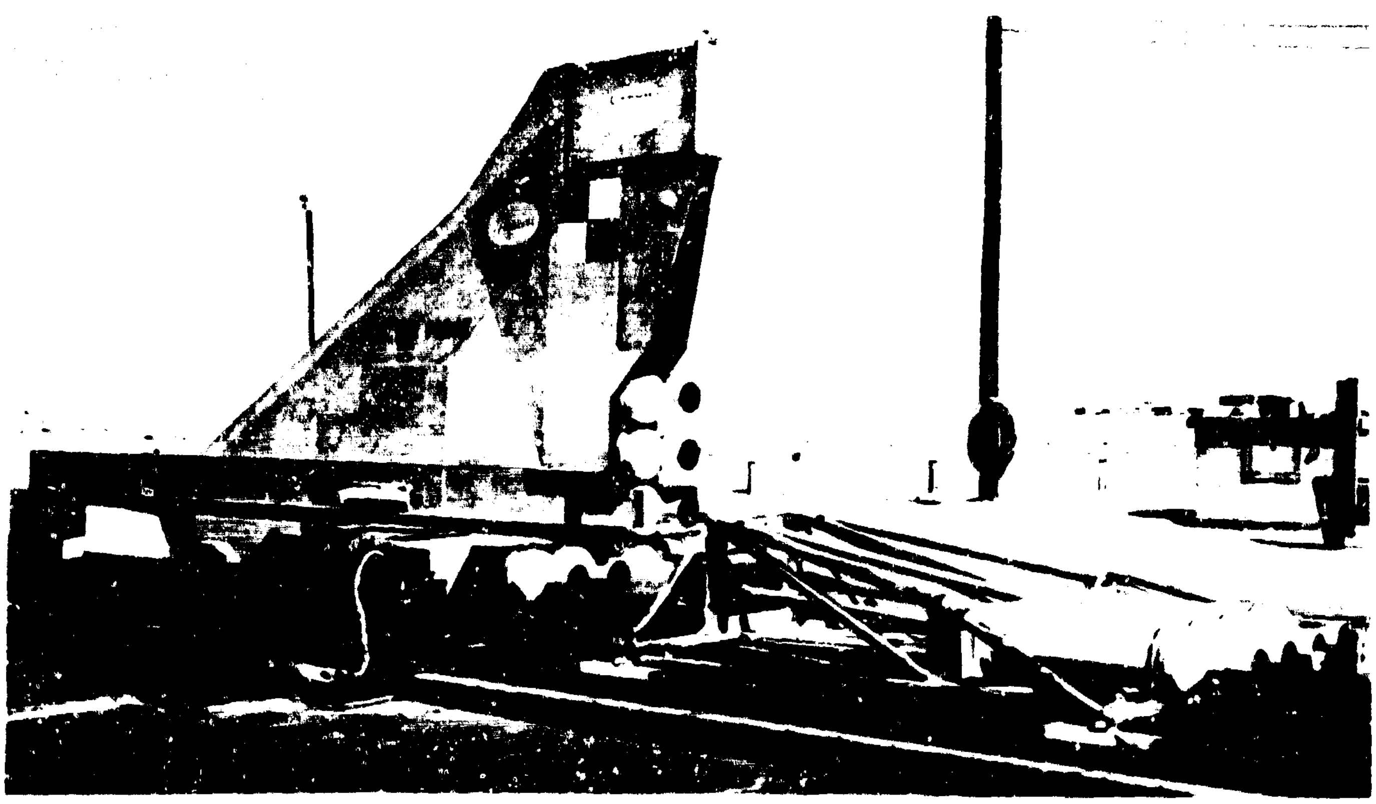

Figure 6.1.2. Tomahawk Parachute Test Vehicle with IDS-5802-1 Pusher Vehicle for Two Stage Operation

coming from the closed pack and by a break line attached to the vent lines of the test parachute and to the pack bridle confluence point. A pictorial diagram showing physical details of the components of the deployment system is shown in Figure 6.2.1.

The parachute compartment cover for the Tomahawk vehicle consisted of a solid metal sheet of 1/4 inch aluminum with an aluminum channel locking bar riveted to the vertical centerline of the cover. To position the cover and restrict its movement, the locking bar was tailored to fit a grooved tab on the lower edge of the compartment. The upper edge of the cover was fitted with an angle which mated with a fitting on the top, aft edge of the compartment. This fitting contained the piston bolt which secured the cover at the top end and also initiated the cover release function. The piston bolt charge consisted of dual six-grain S-68 squibs. Details of the parachute compartment cover release system are shown in Figure 6.2.2.

6.3 PARACHUTE RELEASE SYSTEM

Reliable release of the test parachute prior to terminal deceleration of the test vehicle is an important consideration to proper evaluation of operational damage of the test parachute. If the parachute is not released before the test vehicle brakes to a halt, the parachute will drop to the track behind the test vehicle and be dragged along until the vehicle is finally stopped. This would severely hinder damage evaluation by adding track induced damage to any damage which may have resulted from operational causes.

The parachute release system which was used on all of the tests in this program was a half-ring type attachment and release device designed by Cook Electric Company for this particular application. The basic assembly consists of three main components; the vehicle attachment, the parachute line attachment, and the half-rings. A typical attachment and release device of this type is illustrated in Figure 6.3.1.

The vehicle attachment end is tied into the vehicle structure, through the load transducer (tensiometer) and a flexible link assembly. This part remains with the vehicle after the separation is initiated.

The parachute line attachment end mates with the face of the vehicle attachment end and has provisions for connecting and securing the parachute line loops. The face of this part is recessed on opposite sides to accept electric blasting cap charges.

The half-rings are installed over the blasting caps and mating attachment ends in such a manner that the assembly is effectively locked together.

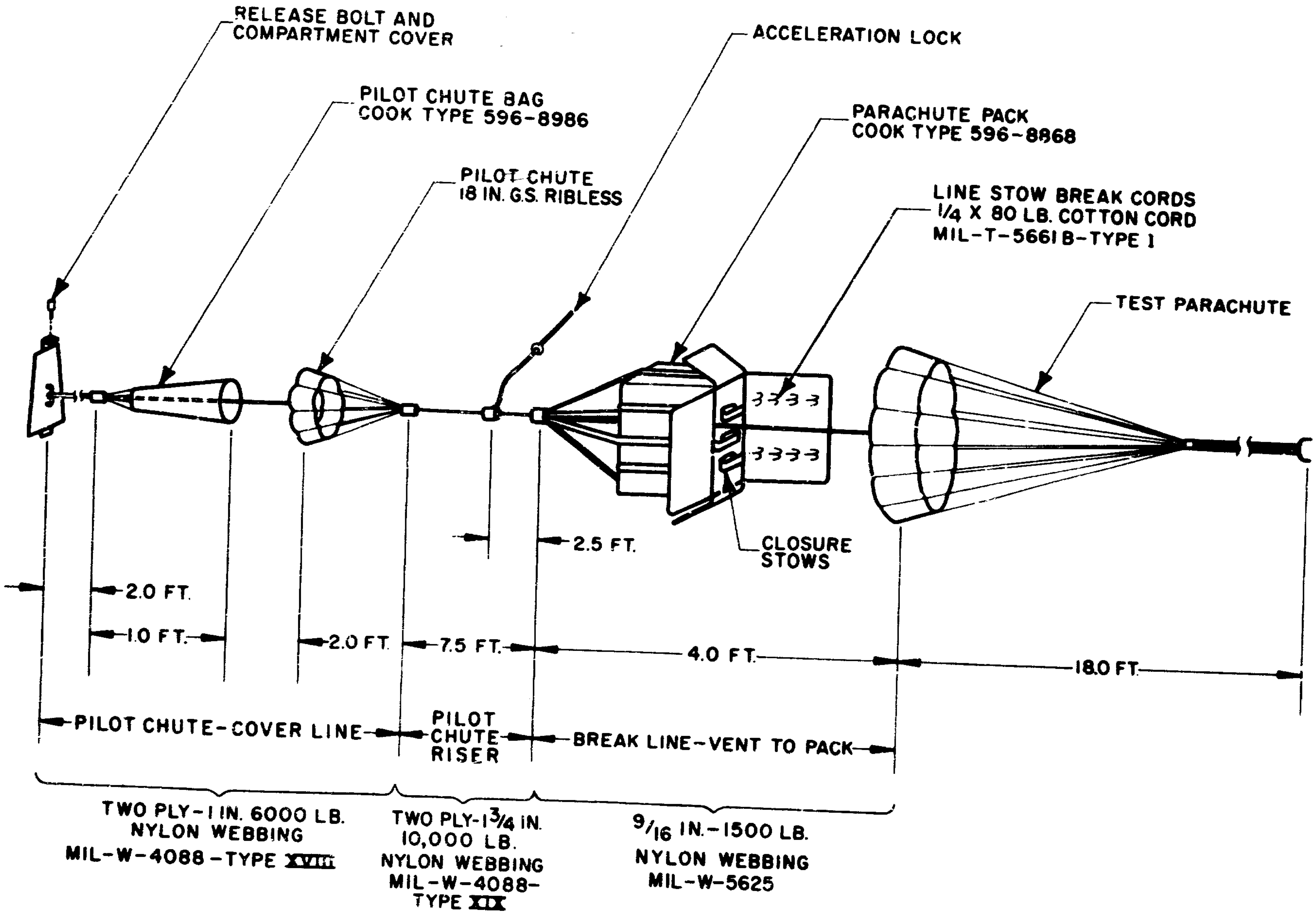

Figure 6.2.1. Deployment System Components

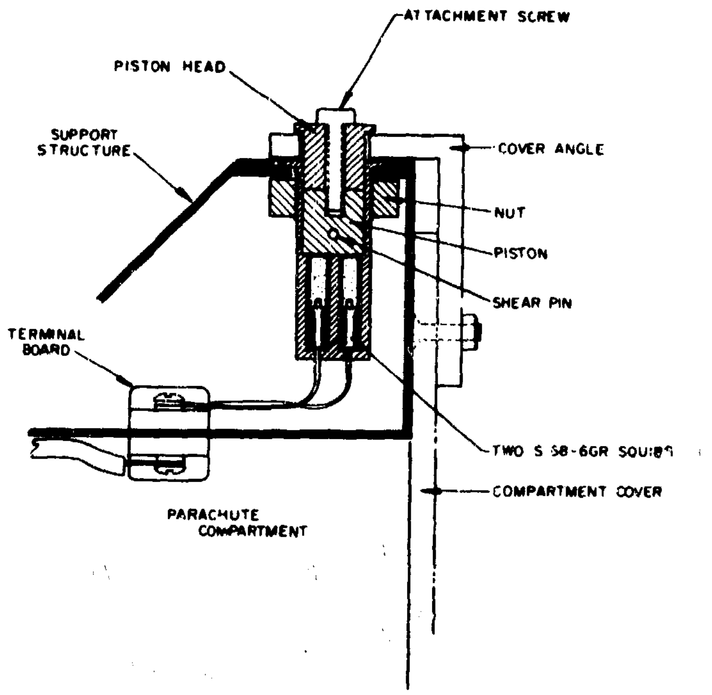

Figure 6.2.2. Compartment Cover Release System

Small shear screws are inserted to hold the assembly firmly together until separation is initiated.

Separation is accomplished when the blasting caps are energized. Sufficient force is exerted to shear the screws and blow the half-rings from the assembly. The two attachment ends are then free to separate.

All of the tests during this program were conducted using this system of parachute release with the separations being initiated within the parachute compartment. No damage to the compartment or components within the compartment ever resulted. This also prevented loss of the half-rings and eliminated the danger of the half-rings becoming projectiles.

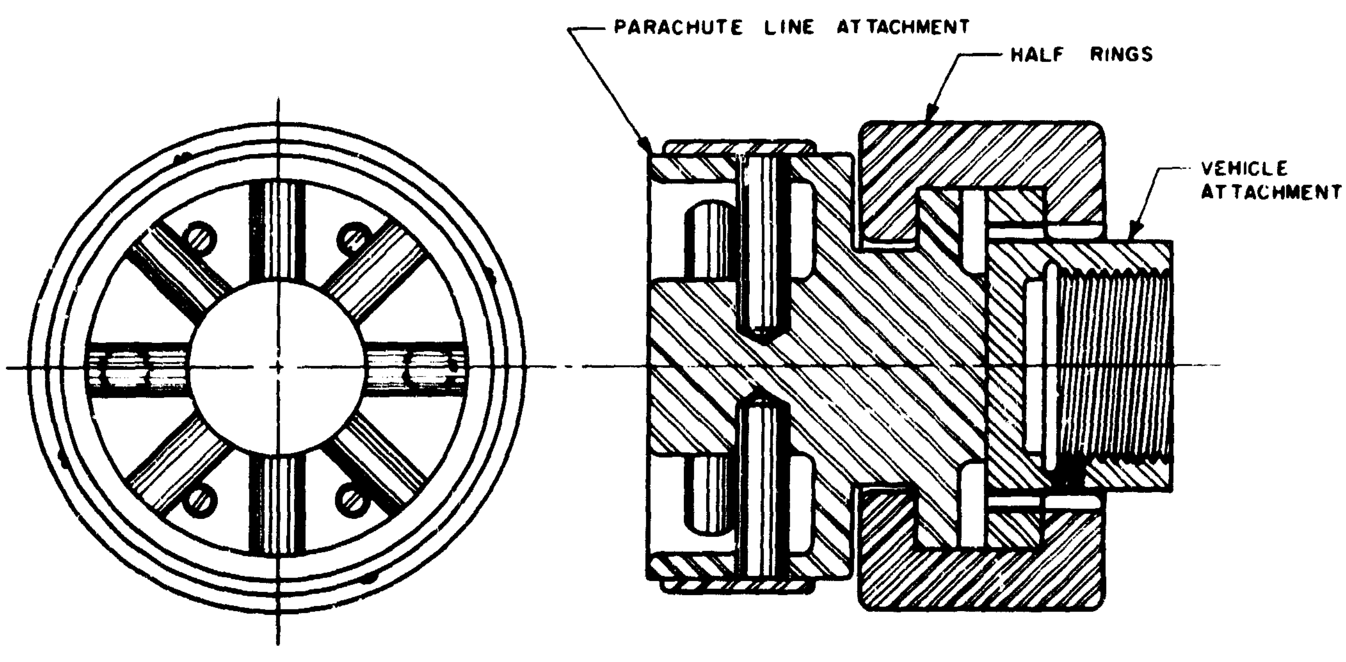

Figure 6.3.1. Parachute Attachment and Release Device

Operation of this separation device was consistent and functional reliability was excellent. There were no separation failures in any of the tests conducted on the program.

Both the deployment and separation systems were initiated by knife electrodes mounted on the sled and rail mounted screen boxes positioned along the track at locations where these events were to occur.

6.4 INSTRUMENTATION

The primary data instrumentation on board the test vehicle consisted of a two subcarrier Vector telemetry package transmitting through an 806 mcs Microdot transmitter. The subcarrier oscillators, 10.5 kc and 14.5 kc millivolt controlled, were driven by Cook Research Laboratories two-channel bridge type load cells. Three ranges of load cells were available to the program; a 30,000 pound force, a 50,000 pound force and a 100,000 pound force.

Space-time data was relayed from the sled to the ground station with an Interstate transmitter driven by its standard sensing head.

Metric cameras were used as a backup for the velocity measuring system and to record the event times for the deployment sequence.

Two high speed motion picture cameras (1000 and 400 frames per second) were installed in the sled to record parachute deployment, inflation and operation during the test. In addition to these sled-mounted cameras, four 70 mm cameras operating at 400 frames per second were stationed 400 feet from the track to record all events from parachute deployment to full parachute inflation. Three tracking cameras provided documentary coverage during each test, and pre-run and post-run still and motion picture documentary photography was obtained. All photographic services were provided by Land-Air.

REFERENCES

1. United States Air Force Parachute Handbook, WADC Technical Report 55-265, December 1956

2. W. E. Nickel, L. W. Sims, Study and Exploratory Free Flight Investigations on Deployable Aerodynamic Decelerators Operating at High Attitudes and at High Mach Numbers, AFFDL Technical Documentary Report 64-35, March 1964

3. L. W. Sims, (UNCLASSIFIED TITLE) Analytical and Experimental Investigation of Supersonic Parachute Phenomena, ASD Technical Documentary Report 62-844, February 1963 (CONFIDENTIAL)

4. B. A. Engstrom, Performance of Trailing Aerodynamic Deceleration at High Dynamic Pressures, Phase V & VI, WADC Technical Report 58-284, Part V, February 1962

5. Cook Research Laboratories, Recovery Systems for Missiles and Target Aircraft, AF Technical Report 5853, Part I (March 1954), Part III (December 1956)

6. P. E. Pedersen, Study of Parachute Performance at Low Supersonic Deployment Speeds; Effects of Changing Scale and Clustering, ASD Technical Report 61-186, May 1961

7. Military Specification, Parachute, FIST Ribbon, General Specification for Construction of, MIL-P-6635A (ASG)

APPENDIX

PARACHUTE DESIGN AND STRENGTH ANALYSIS

A. 1 GENERAL

The choice of test parachute materials, factors of safety used and fabrication and assembly techniques employed were based primarily on the desire to investigate the strength characteristics of the test parachute canopies operating at high dynamic pressures. It was also desirable to obtain aerodynamic and physical performance information on the test parachutes. Therefore the allowable extent of damage to the test parachute canopies had to be minimized. The optimum, of course, was a parachute design which could be made to operate successfully at the design test conditions and at the same time, just begin to show evidence of structural strain.

Because of the limited choice of available Mil-Spec parachute materials optimum designs were not always attainable. This material limitation, in general, dictated the use of somewhat over-strength components in the parachute assembly rather than utilize understrength components and chance the total destruction of the test parachute canopy and thus lose much valuable test data.

It was not considered necessary to include a design factor for parachute canopy aerodynamic heating effects on the tests conducted on the program. This should, however, not be overlooked at higher Mach number sled test operation.

The following paragraphs discuss the strength analysis, geometry and porosity calculations of a Hemisflo type parachute as tested on the program.

A. 1. 1 Strength Analysis

The structural design of any parachute depends primarily upon one main factor; the maximum force incurred by the parachute. This force is given by

$$F = C_{D_o} S_o \, q \, x k \qquad (1)$$

As specified for this program the parachute was to have a drag area of 18 square feet based on a subsonic drag coefficient (C_{D_o}) of 0. 5. Previous tests on Hemisflo type canopies also indicated that the infinite mass opening shock factor, (X = xk), was approximately 1.4. Using the above drag coefficient a total design area of 36 ft^2 (D_o = 6.774 ft) is required.

The deployment conditions for the test of this canopy were:

Mach No. = 1.1

Altitude = 4,000 ft

Dynamic Pressure = 1,550 lb/ft^2

The "x" factor is determined by methods outlined in Reference 1. This factor is given as a function of the A factor, which has the value

$$A = \frac{2W}{C_{D_o} S_o q \rho V_s t_f} \qquad (2)$$

where

W is the vehicle weight (4,000 lb)

g is the gravitational constant (32.2 ft/sec^2)

V_s is the deployment velocity (1,212 ft/sec)

ρ is the atmospheric density (2.112 x 10^{-3} $slugs/ft^3$)

t_f is the filling time $= \dfrac{8\, D_o \sigma}{V_s^{0.9}}$ = (0.092 sec)

Substitution of these values into Equation (2) gives an A factor of 58.7, which indicates relatively no deceleration during the opening process. Thus the decreasing factor (x) has the value of 1, and the xk factor the infinite mass value of 1.4.

The maximum opening force is then calculated to be 39,060 lb.

Material requirements for this Hemisflo canopy were determined by means of the parachute strength analysis developed by Cook Electric Company (Reference 2). This analysis indicates that the canopy stress (L_c) is given by

$$L_c = \frac{F_o\, CRM \cdot f_s}{D_o} \tag{3}$$

where

F_o = maximum opening force (lb)

D_o = nominal parachute diameter (in.)

C = canopy stress factor (1 for Hemisflo)

R = reefing factor (1 for no reefing)

M = material factor (1 for nylon)

Substitution of respective values into Equation (3), a stress of 481 lb/in. can be expected. A design safety factor (f_s) of 1.3 was assumed adequate for the canopy. Thus a material choice of 2 in. x 1500 lb ribbon (MIL-R-5038, Class E, Type III) should be more than adequate, giving a margin of safety of 56 percent.

The suspension line strength (L_s) is given as

$$L_s = \frac{F_o\, f_s}{n \cos\frac{\gamma_s}{2}} \tag{4}$$

where

n = number of gores and suspension lines

γ_s = angle between two diametrically opposite sus. lines

With n taken to be 20 and f_s equal to 1.3 a line strength of 2,570 lb is required. Thus 1 in. x 3000 lb tubular webbing (MIL-W-5625) will give a margin of safety of 12 percent and will be used.

Based upon the above results and standard practice, the various other components were chosen. They are:

Radials	1-1/4 x 650 lb	- MIL-R-5608	- Class E, Type I
Verticals	9/16 x 500 lb	- MIL-T-5038	- Type V
Vent Reinforcing	1 x 6000 lb	- MIL-W-4088	- Type XVIII
Skirt Reinforcing	1-3/4 x 3600 lb	- MIL-W-4088	- Type VIII
Butterflies	1 x 2400 lb	- MIL-W-4088	- Type XVII

A.1.2 Geometry

The following equations are necessary for determining the coordinates of a gore of the Hemisflo parachute (refer to Figure A-1)

$$D = \sqrt{\frac{S_o/n}{\frac{1}{\pi^2}\sin\frac{360}{n} + \frac{a}{\pi}\left(\frac{a+2b}{a+b}\right)\sin\frac{180}{n}\cos\frac{\gamma}{2}}} \tag{5}$$

$$e_{g_b} = \frac{2D}{\pi}\sin\frac{180}{n} \tag{6}$$

$$e_{g_2} = 4D\sin\frac{\gamma}{2} \tag{7}$$

$$h_e = aD\cos\frac{\gamma}{2} \tag{8}$$

$$R_V = \frac{W_V}{\sin\frac{360}{n}} + \left[\frac{.02\,\frac{S_o}{n}}{\sin\frac{360}{n}}\right]^{1/2} \tag{9}$$

$$H_1 = R_V\cos\frac{180}{n} \tag{10}$$

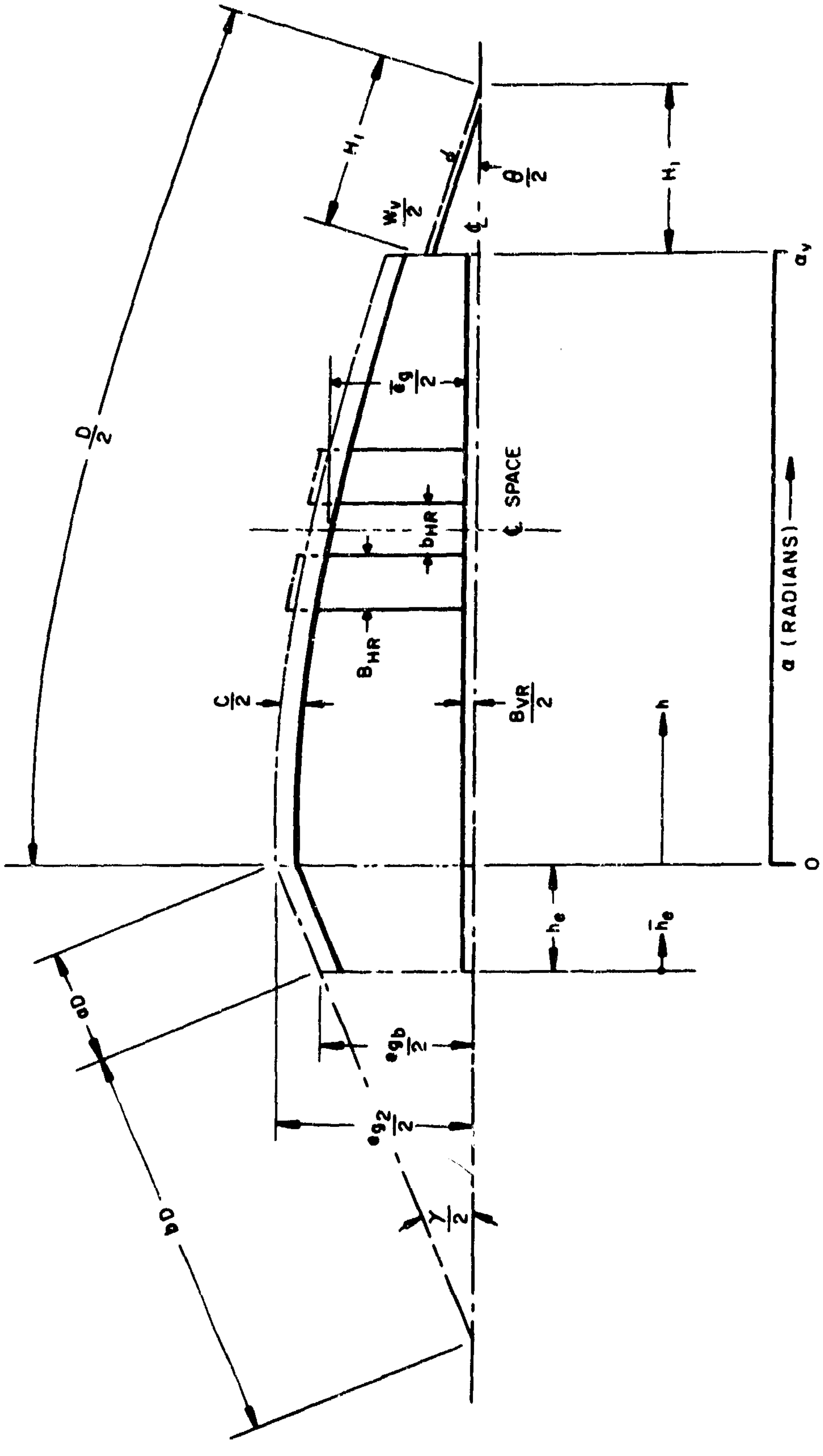

Figure A-1. Gore Coordinate Geometry for a Hemisflo Type Parachute

$$\alpha_V = \left[\frac{\frac{D}{2} \cos \frac{180}{n} - H_1}{\frac{D}{2} \cos \frac{180}{n}} \right] \frac{\pi}{2} \tag{11}$$

The coordinates for the Hemispherical portion are given by the parametric equations:

$$h = \frac{D}{\pi} \cos \frac{180}{n} \alpha \tag{12}$$

$$\pm \frac{^e g}{2} = \frac{^e g_b}{2} \left[\cos \alpha + 0.125 \left(\frac{\cos \alpha_V}{\alpha_V} \right) \alpha \right] \tag{13}$$

for

$$0 \leq \alpha \leq \alpha_V$$

These equations provide for a fullness which is 12.5 percent at the vent and decreases linearly to zero at α equal to 0.

The coordinates of the trapezoidal portion are given as $(\bar{h}_e, \frac{^e g}{2})$, the end points of which are $(o, \pm \frac{^e g_b}{2})$ and $(-h_e, \pm \frac{^e g_2}{2})$.

Substituting the respective values into the equations the following values are obtained

D = 79.608 inches

γ = 8° 40'

$^e g_b$ = 7.896 inches

$^e g_2$ = 7.500 inches

h_e = 7.960 inches

R_v = 7.34 inches

$H_1 = 7.25$ inches

$a_v = 1.281$ radians

The parametric Equations (12) and (13) are then given by,

$$h = 25.028\, a \tag{12A}$$

$$\pm \frac{e_g}{2} = 3.948 \cos a + 0.11\, a \tag{13A}$$

The coordinates at 15° increments are listed in Table A-1

TABLE A-1

HEMISPHERE GORE COORDINATES

a (degrees)	a (radians)	$\pm \frac{e_g}{2}$	h
0	0	3.948	0
15	0.2618	3.843	6.550
30	0.5236	3.477	13.100
45	0.7854	2.878	19.651
60	1.047	2.089	26.196
73.48	1.281	1.270	32.051

The coordinates of the end points of the trapezoidal skirt extension then become (7.960, ±3.948) and (0, ±3.750).

For the determination of $\bar{e}_g/2$, two equations are required. These are, respectively for the trapezoidal and hemispherical sections,

$$\frac{\bar{e}_g}{2} = \frac{e_{g2}}{2} + (e_{g_b} - e_{g_2})\frac{\bar{h}_e}{2h_e} - (\frac{e}{2} + \frac{B_{VR}}{2}) \tag{14}$$

for $0 \leq \bar{h}_e \leq h_e$

and

$$\frac{\bar{e}_g}{2} = \frac{e_{g_b}}{2} (\cos a + 0.125 \frac{\cos a_v}{a_v} \cdot a) - (\frac{c}{2} + \frac{B_{VR}}{2}) \tag{15}$$

for $0 \leq a(h) \leq a_v$

The first term in Equations (14) and (15) gives the gore coordinates, and the second term the decrease in open space height due to the radial and vertical ribbon. The equations become, upon substitution of respective constants,

$$\frac{\bar{e}_g}{2} = 3.750 + 0.0249\,\bar{h}_e - 0.906 \tag{14A}$$

for $0 \leq \bar{h}_e \leq 7.960$

and

$$\frac{\bar{e}_g}{2} = 3.948 \cos a + 0.110\, a - 0.906 \tag{15A}$$

for $0 \leq a \leq 1.281$

The parameters required for the determination of $\frac{\bar{e}_g}{2}$ are tabulated in Table A-2.

A.1.3 Porosity

A.1.3.1 Ribbon Spacing

Based on previous testing of the Hemisflo type parachute a design porosity of approximately 27 percent is desired.

Preliminary analysis of the present design indicated that the number of horizontal ribbons (Z) required, are 13. The spacing between ribbons (b_{HR}) has the value

TABLE A-2

GORE HALF-SPACE HEIGHT

	$\bar{h}_e$	h	α_r	$\cos\alpha$	$\bar{e}_g/2$
1	2.584	-	-	-	2.908
2	5.752	-	-	-	2.987
3		0.960	0.038	0.999	3.042
4		4.128	0.165	0.986	3.005
5		7.296	0.292	0.958	2.908
6		10.464	0.418	0.914	2.749
7		13.632	0.545	0.855	2.530
8		16.800	0.672	0.783	2.259
9		19.968	0.798	0.698	1.938
10		23.136	0.925	0.602	1.573
11		26.304	1.051	0.497	1.172
12		29.472	1.178	0.383	0.736
				Σ	28.046

$$b_{HR} = \frac{h_e + h_{\alpha_v} - Z\,B_{HR}}{Z - 1} \qquad (16)$$

where $h_e + h_{\alpha_v}$ is the total gore height (40.011 inches).

Substitution of the respective values into the above equation yields:

$$b_{HR} = 1.168 \text{ inches}$$

A.1.3.2 Geometric Porosity

The geometric porosity is determined by

$$\lambda_g = 100\,\frac{\frac{S_g}{2n}}{\frac{S_o}{2n}} = 100\,\frac{b_{HR}\sum\frac{\bar{e}_g}{2} + 0.01\frac{S_o}{2n}}{\frac{S_o}{2n}} \qquad (17)$$

Thus the geometric porosity becomes

$$\lambda_g = (100)\,\frac{(1.168)\,(28.046) + 1.296}{(129.600)} = 26.31\ \% \tag{17A}$$

A.1.3.3 Total Porosity

To determine the total porosity λ_T, the material area and permeability must be taken into account. For this, it is assumed that any two ply material and the vent lines have zero permeability. Thus the area having only one ply of material per half gore is given as

$$\frac{S_m}{2n} = \frac{S_o}{2n} - \left(\frac{S_g}{2n} - 0.01\,\frac{S_o}{2n}\right) - \frac{\left(R_v \cos\frac{180}{n}\,\frac{e_{g_v}}{2}\right)}{2} - \frac{B_{VR}}{2}\,h_1 - \left(\frac{D}{2} + 0.1\,D - R_v\right)\frac{c}{2} \tag{18}$$

Substitution of appropriate values results in

$$\frac{S_m}{2n} = 63.032\ \text{in.}^2$$

If the assumption that the material has a 2 percent porosity, then the porosity due to the material becomes

$$\lambda_m = \frac{\frac{S_m}{2n}}{\frac{S_o}{2n}}\,(2\%) = 0.973\ \% \tag{19}$$

Thus the total porosity λ_T is,

$$\lambda_T = \lambda_g + \lambda_m = 26.31 + 0.973 = 27.283\ \% \tag{20}$$

REFERENCES

1. United States Air Force Parachute Handbook, WADC TR 55-265, Dec. '56.

2. The Study of Design and Material for Development of Low Cost Aerial Delivery Parachutes, WADC TR-59-385, Sept. '59, Cook Research Laboratories.